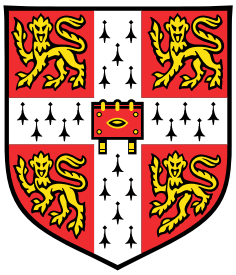

The imprint of scalar clouds around Kerr black holes: hairy solutions and weak cosmic censorship

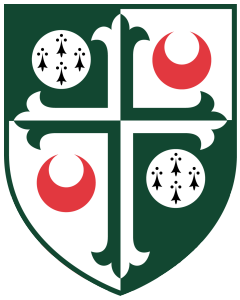

Bogdan Vladimirov Ganchev

Supervisor: Dr. Jorge E. Santos

Department of Applied Mathematics and Theoretical Physics
University of Cambridge

This dissertation is submitted for the degree of
Doctor of Philosophy

Girton College

September 2020

Declaration

I hereby declare that except where specific reference is made to the work of others, the contents of this dissertation are original and have not been submitted in whole or in part for consideration for any other degree or qualification in this, or any other university. This dissertation is my own work and contains nothing which is the outcome of work done in collaboration with others, except as specified in the text and Acknowledgements. This dissertation contains fewer than 65,000 words including appendices, bibliography, footnotes, tables and equations and has fewer than 150 figures.

Bogdan Vladimirov Ganchev
September 2020

Acknowledgements

I would like to thank my supervisor Jorge Santos for the continuous support, guidance and patience throughout my PhD. I am grateful I was given the opportunity to carry this out in Cambridge where I have met so many interesting people and have had so many engaging discussion within my department and outside of it. The work done in Chapter 3 was carried out in collaboration with Jorge Santos and published in [95]. Chapter 4 is based on [78], done with Felicity Eperon and Jorge Santos.

I want to express my gratitude to all my friends and beloved ones who were part of my life during my PhD studies - whether through discussions about physics, making silly jokes or giving me emotional support. Special thanks goes to Theodor Björkmo and Neeraja Bhamidipati for everything they did.

Of course, none of this would have been possible in the slightest without the unlimited love and support of my parents that I have been lucky enough to have throughout my whole life.

The imprint of scalar clouds around Kerr black holes: hairy solutions and weak cosmic censorship

Bogdan Vladimirov Ganchev

Abstract

In this thesis we explore Einstein gravity coupled to matter, and more specifically, we focus on the Kerr black hole in the presence of a massive scalar field. We investigate the superradiant phenomenon present in this setting - amplified scattering of scalar waves by the black hole given the right conditions on the scalar field's frequency are satisfied. Due to the mass term the spacetime develops a trapping region where the scalar waves can get localised instead of dispersing to infinity. In this way, the energy extracted from the black hole leads to the formation of a quasi bound state of the scalar field around it, known as a scalar cloud. This parallels the situation in Kerr-AdS [61], where due to the timelike character of the boundary this phenomenon appears more naturally and one does not necessarily need to make the field massive. We explore some of the consequences due to the formation of the scalar clouds in the asymptotically flat context.

In the case of a complex scalar field the configuration can actually settle to a stationary solution to the Einstein equation which represents a scalar hairy Kerr black hole in asymptotically flat four dimensions - the first example of such black holes that does not violate energy conditions, discovered recently [109, 35]. These scalar hairy black holes branch off from the Kerr solution at the onset of scalar superradiance, when the scalar cloud starts forming. Since their discovery a number of studies have been carried out, trying to relate their properties to astrophysics. However, prior to our work, no stability analysis was performed. This is particularly important if we want to argue for the astrophysical significance of such solutions. We made the initial step in answering this question by showing that such black holes are unstable towards higher excited superradiant modes than the mode from whose onset they branched off. This required the construction of the black hole backgrounds numerically, utilising the DeTurck method and solving a system of PDEs with extended precision using spectral methods. Afterwards, a clever choice of gauge allowed us to decouple the scalar field perturbations form the gravitational sector and perform the analysis by looking at the quasinormal mode spectrum of the hairy solutions.

When the scalar field is real, these stationary hairy solutions do not exist, but scalar clouds still form around the black hole. Moreover, our previous work suggested that for any parameters of the Kerr black hole, an unstable scalar mode will be present. We showed this analytically using a hybrid WKB and matched asymptotic expansion technique and confirmed it with numerical data. This led us to explore an idea for a plausible counterexample to the Weak Cosmic Censorship Conjecture in flat four dimensions, based on the cascading of energies, as seen in AdS [62, 142], whereby with time even higher superradiant modes become dominant and form clouds around the black hole. In support of our claim we have integrated the sourced Teukolsky equation for gravitational perturbations of Kerr numerically with extended precision in order to obtain the backreaction of the scalar field on the geometry and also analysed the system analytically, as detailed above, in order to confirm our numerics and discuss the endpoint of the evolution of the system.

Table of contents

List of figures

Chapter 1

Introduction

1.1 General Relativity

Since its formulation just over one hundred years ago General Relativity has gone through many exciting developments, but nevertheless still provides us with a multitude of challenges to tackle both theoretically and experimentally. In the most basic terms, General Relativity describes the interplay between the geometry of spacetime and the matter present in it. This intricate dynamical behaviour is governed by the famous Einstein field equation

$$R_{ab} - \frac{1}{2} R\, g_{ab} + \Lambda\, g_{ab} = \frac{8\,\pi\, G}{c^4} T_{ab}, \tag{1.1}$$

where R_{ab} is the Ricci curvature tensor, R is the Ricci scalar, g_{ab} is the metric tensor, Λ is the cosmological constant, G is Newton's constant, c is the speed of light and T_{ab} is the stress-energy-momentum tensor of matter distributed within the spacetime. The latter is represented by (M, g) - a Lorentzian manifold without a boundary (a type of pseudo-Riemannian manifold) equipped with an inner product on the tangent space at each point of the manifold - the so called metric g_{ab} we referred to in the previous sentence. The metric tensor is a generalisation of the dot product of ordinary Euclidean space and it bears physical significance as it encodes the information about the geometric and causal structure of spacetime. The Einstein field equation is a tensor equation between symmetric 4×4 tensors (or $D \times D$ in D-dimensions, as Einstein's General Relativity can be formulated in any number of dimensions), hence there are actually only 10 independent components (or $D\,(D+1)/2$ in D-dimensions) in Eq. (1.1). The Ricci tensor and scalar are non-linear functions of the metric and, in general, (1.1) represents a system of coupled, non-linear, second order partial differential equations

for the metric g_{ab} and its first and second derivatives. The Ricci scalar is the trace of R_{ab}, which itself is defined as the trace of the Riemann curvature tensor:

$$R_{ab} = R^{c}{}_{acb}, \quad R = R^{a}{}_{a}. \tag{1.2}$$

The Riemann curvature tensor $R^{a}{}_{bcd}$, which is one of the central mathematical objects in the theory of General Relativity, enables us to quantify the curvature of any Riemannian or pseudo-Riemannian manifold[1]. Roughly speaking, it measures the local deviation of the metric tensor g_{ab} from being isometric to that of flat space. Furthermore, spacetime curvature is an observable quantity via the geodesic deviation equation, which determines the relative acceleration of nearby geodesics due to the curvature of spacetime. This acceleration is a result of the gradient of the gravitational field between the geodesics, which results in gravitational tidal forces that cause them to move together or apart. Hence, more accurately, the Riemann curvature tensor is the quantity that measures tidal forces in the spacetime. In contrast to geodesic motion in curved spacetimes, in flat space, two initially parallel trajectories will remain parallel forever.

Moreover, the properties and symmetries of the Riemann tensor, and in particular the so called Bianchi identities, together with the Einstein equation (1.1) ensure that General Relativity is consistent with local conservation of energy and momentum through the conservation of the stress tensor T_{ab}:

$$\nabla_a T^{ab} = 0, \tag{1.3}$$

whereby ∇ is the covariant derivative with respect to the metric g_{ab}.

From here onwards, we will assume that we are working in four spacetime dimensions, unless explicitly stated otherwise.

General Relativity can therefore be thought of as a mathematical model for a Lorentzian manifold M with metric g that obeys three postulates: local causality, local conservation of energy and momentum and the validity of the Einstein field equation (1.1) on M. The first two postulates have been tested extensively experimentally. Concerning the third one, it is possible to think of extensions of Einstein's theory (modified theories of gravity) which would agree with all observations made up to day, but would have different predictions in certain regions of parameter space. In fact, ever since its publication, General Relativity has been subject to experimental tests probing its validity as a theory of gravity and it has so far managed to pass

[1] Or any manifold with an affine connection.

all of them successfully. The very first such test was cleared by the theory on the day of its birth - it determined the rate of precession of the perihelion of Mercury correctly, which had already been measured at this point and was in conflict with the Newtonian prediction. More tests followed - the bending of light in gravitational fields, gravitational redshift and Shapiro time delay[2] - all confirming Einstein's theory. Even though the previously mentioned tests are all probing the weak field regime of gravity, in more recent history, there have also been confirmations of the theory in the presence of very strong gravitational fields. One such example is the observation of the Hulse-Taylor binary pulsar in 1974 [121, 173, 181] - a pair of neutron stars orbiting each other with a period of just a few hours and at a distance of just a few solar radii. The two stars are gradually spiralling towards each other and emitting gravitational waves in the process, thereby causing their orbital period to decay at a rate which agrees very well with predictions from General Relativity. Furthermore, in February 2016 the first detection of the merger of two black holes into a final larger black hole was announced by the LIGO collaboration [2, 1, 5–8]. This constituted the first direct observation of gravitational waves and the observed waveform matches the theoretical expectations from Einstein's theory for the inspiral and merger of a pair of black holes, and, the ringdown of the resulting single black hole. Since then dozens more binary mergers have been detected, including the merger of two neutron stars. These observations allow us to access the properties of spacetime in the strong-field regime of gravity and test predictions of General Relativity for the non-linear dynamics of black holes and other ultra compact objects. With several more gravitational wave detectors on the way around the world to add to the existing three (2 LIGO facilities and VIRGO), direct observations of gravitational waves are gradually making their way towards becoming a tool for precision tests of General Relativity in the strong field regime.

As mentioned earlier, General Relativity gives a different answer for the rate of precession of the perihelion of Mercury (agreeing with observations). However, we also know that there are certain regimes in which Newtonian gravity produces reliable answers (like throwing a ball in your backyard). One would thus hope that in these situations Einstein's theory does agree with Newtonian gravity. And indeed it can be shown that General Relativity reduces to Newtonian gravity in the limit of non-relativistic velocities and a weak gravitational field.

In the opposite regime of strong gravitational fields, where relativistic effects are important, the aforementioned black holes were actually an unexpected prediction

[2]Increase in the travel time of light near massive objects, compared to if the object was not there.

of Einstein's theory. Even though the first black hole metric was written down as a solution to Eq. (1.1) in 1916 by Schwarzschild [164], it was not until the 1960s when physicists realised that black holes are regions of spacetime from where nothing, including light, can escape and that they are indeed a prediction of Einstein's theory. In what follows we will give a definition of what a black hole in General Relativity is and we will recap some of the important classical results concerning them.

1.1.1 Causal structure of spacetime

Before we can give a proper definition of a black hole in General Relativity we need to introduce a few concepts of causality that will be helpful for the rest of this section. Our sign convention is mostly positive, $(-,+,+,+)$, and we work in units with $c = G = \hbar = 1$.

In Special Relativity, where the background is fixed Minkowski spacetime, with metric

$$\eta = -dt^2 + dx^2 + dy^2 + dz^2, \tag{1.4}$$

one can easily identify a light cone with each event, p, in the spacetime. Its upper half is called the future light cone and the lower part is the past light cone. All spacetime events strictly inside the future light cone can be reached by massive particles starting at p, and this is referred to as the chronological future of p in Special Relativity. Combining these with all the events lying on the future light cone itself gives us the causal future of p, which corresponds to all the events that can be influenced by a signal, travelling at the speed of light, emitted at p.

While in General Relativity that structure exists locally, it may be subject to change globally due to the "non-trivial" geometry of curved spacetimes - the light cones might get rotated (for example, inside a black hole event horizon) or there might be singularities present in the spacetime.

As already mentioned, the spacetime is a Lorentzian manifold (M, g), and at each point p of this manifold we can identify a tangent space of vectors $T_p(M)$. This is the set of all tangent vectors at p and it forms an n-dimensional vector space, $T_p(M)$. Recall that, a tangent vector to a smooth curve at a point p on the manifold M is a linear map from the space of smooth functions on M to $\mathbb{R}$. Furthermore, we can then make the following disambiguation:

Definition 1. *On a Lorentzian manifold (M, g), a non-zero vector $X \in T_p(M)$ is **timelike** if $g(X, X) < 0$, **null** if $g(X, X) = 0$, and **spacelike** if $g(X, X) > 0$. A non-spacelike vector will be referred to as a **causal** vector.*

In our everyday lives we are used to the concept of an arrow of time. For our small neighbourhood of spacetime we can most directly link it to the increase of entropy in quasi-isolated thermodynamic systems. Demanding the ability to define a local thermodynamic arrow of time at every point of our manifold, even if certainly physically reasonable, is more than one needs in order to talk about the causal structure of spacetime in General Relativity. Instead we will introduce the notion of a *time-orientation*:

Definition 2. *Let (M, g_{ab}) be a spacetime. It is* ***time-orientable*** *if there exists a continuous causal vector field T^a on M. T^a is sometimes referred to as* ***time-orientation*** *and is non-unique.*

Any other causal vector V^a is said to be *future-directed* if it lies in the same light cone as the time-orientation T^a. Two causal vectors are within the same light cone if their inner product is negative $g(T, V) < 0$. Otherwise, V^a is *past-directed*. In this way time-orientability allows us to continuously differentiate between future- and past-directed causal vectors, which one can think of as a "choice" of an arrow of time at each point. Also, we define a future-directed causal curve as one whose tangent vector is everywhere causal and future-directed.

Next, we introduce a few notions pertaining to the causal structure of a spacetime which are necessary for our definition of asymptotic flatness later that will ultimately enable us to define a black hole.

Definition 3. *The* ***chronological future*** *of $p \in M$, denoted $I^+(p)$, is the set of points in M that can be reached by a future-directed timelike curve starting from p.*

$$I^+(p) = \Big\{ q \in M,\ \exists \text{ a future-directed timelike curve } \lambda(t), \quad \lambda(0) = p,\ \lambda(t_0) = q,\ t_0 > 0 \Big\}. \tag{1.5}$$

A similar definition holds for the ***chronological past*** *$I^-(p)$ of p.*

We should note that in general $p \notin I^\pm(p)$ unless there are closed timelike curves in the spacetime. Furthermore, one can always deform the endpoint of a timelike curve slightly, while keeping its timelike character (that will not hold for null curves), indicating that there exists a small neighbourhood of q that is also contained within $I^\pm(p)$, implying that $I^\pm(p)$ is an open subset of M. Moreover, for any subset $S \subset M$, we define $I^\pm(S)$ in the expected way

$$I^\pm(S) = \bigcup_{p \in S} I^\pm(p), \tag{1.6}$$

and observe that a union of open sets is also open, thus $I^{\pm}(S)$ is an open subset of M.

Definition 4. *The* ***causal future*** *of $p \in M$, denoted $J^{+}(p)$, is the union of p with the set of points in M that can be reached by a future-directed causal curve starting from p.*

$$J^{+}(p) = p \cup \Big\{ q \in M,\ \exists \text{ a future-directed causal curve } \lambda(t), \quad \lambda(0) = p,\ \lambda(t_0) = q,\ t_0 > 0 \Big\}. \tag{1.7}$$

A similar definition holds for the ***causal past*** *$J^{-}(p)$ of p,*

and, as above, for a subset $s \subset M$ we have

$$J^{\pm}(S) = \bigcup_{p \in S} J^{\pm}(p). \tag{1.8}$$

As we noted earlier, in Minkowski spacetime, $I^{\pm}(p)$ are precisely the sets that contain all the points that can be reached by a future/past-directed timelike geodesic starting from p (the insides of the past/future light cones), whereas $J^{\pm}(p)$ is built up of all the points that are accessible via future/past-directed causal geodesics starting from p (all the points on or inside the past/future light cones) and p. From topology we remember that the closure of a set is equal to the union of that set with its limit points. We will denote this closure with an overbar and from the above we see that in Minkowski $\overline{I^{\pm}(p)} = J^{\pm}(p)$, implying that $J^{+}(p) = \overline{J^{+}(p)}$ and thus $J^{+}(p)$ is closed. In addition, in topology one says that a point $p \in U$ is an interior point if there is a neighbourhood of p that is contained within U. The set of interior points of U (the interior of U) is denoted $\mathrm{int}(U)$. It must be clear from the definition that if U is open then $\mathrm{int}(U) = U$. Furthermore, from these we also have the boundary of U, given by $\dot{U} = \bar{U} \setminus \mathrm{int}(U)$. Going back to Minkowski, there $\dot{I}^{\pm}(p)$ is the set of points along future/past-directed null geodesics starting from p. The examples in flat space might be easy to understand, however, they are not true in general, as the setup in Fig. (1.1) shows.

Nevertheless, as already stated, they are still true in a local sense, as indicated by the next theorem.

Theorem 1. *Given $p \in M$ there exists a* ***convex normal neighbourhood*** *of p. This is an open set U with $p \in U$ such that for any $q, r \in U$ there exists a unique geodesic connecting q and r that stays entirely in U. $I^{+}(p)$ in the spacetime (U, g) consists of all points in U along future-directed timelike geodesics that start at p and are contained in U. The boundary of this region is the set of all points in U along future-directed null geodesics in U that start at p.*

Figure 1.1 Minkowski spacetime with a point removed from the future light cone of another point p in the spacetime. No causal curve connects p and q, hence $q \notin J^+(p)$, however, $q \in \overline{J^+(p)}$, implying that $J^+(p)$ is not closed in this spacetime.

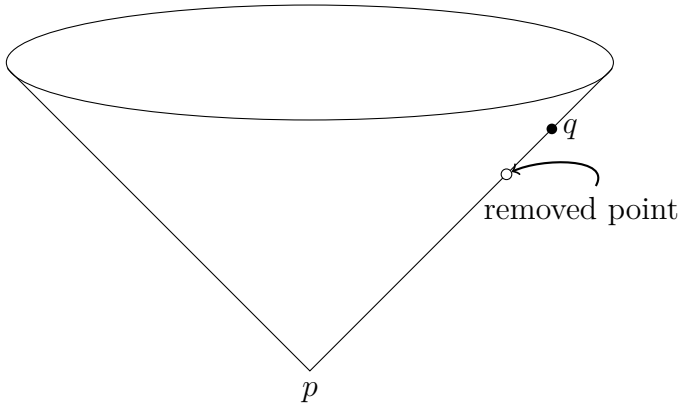

The theorem is given in [179] with references on where to find all of the individual parts of the proof.

1.1.2 Conformal compactification

In physics, we often study idealised isolated systems and then perturb them slightly in order to get an understanding of how they might behave in real world situations, which are usually way too complex to approach directly with our mathematical (and numerical) tools. We would like to implement this approach in General Relativity as well. It seems intuitive that if we are interested in the properties of a very dense star, we should not need to worry about some other matter in a galaxy far, far away or the effect of the tiny, but non-zero, cosmological constant which is only important on very large scales. To this end, relativists have defined the concept of an asymptotically flat spacetime, which allows one to study stars and black holes as though they were in a spacetime that approaches Minkowski at large distances from the object in question.

Making a hand-wavy argument about the need for a notion of asymptotic flatness seems easy, but its formulation is not a straightforward task and in particular we are not going to explore it thoroughly. Not only that, but in General Relativity there is an additional complication that one needs to be aware of. The spacetime metric is no longer a fixed background (like in Electrodynamics) as it is dynamically determined by the Einstein equation (1.1). Hence, there is no preferred global coordinate system to use for specifying how quantities of interest (including the dynamic metric g_{ab}) behave in distant regions. Therefore, one needs a coordinate independent way of talking

about "very far away" and evaluating "limits at infinity". It turns out that conformal compactifications provide a solution to that problem and in order to illustrate how this works, we will carry out the conformal compactification of Minkowski in what follows next.

Minkowski spacetime, $(M, \eta) = (\mathbb{R}^4, \eta)$, in spherical polar coordinates is given by the following line element:

$$ds^2 = -dt^2 + dr^2 + r^2 d\theta^2 + r^2 \sin^2\theta \, d\phi^2. \tag{1.9}$$

Defining null coordinates

$$u = t - r \quad v = t + r, \tag{1.10}$$

transforms the metric into

$$ds^2 = -du\, dv + \frac{1}{4}(u - v)^2 (d\theta^2 + \sin^2\theta \, d\phi^2), \tag{1.11}$$

whereby, since the radial coordinate $r \geq 0$, we have $-\infty < u \leq v < \infty$ for the retarded and advanced times respectively. In this form, the infinitely far region still corresponds to taking one of the coordinates to infinity, for example u fixed and $v \to \infty$. However, making the trigonometric coordinate transformation

$$u = \tan p, \quad v = \tan q \tag{1.12}$$

gives us

$$ds^2 = \Big[\frac{1}{2\,\cos p\,\cos q}\Big]^2 \Big[-4\, dp\, dq + \sin^2\Big(q - p\Big)\Big(d\theta^2 + \sin^2\theta \, d\phi\Big)\Big], \tag{1.13}$$

with coordinate ranges $-\pi/2 < p \leq q < \pi/2$. We see that in this way we have managed to pull infinity back to a finite distance, in the sense that $r \to \infty$ at fixed t now corresponds to $q \to \pi/2$, $p \to -\pi/2$, while $t \to \infty$ at fixed r is given by $q \to \pi/2$, $p \to \pi/2$ and $t \to -\infty$ at fixed r is $q \to -\pi/2$, $p \to -\pi/2$. Nevertheless, Eq. (1.13) still contains a prefactor that diverges at these limits, hence we cannot actually extend the spacetime metric to the very distant region, which we want to associate with infinity. However, if we define the function

$$\Omega = 2\,\cos p\,\cos q, \tag{1.14}$$

we see that in the allowed coordinate ranges for q and p, the prefactor is always positive. We can, therefore, use it to introduce a conformal transformation of our metric,

$$\bar{g} = \Omega^2 g = -4\, dp\, dq + \sin^2\Big(q - p\Big)\Big(d\theta^2 + \sin^2\theta\, d\phi\Big), \tag{1.15}$$

where $\bar{g}$ is called the unphysical metric. Before proceeding with the discussion, we make a final coordinate transformation in order to bring $\bar{g}$ into a more familiar form via

$$T = q + p, \quad \chi = q - p, \tag{1.16}$$

with

$$T \in (-\pi,\, \pi), \quad \chi \in [0,\, \pi), \tag{1.17}$$

which allows us to obtain

$$\bar{g} = -dT^2 + d\chi^2 + \sin^2\chi\Big(d\theta^2 + \sin^2\theta\, d\phi\Big). \tag{1.18}$$

The $d\chi^2 + \sin^2\chi\Big(d\theta^2 + \sin^2\theta\, d\phi\Big)$ part of the metric is just the unit round metric on an S^3 and had we had $T \in (-\infty, \infty)$ and $\chi \in [0,\, \pi]$, then $\bar{g}$ would represent the metric on the Einstein Static Universe (ESU) with topology $\mathbb{R} \times S^3$, which we will label as $(\bar{M}, \bar{g})$. Nonetheless, due to the restricted coordinate ranges we can only cover a portion of it.

On the other hand, we see that the unphysical metric $\bar{g}$ (1.18) is finite everywhere in the allowed coordinate domain, hence we can smoothly extend it to the region of interest (the boundary of the restricted coordinates (1.17)). We have thus shown that there exists a conformal mapping of Minkowski spacetime $(M,\, \eta)$ into the open subset $(U,\, \bar{g})$ of the ESU $(\bar{M}, \bar{g})$, defined by the ranges (1.17). Furthermore, the region we refer to as infinity of Minkowski spacetime corresponds to the boundary of M inside the ESU, given by $\dot{U}$, and we call this the *conformal infinity* of Minkowski. This mapping, as part of the ESU, is shown in Figure (1.2). There we can see that conformal infinity of Minkowski consists of: (1) the points $i^{\pm}$, called future/past timelike infinity $(t \to \pm\infty)$, given by $T = \pm\pi$, $\chi = 0$; (2) the point i^0, spacelike infinity $(r \to \infty)$, $T = 0$, $\chi = \pi$; (3) a pair of three-dimensional null hypersurfaces $\mathcal{I}^{\pm}$, future/past null infinity, with equations $T = \pm(\pi - \chi)$, for $\chi \in (0,\, \pi)$ and also parametrised by θ and ϕ, with topology $\mathcal{R} \times S^2$ (for $\mathcal{I}^{\pm}$, χ can be mapped onto the real line, due to the openness of the interval $(0,\, \pi)$).

It is important to note that conformal transformations preserve the causal structure of the metric so that g and $\bar{g}$ have the same null geodesics. The behaviour of geodesics can be identified on the diagram (1.2). As one might be anticipating from the names,

Figure 1.2 A diagram of the Einstein Static Universe. Defined in the text as U, the conformal mapping of Minkowski spacetime, is the shaded region, which is also given by $U = I^-(i^+) \cap I^+(i^-)$. Its boundary, $\dot{U}$,consisting of i^-, i^0, i^+ and the null hypersurfaces $\mathcal{I}^-$ and $\mathcal{I}^+$, defines our notion of infinity for flat space.

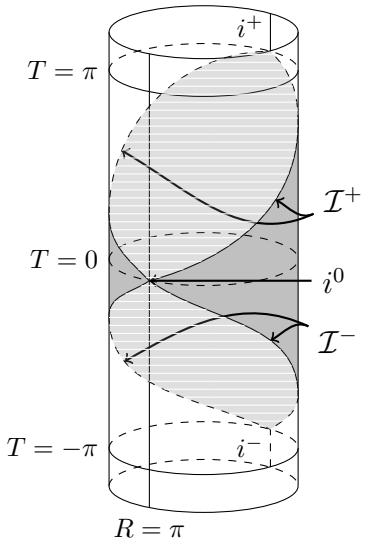

timelike geodesics start at i^- and end at i^+; null geodesics, which are straight lines at 45°, start at $\mathcal{I}^-$ and end at $\mathcal{I}^+$; and spacelike geodesics start and end at i^0. Non-geodesic curves do not obey these relations - a non-geodesic timelike curve may start at $\mathcal{I}^-$ and end at $\mathcal{I}^+$. Studying and understanding the causal structure of spacetimes is an indispensable part of General Relativity, hence relativists have come up with a way of extracting the most important features from the diagram in Figure (1.2) and presenting them simply by means of a 2D projection, called a *Penrose diagram*. In our case, we project onto the (T, χ)-plane and the result is given in Figure (1.3). Every point on that diagram represents a two-sphere, except for $i^\pm$ and i^0, which are single points, as well as $r = 0$, where polar coordinates are not defined. These are common features of Penrose diagrams of asymptotically flat spacetimes and we will see more such diagrams later when we introduce different black hole spacetimes.

1.1.3 Asymptotic flatness

The construction presented in the previous section enabled us to prescribe a notion of infinity in a coordinate independent way, allowing us to finally define what it means for an arbitrary curved spacetime to be flat far away from any mass. We should say here that as the need for such a notion stems from the way we seek to observe physical systems, in a similar way the definition of asymptotic flatness is carefully balanced

Figure 1.3 Penrose Diagram of Minkowski spacetime. Each point corresponds to an S^2, except for $i^{\pm}$ and i^0, which are single points, and the line $r = 0$ where polar coordinates are not defined.

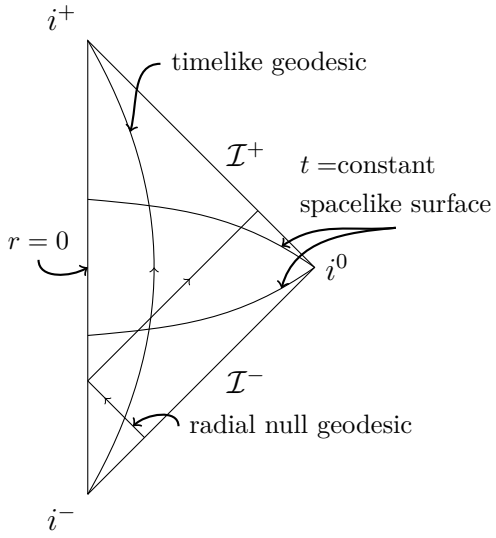

between two main considerations. First, we would like a definition that encompasses only spacetimes that do indeed represent isolated gravitational systems that we can study in a systematic way as physicists, and second, this same definition should not be too restraining so that it excludes examples that are physically reasonable to consider. The idea is to require that using a conformal transformation, the curved spacetime in question can be mapped onto an "unphysical" one that has properties similar to these of Minkowski at infinity.

We use the definition given by Ashtekar and Hansen [14] and Ashtekar [13] for a vacuum spacetime (M, g_{ab}) to be called *asymptotically flat at null and spatial infinity*:

Definition 5. *A vacuum spacetime (M, g_{ab}) is said to be **asymptotically flat at null and spatial infinity** if there exists a spacetime $(\bar{M}, \bar{g}_{ab})$ with g_{ab} being C^∞ everywhere except possibly at a point i^0 where it is $C^{>0}$ (defined below) and a conformal isometry $\psi : M \to \psi[M] \in \bar{M}$ with conformal factor Ω (so that $\bar{g}_{ab} = \Omega^2 \psi^* g_{ab}$ in $\psi[M]$) satisfying the following conditions:*

1. *$\overline{J^+(i^0)} \cup \overline{J^-(i^0)} = \bar{M} - M$. Thus, i^0 is spacelike related to all points in M and the boundary $\dot{M}$ of M consists of the union of i^0, $\mathcal{I}^+ = \dot{J}^+(i^0) - i^0$ and $\mathcal{I}^- = \dot{J}^-(i^0) - i^0$.*

2. *There exists an open neighbourhood V of $\dot{M} = i^0 \cup \mathcal{I}^+ \cup \mathcal{I}^-$ such that the spacetime $(V, \bar{g}_{ab})$ is strongly causal.*

3. Ω *can be extended to a function on all of* $\bar{M}$ *which is* C^2 *at* i^0 *and* C^∞ *elsewhere.*

4. *(a) On* $\mathcal{I}^\pm$ *we have* $\Omega = 0$ *and* $\bar{\nabla}_a\Omega \neq 0$.

(b) $\Omega(i^0) = 0$, $\lim_{i^0} \bar{\nabla}_a\Omega = 0$ *and* $\lim_{i^0} \bar{\nabla}_a\bar{\nabla}_b\Omega = 2\,\bar{g}_{ab}(i^0)$, *whereby we take limits at* i^0 *since* $\bar{g}_{ab}$ *need not be* C^1 *there, meaning that* $\bar{\nabla}_a$ *need not be defined at* i^0.

5. *(a) The map of null directions at* i^0 *into the space of integral curves of* $n^a = \bar{g}^{ab}\bar{\nabla}_a\Omega$ *on* $\mathcal{I}^\pm$ *is a diffeomorphism.*

(b) For a smooth function ω *on* $\bar{M} - i^0$ *with* $\omega > 0$ *on* $M \cup \mathcal{I}^+ \cup \mathcal{I}^-$ *which satisfies* $\bar{\nabla}_a(\omega^4 n^a) = 0$ *on* $\mathcal{I}^+ \cup \mathcal{I}^-$, *the vector field* $\omega^{-1}n^a$ *is complete on* $\mathcal{I}^+ \cup \mathcal{I}^-$.

Before commenting on these conditions - which we will not attempt in full technical detail as that is beyond the scope of this introduction - we need to make a few definitions. First, we introduce the notation for differentiability classes. Namely, a function $f(x)$ is said to be of differentiability class C^k if the first k derivatives $f'(x)$, $f''(x)$, ..., $f^{(k)}(x)$ all exist and are continuous. By $C^{>0}$ here we mean that a function is continuous (C^0) and its first derivatives have direction-dependent limits at i^0 which are smooth in their angular dependence. Second, we need to differentiate between curves that can be extended and such that cannot:

Definition 6. *$p \in M$ is a **future endpoint** of a future-directed causal curve $\gamma : (a, b) \to M$ if, for any neighbourhood O of p, there exists t_0 such that $\gamma(t) \in O$ for all $t > t_0$. We say that γ is **future-inextendible** if it has no future endpoint. Similarly for **past endpoints** and **past inextendibility**. γ is inextendible if it is both future and past inextendible.*

Definition 7. *A geodesic is complete if an affine parameter for the geodesic extends to $\pm\infty$. A spacetime is geodesically complete if all inextendible causal geodesics are complete.*

The reason we need the reduced differentiability conditions at spatial infinity i^0 is due to the way conformal compactification works. In the unphysical spacetime spatial infinity is just a single point, implying that all curves that approach it will end at the same point i^0. On the other hand, in the physical spacetime, curves that reach spatial infinity might do so along different angular directions, meaning that they could be moving further and further away from each other. Henceforth, while demanding that physical fields, multiplied by a suitable power of the conformal factor, have well

defined limits as they go towards spatial infinity makes sense, requiring the limits of curves approaching i^0 along different angular directions to give the same limit at spatial infinity is not physically motivated. In empty Minkowski, this works because of the high degree of symmetry of the spacetime, but as soon as one adds matter, it can be shown that problems will arise.

The first three conditions in the definition for asymptotic flatness above express the requirement that an appropriate conformal compactification exists, with features similar to those of Minkowski, as seen in the previous subsection. In particular, locally, General Relativity has a qualitatively similar causal structure as Special Relativity, as confirmed by Theorem 1, but can be seriously different globally. *Strong causality* requires that these differences do not result in physically unreasonable causal phenomena and it is defined as follows:

Definition 8. *A spacetime (M, g_{ab}) is **strongly causal** if for all $p \in M$ and every neighbourhood O of p there exists a neighbourhood $V \subset O$ of p, such that no causal curve intersects V more than once.*

In the case of higher dimensional surfaces 'intersect' is taken to mean 'pass through' - that is, a curve goes in, leaves and does not enter again. A spacetime failing to be strongly causal at a point p implies that near p there are causal curves that come arbitrarily close to intersecting themselves. Furthermore, a small perturbation of the metric in a small region about p might enable such intersections, leading to the creation of closed causal curves and thus causality violations.

The vanishing of the conformal factor, Ω, at the boundary of M, $\dot{M} = i^0 \cup \mathcal{I}^+ \cup \mathcal{I}^-$, in condition 4, is a mathematical way of saying that in order to go from the unphysical spacetime, where we have brought infinity to a finite distance (via $\mathcal{I}^\pm$ and i^0), to the the physical one, we need to introduce an infinite amount of stretching. Furthermore, it is the derivative conditions on Ω in the fourth condition that ensure g_{ab} approaches flat space at an appropriate rate as one goes off to null and spatial infinity. This can be stated in a more precise way, which will be illustrated for $\mathcal{I}^\pm$ here only. Namely, one starts from the rule for the conformal transformation of the Ricci tensor R_{ab} in terms of the unphysical variables $\bar{g}_{ab}$, $\bar{R}_{ab}$, $\bar{\nabla}_a$ and the conformal factor Ω. One can then further use the gauge freedom of choosing Ω, which comes about due to the fact that if $(\bar{M}, \bar{g}_{ab})$ is an unphysical spacetime with the properties we need and conformal factor Ω, then so is the spacetime $(\bar{M}, \omega^2 \bar{g}_{ab})$ with conformal factor $\omega\,\Omega$, where $\omega > 0$ and is smooth everywhere except possibly at i^0, where it is $C^{>0}$ and $\omega(i^0) = 1$. It is then possible to quantify in a coordinate form the requirement on the asymptotic behaviour

of the spacetime as one approaches null infinity, namely Minkowski plus corrections in $1/r$. Similar conclusion can be reached for the approach to spatial infinity.

Finally, condition five ensures that in the appropriate gauge the null geodesic generators of $\mathcal{I}^{\pm}$ are complete, or in other words all of null infinity is present as in Minkowski spacetime.

A final remark before continuing: our definition concerns vacuum spacetimes, however it is possible to consider spacetimes with non-vanishing stress-energy tensor T_{ab}, as long as it decays (or more precisely $\Omega^{-2}T_{ab}$) sufficiently quickly near future $\mathcal{I}^{+}$ and past $\mathcal{I}^{-}$ null infinity and has an appropriate limiting behaviour at i^0.

1.2 Black Holes

1.2.1 Definition

Before finally defining what a black hole in General Relativity in an asymptotically flat spacetime is, we need a few more straightforward definitions.

Definition 9. *Let (M, g) be a time-orientable spacetime. A **partial Cauchy surface** Σ is a hypersurface for which no two points are connected by a causal curve in M. The **future domain of dependence** of Σ, denoted $D^{+}(\Sigma)$, is the set of $p \in M$, such that every past-inextendible causal curve through p intersects Σ. The **past domain of dependence**, $D^{-}(\Sigma)$, is defined similarly. The **domain of dependence** of Σ is $D(\Sigma) = D^{+}(\Sigma) \cup D^{-}(\Sigma)$.*

Definition 10. *A spacetime (M, g) is **globally hyperbolic** if it admits a Cauchy surface: a partial Cauchy surface Σ such that $M = D(\Sigma)$.*

Definition 11. *Let (M, g_{ab}) be an asymptotically flat spacetime with corresponding unphysical spacetime $(\bar{M}, \bar{g}_{ab})$. We say that (M, g_{ab}) is **strongly asymptotically predictable** if there exists an open region $\bar{V} \subset \bar{M}$ with $\overline{M \cap J^{-}(\mathcal{I}^{+})} \subset \bar{V}$, such that $(\bar{V}, \bar{g}_{ab})$ is globally hyperbolic.*

We now have all the ingredients to give a precise definition of a black hole in General Relativity in an asymptotically flat spacetime. Our formulation is based on the fact that an observer that falls inside the black hole cannot send a signal to infinity and will be dragged further inside it, with no way of coming back, with all this being unobservable by someone outside. Following our constructions from the previous chapters, infinity is part of the unphysical spacetime $\bar{M}$, meaning that $J^{-}(\mathcal{I}^{+}) \subset \bar{M}$

and the region of M that can send signals to null infinity is given by $M \cap J^-(\mathcal{I}^+)$. Its complement then is what we will take to be the black hole and the boundary of that complement is the future event horizon (similarly for the white hole region):

Definition 12. *Let (M, g_{ab}) be a strongly asymptotically predictable spacetime. M contains a black hole if M is not contained in $J^-(\mathcal{I}^+)$. The black hole region is $\mathcal{B} = M \backslash [M \cap J^-(\mathcal{I}^+)]$ where $J^-(\mathcal{I}^+)$ is defined using the unphysical spacetime $(\bar{M}, \bar{g})$. The future event horizon is $\mathcal{H}^+ = \dot{\mathcal{B}}$ (the boundary of $\mathcal{B}$ in M), equivalently $\mathcal{H}^+ = M \cap \dot{J}^-(\mathcal{I}^+)$. Similarly, the white hole region is $\mathcal{W} = M \backslash [M \cap J^+(\mathcal{I}^-)]$ and the past event horizon is $\mathcal{H}^- = \dot{\mathcal{W}} = M \cap \dot{J}^+(\mathcal{I}^-)$.*

One can make the above definition omitting the strong asymptotic predictability requirement without making any other changes. The reason we have included it is twofold. First, we need it for the discussion on the uniqueness theorems for stationary, asymptotically flat, four dimensional black hole spacetimes later, as most of the results that we quote assume strong asymptotic predictability. Second, if we were to not require it, then we would have to account for the possibility of *naked singularities*. These are singularities that are in causal contact with null infinity, or in other words - places where physics breaks down but information/light rays can still propagate to an observer from there - which is an indication of our theory failing to describe the real physics at play. Therefore, requiring strong asymptotic predictability is equivalent to demanding that we should be able to use General Relativity to predict everything that happens on and outside a black hole horizon, which is the region we have causal access to as observers outside of the black hole.

On the other hand, as we will see in the next sections, exact black hole solutions in General Relativity usually do contain singularities hidden behind their event horizons, thus inaccessible to observers in the exterior region - that is, to us. Furthermore, the celebrated singularity theorems [153, 145, 165] show us that in fact these are not artefacts of symmetry (as the black hole solutions we will look at below indeed possess a lot of symmetry), but are a generic feature of General Relativity and gravitational collapse [160, 40], in contrast to Newtonian gravity, where singularities form only in exact spherical symmetry and small perturbations or addition of angular momentum prevent that from happening [103]. What is more, there is a sizeable body of research since the publication of the singularity theorems, suggesting that gravitational collapse produces black holes instead of naked singularities. This has led people to conjecturing that in nature singularities will always be hidden by event horizons. This intuition has been turned into a conjecture - the *Weak Cosmic Censorship Conjecture* [146, 180] that we will discuss later. We should note that the conjecture and strong asymptotic

predictability are related. In particular, if the conjecture does not hold in a certain scenario (as it might be the case in dimensions higher than four), then it should be possible to form a naked singularity starting from well-behaved initial data (to be elaborated on later). This would most likely prevent the resulting spacetime from being strongly asymptotically predictable. Before we explore the Weak Cosmic Censorship Conjecture in more detail, we will present a few explicit examples of black hole spacetimes, starting with the first one to ever be written down.

1.2.2 Schwarzschild Black Hole

The first black hole solution to the Einstein equation (1.1) was written in 1916 by Schwarzschild [164]. It describes an asymptotically flat, spherically symmetric, non-rotating black hole with metric

$$ds^2 = -f(r)\,dt^2 + \frac{dr^2}{f(r)} + r^2\left(d\theta^2 + \sin^2\theta\,d\phi^2\right), \quad f(r) = 1 - \frac{2\,M}{r}. \tag{1.19}$$

It should be noted that the interpretation of the above metric as a black hole is valid when one considers it as an empty space solution of the Einstein equation (1.1) for all values of r. Otherwise the Schwarzschild solution describes the geometry outside of a spherical body of mass M for values of r greater than some radius $r_0 > 2\,M$, whereby the metric inside the body, for $r < r_0$, is determined by the stress-energy tensor of the matter making up the object. Here we will focus on the black hole case.

Regarding (1.19) as a solution of the vacuum Einstein equation (1.1) for all values of r immediately presents us with a problem: some of the components of the metric blow up for $r = 0$ and $r = 2\,M$. We could just remove these points from our manifold, but if we were to instead look at some scalar invariant of the Riemann curvature tensor - for example the *Kretschmann scalar*, $K = R_{abcd}R^{abcd}$ - then it is suggestive that $r = 2\,M$ is not a real physical singularity, but is simply a result of a bad choice of coordinates, as K does not blow up there. This also means that one should be able to find an extension of the manifold $\mathcal{M}$ with metric g, (1.19), to a larger manifold $\mathcal{M}'$ with an appropriate metric g' that will reduce to g on $\mathcal{M}$. This can be achieved via the introduction of a new radial variable (also called the tortoise coordinate)

$$dr^* = \frac{dr}{f(r)}, \tag{1.20}$$

and a transformation to ingoing Edington-Finkelstein (EF) coordinates, given by

$$v = t + r^*, \quad dt = dv - \frac{dr}{f(r)}. \tag{1.21}$$

The metric then takes the form

$$ds^2 = -f(r)dv^2 + 2\,dv\,dr + r^2\left(d\theta^2 + \sin^2\theta\,d\phi^2\right) \tag{1.22}$$

and one can check that it is invertible and its components are smooth functions of the radial variable r for $r > 0$. One can therefore extend the spacetime to the region $0 < r < 2\,M$ as a solution to the vacuum Einstein equation (1.1).

The above transformations can be inferred by looking at radial null geodesics in the Schwarzschild spacetime, and in particular, v is constant along ingoing such geodesics. Analogously, one can define outgoing EF coordinates with $u = t - r^*$, which is constant along outgoing radial null geodesics and a similar metric can be derived, which again allows for an extension to the region $0 < r < 2\,M$. This region, $0 < r < 2\,M$, is not the same as the one that follows from the ingoing transformation, as we will see further below.

On the other hand, the blow-up for $r = 0$ cannot be eliminated via a coordinate transformation, and thus it represents a true curvature singularity. Here the Kretschmann scalar diverges as well. Therefore, we must cut out $r = 0$ from the spacetime manifold because the metric is not defined there.

However, by looking at the behaviour of the tangent vector to future-directed causal curves in ingoing EF coordinates in the regions $0 < r \leq 2\,M$ and $r > 2\,M$, it can be shown that the former corresponds to our earlier definition of a black hole, while the latter is its exterior. Indeed, the curves that fall inside the $0 < r \leq 2M$ region are confined within, as they cannot escape to infinity - that is, to $r \to \infty$ - and in fact reach the $r = 0$ curvature singularity in finite affine parameter time. At the same time, there are future-directed causal curves that start out from places with $r > 2\,M$ and reach asymptotic infinity, where $r \to \infty$. Therefore, we see that it is impossible to send a signal from a point with $0 < r < 2\,M$ to another point with $r > 2\,M$ and in particular to the infinitely distant region, given by $r \to \infty$. Hence, in accordance with our definition for a black hole, we identify the region $0 < r \leq 2\,M$ in the Schwarzschild spacetime as a black hole. Its boundary, $r = 2\,M$, called the Schwarzschild radius, is where the *event horizon* of the black hole is located. The event horizon $r = 2\,M$ is a null surface which can be easily seen by looking at its normal dr in ingoing EF coordinates.

A similar exercise can be performed in outgoing EF coordinates[3], however, with a different conclusion: No signal can be sent from the $r > 2\,M$ region to a point with $r < 2\,M$. Furthermore, any causal curve starting with $r < 2\,M$ must cross the $r = 2\,M$ surface in finite affine parameter time. This is identified as a white hole - a region that cannot be accessed by a signal from infinity. It is the time-reverse of a black hole. To see this, change variables $v = -u$ in (1.22), which leads to the Schwarzschild metric written in outgoing EF coordinates.

The metric (1.19) describes a one parameter family of solutions labelled by M. The latter can take any real value, but here we focus on the positive $M > 0$ case and interpret it as mass. Negative values of M correspond to a spacetime without an event horizon, which possesses geodesics that can reach the $r = 0$ curvature singularity in finite affine parameter time - such a spacetime is referred to as geodesically incomplete. Therefore, one says that a naked singularity, one that can be observed, is present in the spacetime and it is deemed physically unrealistic.

As already mentioned, the Schwarzschild metric (1.19) is spherically symmetric - that is, the spacetime admits $SO(3)$ as a group of isometries, whereby there are spacelike two-surfaces ($(t,\, r)$ being constant in our coordinates) which are invariant under its action (the group orbits) and have constant positive curvature. Moreover, it possesses a hypersurface-orthogonal Killing vector field (KVF), which is timelike for $r > 2\,M$, implying that the exterior $r > 2\,M$ of the Schwarzschild solution is static. In fact, staticity in the exterior follows from spherical symmetry. This is due to Birkhoff's theorem (a proof can be found in [103]):

Theorem 2 (Birkhoff's theorem)**.** *Any C^2 solution of the vacuum Einstein equation, which is spherically symmetric in an open set V, is locally equivalent to part of the maximally extended Schwarzschild solution in V.*

In particular, this implies that the spacetime outside any spherical object in empty space, even if the body's interior itself is time-dependent, is described by the exterior Schwarzschild solution.

The ingoing and outgoing EF coordinates provide access to two different regions in the spacetime. In addition, Birkhoff's theorem makes use of the term *maximally extended*, which has not been defined yet, and we have already used the concept of extending a spacetime a few times, hence it is now time to introduce the following:

Definition 13. *A spacetime (M, g) is **extendible** if it is isometric to a proper subset of another spacetime (M', g'). The latter is called an extension of (M, g).*

[3]Recall that the $0 < r \leq 2\,M$ regions in ingoing and outgoing EF coordinates are not the same.

We can now talk about the maximal analytic extension of the Schwarzschild spacetime - the Kruskal spacetime. First, we introduce double null coordinates (u, v, θ, ϕ) via

$$v = t + r^*, \quad u = t - r^*, \tag{1.23}$$

which we then transform into Kruskal-Szekeres coordinates with the help of

$$U = -e^{-u/(4\,M)}, \quad V = e^{v/(4\,M)}, \tag{1.24}$$

whereby $U < 0$, $V > 0$ and

$$U\,V = -e^{r/(2\,M)}\left(\frac{r}{2\,M} - 1\right), \tag{1.25}$$

which is a monotonic function of r, providing us with an equation that determines r as a function of U and V uniquely. Similarly for t through

$$\frac{V}{U} = -e^{t/(2\,M)}. \tag{1.26}$$

The resulting metric is given by

$$ds^2 = -\frac{32\,M^3 e^{-r(U,V)/(2\,M)}}{r(U,V)} dU\,dV + r(U,V)^2\left(d\theta^2 + \sin^2\theta\,d\phi^2\right). \tag{1.27}$$

Analogously to what we did for the metric in ingoing EF coordinates (1.22), the above metric can be analytically extended (non-vanishing determinant and smooth metric components) through the surfaces $U = 0$ and $V = 0$, to the regions where $U > 0$ and $V < 0$. This can be seen on the *Kruskal diagram* (1.4) of Schwarzschild spacetime, which represents its maximal analytic extension.

As seen in Fig. (1.4), and evident from (1.25), the event horizon, $r = 2\,M$, corresponds to two null surfaces, $U = 0$ and $V = 0$, that intersect at $U = V = 0$ (the bifurcation 2-sphere B). Similarly, the curvature singularity at $r = 0$, given by $U\,V = 1$ is a hyperbola with two branches. The diagram has four regions. The exterior, $r > 2\,M$, of the Schwarzschild solution, where we started, is region I. The black hole is in region II. The ingoing EF coordinates that we used to infer its existence cover regions I and II. Region III is the white hole. Analogously, outgoing EF coordinates cover regions I and III. Region IV, on the other hand, is new to us. There we have $r > 2\,M$ hence it also represents the exterior of a spherical body of mass M, given by the Schwarzschild solution (1.19). It is isometric to region I, which can be seen by changing $(U, V) \to (-U, -V)$, implying that it is also asymptotically flat. An observer

Figure 1.4 Kruskal diagram of Schwarzschild spacetime. Radial null geodesics are lines of constant U or V, that is 45° lines. Region I is the exterior ($r > 2\,M$) where we started. II is the black hole, while III is the white hole. IV is a new asymptotically flat region, isometric to region I, but causally disconnected from it.

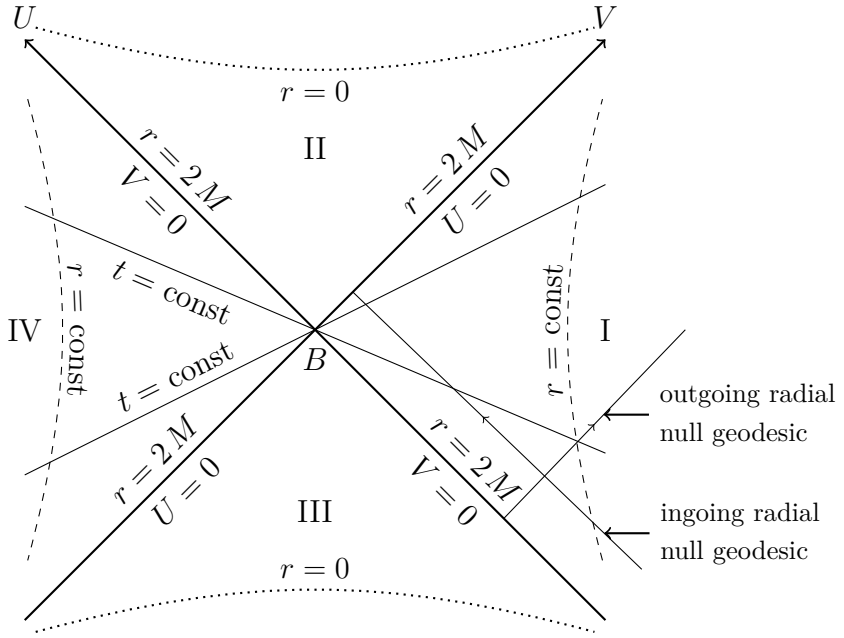

in region IV cannot send a signal to an observer in region I, as that will involve faster than light travel. Communication is only possible if they were to both fall into the black hole (unfortunately also leading to them eventually hitting the singularity at $r = 0$).

Not all of the Kruskal diagram is physical. In particular, if we were to look at the spacetime resulting from spherical gravitational collapse, then we would be left with regions I and II and a timelike curve through them that traces the surface of the collapsing star. The interior of the star (to the left of the timelike curve) will be described by a different non-vacuum metric, and in particular, $r = 0$ will be smooth.

We can also construct a Penrose diagram for the Kruskal spacetime. The required derivation will not be presented here, but to compactify the spacetime one can take

$$\tilde{v} = \arctan \frac{V}{\sqrt{2\,M}}, \quad \tilde{u} = \arctan \frac{U}{\sqrt{2\,M}}. \tag{1.28}$$

The Kruskal spacetime contains two asymptotically flat regions, which by the definition of the latter will look like infinity in Minkowski. Moreover, both diagrams depict null curves as straight lines tilted at 45°. The crucial difference is that on a Penrose diagram asymptotic infinity is brought to a finite distance, which also represents the boundary of the digram. Therefore, it should be possible to deduce what the Penrose diagram looks like and it is given in Fig. (1.5).

The Penrose diagram makes it very easy to see that the $t =$ constant surface that we have drawn is a Cauchy surface for the maximally-extended Schwarzschild spacetime, implying that the latter is globally hyperbolic.

We conclude this, by no means complete, introduction to the Schwarzschild spacetime with a small note. The curvature singularity at $r = 0$ inside region II, where tidal forces diverge, is not a place, but rather a "time". It lies to the future of any other point on the diagram. This can also be understood by noting that for $r < 2\,M$, t and r swap their roles as time and radial coordinates, respectively. To infer this, one could take the ingoing EF metric (1.22) inside region II and switch back to Schwarzschild coordinates (t, r, θ, ϕ). This recovers (1.19) but with $r < 2\,M$.

1.2.3 Kerr Black Hole

The Schwarzschild solution is a special, $a = 0$, case of a broader class of solutions to the Einstein equation (1.1) - the Kerr spacetime [127]. The latter represents the gravitational field outside a stationary, axisymmetric, asymptotically flat, massive and rotating body, with a small caveat. Unlike in the case of Schwarzschild, the Kerr metric

Figure 1.5 Penrose diagram of the Kruskal spacetime

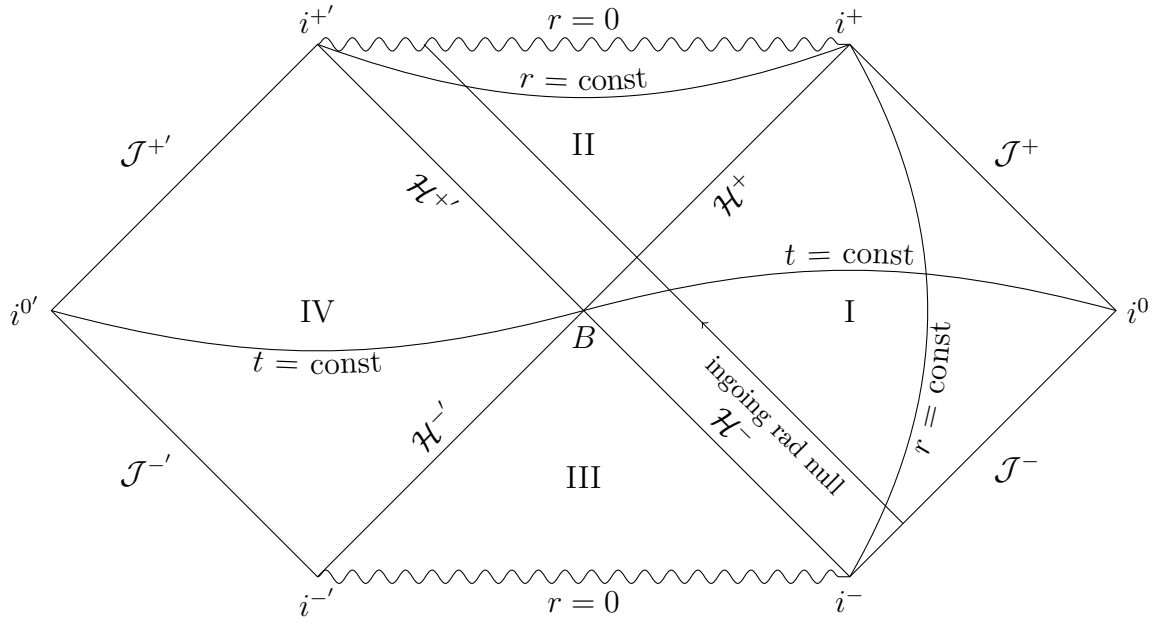

does not represent the spacetime outside any object with the previously enumerated properties, rather it corresponds to a body with a specific combination of multipolar modes. What we will discuss later is that the Kerr metric is the unique exterior solution of the said kind when the object under consideration is a black hole. It is given, in Boyer–Lindquist (BL) coordinates, by

$$ds^2 = -\frac{\Delta}{\Sigma^2}\left(dt - a\sin^2\theta d\phi\right)^2 + \frac{\sin^2\theta}{\Sigma^2}[a\,dt - (r^2+a^2)d\phi]^2 + \Sigma\left(d\theta^2 + \frac{dr^2}{\Delta}\right), \quad (1.29)$$

where

$$\Sigma = r^2 + a^2\cos^2\theta, \quad \Delta = r^2 - 2\,M\,r + a^2, \quad (1.30)$$

and M is the mass of the black hole, whereas $J = a\,M$ is its angular momentum. The metric is symmetric under the transformation $t \to -t$ and $\phi \to -\phi$ (time inverting a rotating body makes it spin in the opposite direction), which combined with the fact that $\phi \to -\phi$ is equivalent to $a \to -a$ implies we can take $a \geq 0$ without loss of generality. As already mentioned, it can be shown that the Kerr spacetime is asymptotically flat and for $a = 0$ it reduces to the Schwarzschild metric (1.19). In the infinitely far away region, the coordinates (t, r, θ, ϕ) reduce to the normal spherical polars in flat space, implying that (θ, ϕ) are the usual angles of a 2-sphere, hence $\theta \in (0, \pi)$ and ϕ has period of $2\,\pi$.

The spacetime possesses two commuting KVFs, stationary and axisymmetric,

$$k^a = (\partial_t)^a\,, \quad m^a = (\partial_\phi)^a\,. \tag{1.31}$$

k^a is not globally timelike, but is timelike near infinity and outside the so called *ergoregion* that we will discuss in a moment. For $a^2 > M^2$ there is in fact no black hole event horizon and only a "naked" curvature singularity at $\Sigma = 0$ ($r = 0$ and $\theta = \pi/2$). We will therefore assume that $M^2 \geq a^2$. The function Δ can then also be written as

$$\Delta = (r - r_+)(r - r_-), \quad r_\pm = M \pm \sqrt{M^2 - a^2}, \tag{1.32}$$

whereby $r_\pm$ are coordinate singularities and the locations of the event and Cauchy horizons (to be defined further below) respectively. To see that the metric can in fact be extended through these locations, we can use coordinates analogous to the ingoing/outgoing EF coordinates for Schwarzschild. These are called Kerr coordinates and for the ingoing case they are given by

$$dv = dt + \frac{r^2 + a^2}{\Delta} dr, \quad d\chi = d\phi + \frac{a}{\Delta} dr, \tag{1.33}$$

while the outgoing version has minus signs in front of the dr terms. The transformations can again be inferred by looking at ingoing radial null geodesics in the original BL coordinates. The transformed metric is

$$\begin{aligned} ds^2 = &-\frac{(\Delta - a^2 \sin^2\theta)}{\Sigma} dv^2 + 2\, dv\, dr - 2\, a\, \sin^2\theta \frac{(r^2 + a^2 - \Delta)}{\Sigma} dv\, d\chi \\ &- 2\, a\, \sin^2\theta\, d\chi\, dr + \left(\frac{(r^2 + a^2)^2 - \Delta\, a^2 \sin^2\theta}{\Sigma} \right) \sin^2\theta\, d\chi^2 + \Sigma\, d\theta^2, \end{aligned} \tag{1.34}$$

and it is smooth and non-degenerate at $r_\pm$, hence it can be analytically extended through these surfaces to the region $0 < r < r_+$, which for the ingoing case is a black hole, whereas for the outgoing one is a white hole. Note that $r = 0$ ($\Sigma = 0$ with $\theta = \pi/2$) is again a curvature singularity. However, unlike in Schwarzschild, it is not a point, but rather a ring. Although this is not straightforward to see and the full calculation will not be shown here, the idea is to transform from (1.29) to Kerr-Schild Cartesian coordinates via

$$x + i\, y = (r - i\, a) e^{i\,\phi} \sin\theta, \quad z = r\, \cos\theta, \tag{1.35}$$

where it is useful to note that

$$\frac{x^2+y^2}{r^2+a^2}+\frac{z^2}{r^2}=1, \tag{1.36}$$

which comes from the implicit definition of r in terms of x, y and z. Then the equation for the singularity at $r=0$ transforms into $x^2+y^2=a^2$, with $z=0$, which is a circle.

Obtaining the maximal analytic extension of the Kerr spacetime is slightly more complicated than for Schwarzschild, but the guiding principle is similar. As before, one starts by introducing double null variables via the ingoing and outgoing Kerr transformations, and then defines Kruskal-like coordinates that reveal a spacetime consisting of four regions separated by two intersecting null hypersurfaces: a black hole, a white hole, and two asymptotically flat exteriors. This time, however, there are no curvature singularities in the black (II) and white (III) hole regions, as from the ingoing and outgoing Kerr coordinates we know that we can extend the spacetime past the surfaces at $r=r_-$, which are the boundaries of these regions. In particular it can be shown that radial null geodesics will reach $r=r_-$ inside the black hole region in finite time. To access the regions across that surface we start from the ingoing Kerr metric (1.34) inside region II and invert back to BL coordinates, which gives us back the original metric (1.29), but for $r_-<r<r_+$. We can then switch to double null and then to Kruskal-like coordinates as before. The latter can then be extended analytically across the $r=r_-$ surface revealing another two regions (V and VI) that contain the $\Sigma=0$ ring singularity, which is now timelike and not spacelike as for Schwarzschild (it is only in the region between the two horizons $r_-<r<r_+$ that time and space interchange roles). To be specific, it is possible for a future-directed timelike curves going through region V (or VI) to avoid the singularity all together and, continue onwards, and emerge into a new region, which is isometric to the white hole region III. At this stage one realises that the maximal analytic extension is actually going to consists of infinite number of regions. By defining outgoing and then Kruskal-like coordinates in this new, isometric to the white hole region, it becomes clear that there are further regions isometric to the two asymptotically flat regions I and IV. This procedure can be continued indefinitely in both "up" and "down" directions.

The final part of the maximal analytic extension puzzle has to do with the ring singularity at $r=0$. Curvature invariants like the Kretschmann scalar diverge only on the ring itself and are finite on the disc bounded by it, given by $x^2+y^2<a^2$, $z=0$. It is then possible to analytically extended the radial coordinate to negative values through the disc. This is not as straightforward as the previous extensions, however

the main idea is to take two copies of the manifold and glue them together at the disc. One then identifies the top side (as approaching from positive z) of the disc of one manifold with the bottom side (as approaching from negative z) of the disc of the other manifold and vice-versa. At large negative values of r (after passing through the disc bounded by the ring singularity) the spacetime is asymptotically flat, but with negative mass. Furthermore, for small negative values of r and for $\theta \sim \pi/2$, we have $g_{\phi\phi} < 0$, implying that ∂_ϕ becomes timelike. However, we know that for asymptotic flatness to hold at $r \to \infty$, ϕ must be periodically identified, meaning that the orbits of ∂_ϕ must be closed. This leads to the existence of closed timelike curves near the ring singularity. These are, of course, not visible to observers outside the black hole region II.

A diagram presenting the above-described structure is given in Fig. (1.6). It should be mentioned that this is not exactly a Penrose diagram in the sense that we defined for Schwarzschild, as the Kerr solution is not spherically symmetric, so it is not possible to identify every point with a 2-sphere. Nevertheless, considering the submanifold obtained by restricting to the axis of axisymmetry, $\theta = 0$ or $\theta = \pi$, one can draw the diagram we have presented, whereby each point is a circle.

A small, but important note before moving on: in the case of $a = M$, we have an *extremal* Kerr black hole. The event horizon becomes degenerate - the locations of the inner and outer horizons coincide, $r_+ = r_-$. There is no region II anymore, rather we have an infinite sequence of regions I and V, the latter also being the black hole, and some of the properties of extremal black holes do differ from those of subextremal ones. Neverthless, in this work we are focussed on the latter, thus will refrain from providing more information on the former.

Going back to the ring singularity - due to its timelike nature we cannot find a Cauchy surface for this spacetime. However, the $t =$ constant surface drawn in Fig. (1.6) is a Cauchy surface for regions I, II and IV. On the other hand, in the future of region V (and VI) there are past-directed inextendible causal curves that approach the singularity, but do not intersect the inner horizon, $r = r_-$. The latter is therefore called the future Cauchy horizon for the surface $t =$ constant that we have drawn. These are defined in the following way:

Definition 14. *The* ***future Cauchy horizon*** *of a partial Cauchy surface* Σ *is* $H^+(\Sigma) = \overline{D^+(\Sigma)} \backslash I^-(D^+(\Sigma))$. *Similarly for the* ***past Cauchy horizon*** $H^-(\Sigma)$.

The implication of the above is that the solution to the Einstein equation is not uniquely determined by initial data on our $t =$ constant surface beyond the Cauchy horizon. The extension we have presented is still the unique locally inextendible

Figure 1.6 Maximal analytic extension of the Kerr spacetime

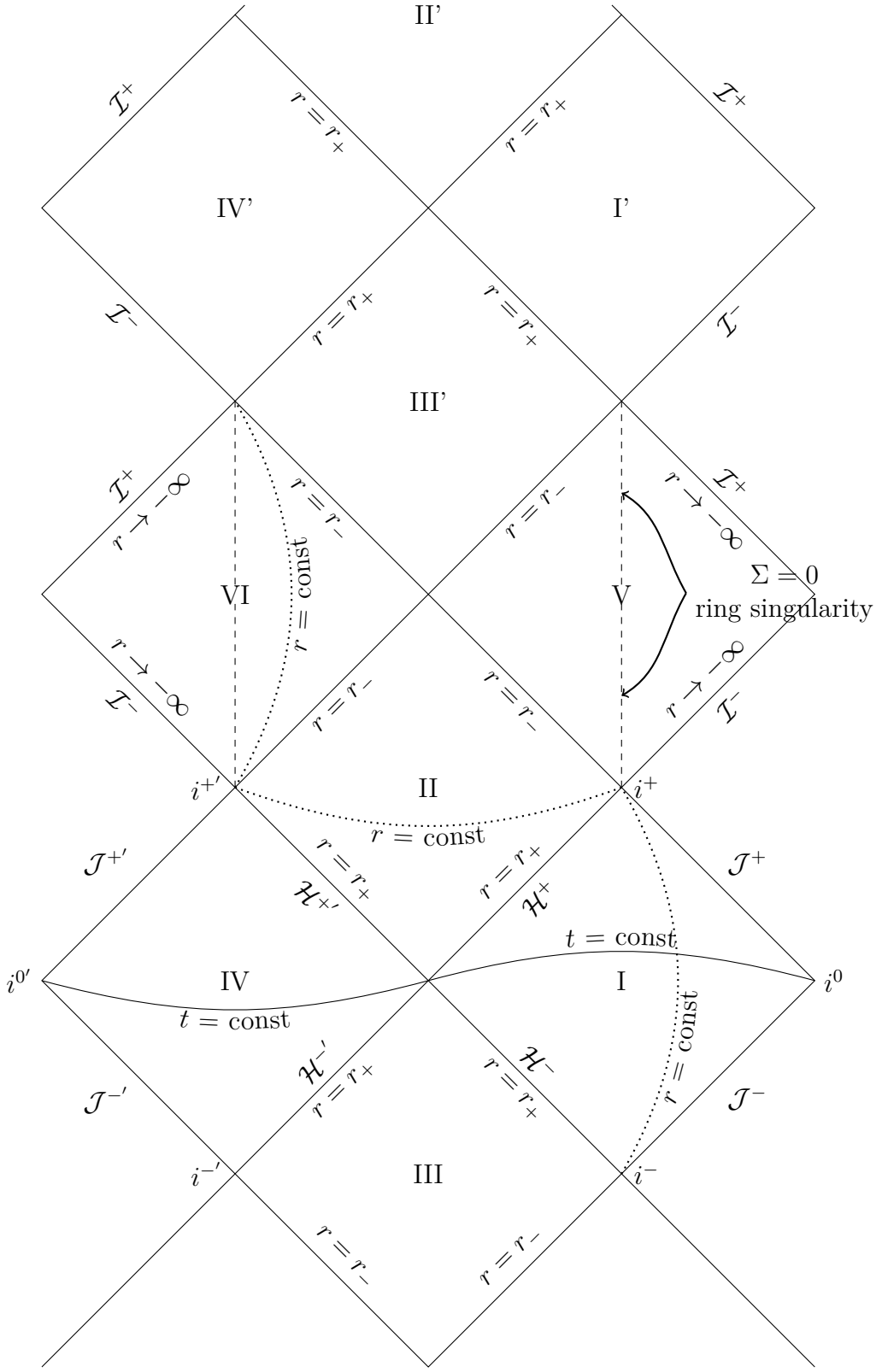

analytic continuation, but beyond the Cauchy horizon at $r = r_-$ there are other possible non-analytic extensions that satisfy the Einstein equation.

The above implies that beyond the Cauchy horizon one would lose the ability to uniquely make predictions about the future based on initial data solely, which is not the behaviour one would want from a physical theory. This issue is addressed by the so called Strong Cosmic Censorship [149, 42, 49, 52, 50, 43], which is still an active area of research in General Relativity. We are not going to delve into the rigorous mathematical results derived on the subject, but there is a simple heuristic argument that one can make which points to a possible resolution. If one considers an observer falling in through the outer horizon, $r = r_+$, into the black hole, they are then drawn to the Cauchy surface $r = r_-$. On approaching the latter, they would see the whole history of the asymptotically flat region (I or IV) that they fell in from, in finite time, implying that they will receive an infinite number of signals from all the objects in the exterior region as the latter approach future timelike infinity i^+. This will result in infinite amounts of energy accumulating at the Cauchy horizon (infinite blue-shift). This suggests that the Cauchy horizons might be unstable to small perturbations in the initial data on the spacelike surface $t = \text{const}$. One would then hope that this instability would lead to a strong enough blow-up at the $r = r_-$ surfaces, which would make it impossible to extend the solution to the initial value problem past the Cauchy horizons.

The event horizon $\mathcal{H}^+$ is, of course, a null hypersurface. Its normal is

$$\xi_a = k_a + \Omega_H \, m_a, \tag{1.37}$$

where

$$\Omega_H = \frac{a}{r_+^2 + a^2}. \tag{1.38}$$

ξ^a is a linear combination of KVFs, hence itself a KVF and is tangent to the generators of $\mathcal{H}^+$. Furthermore, in BL coordinates one can show that on integral curves of ξ^a, we have $\phi = \Omega_H \, t+ \text{const}$. Combining this with the fact that $\phi = \text{constant}$ on orbits of $k = \partial_t$, it becomes clear that particles on orbits of ξ^a rotate with angular velocity Ω_H with respect to stationary observers. Moreover, since ξ^a are the null generators of the event horizon $\mathcal{H}^+$, this implies that these generators will rotate with angular velocity Ω_H with respect to a stationary observer at infinity, thus leading us to the identification of Ω_H as the angular velocity of the black hole.

Another feature of the Kerr spacetime that differentiates it from its spherically symmetric counterparts (Schwarzschild and Reissner-Nordström) is the existence of

the so called ergosphere. To find it we look at the norm of the timelike KVF in BL coordinates

$$k^2 = g_{tt} = -\frac{(\Delta - a^2 \sin^2\theta)}{\Sigma} = -\left(1 - \frac{2\,M\,r}{r^2 + a^2\cos^2\theta}\right). \tag{1.39}$$

We see that the RHS becomes positive when $r^2 - 2\,M\,r + a^2 < 0$, and in this case, k^a is no longer timelike but is instead spacelike. The boundaries of this region are given by

$$r^{\pm}_{erg} = M \pm \sqrt{M^2 - a^2\cos^2\theta}. \tag{1.40}$$

In particular note that

$$r^{-}_{erg} \leq r_- < r_+ \leq r^{+}_{erg}, \tag{1.41}$$

with the equalities only being satisfied at the poles $\theta = 0$ and $\theta = \pi$. The points given by $r^{\pm}_{erg}$, where k^a changes character, are also known as stationary limit points. The region between them is usually referred to as the ergoregion, and more often than not, the space between the outer horizon $\mathcal{H}^+$ and the outer stationary limit point, r^{+}_{erg}, is defined as the ergosphere, with its outer boundary at r^{+}_{erg} being the ergosurface.

The timelike KVF k^a becoming spacelike inside the ergosphere implies that stationary observers can no longer remain as such, as they will have to move faster than light in order to follow an orbit of the KVF. One proper way of seeing this is by looking at the norm of u^a - the tangent vector to a timelike curve - that is, we consider $g_{\mu\nu}\,u^\mu\,u^\nu < 0$. Carrying this out in BL coordinates quickly shows us that the only non-positive term on the LHS is $g_{t\,\phi}\,u^t\,u^\phi$. Moreover, one can show that $\nabla^a\,t$ is past-directed and timelike inside the ergosphere, hence

$$u^t = \frac{dt}{d\tau} = g_{ab}\,u^a\,\nabla^b\,t > 0, \tag{1.42}$$

which, together with $g_{t\phi} < 0$ inside the ergosphere, leads to the condition

$$\frac{d\phi}{d\tau} > 0. \tag{1.43}$$

This is the statement that any timelike curve inside the ergosphere must rotate in the same direction as the black hole and thus cannot remain at rest.

1.2.4 Energy extraction from black holes: Penrose process

The fact that the KVF $k^a = (\partial_t)^a$, which is timelike near infinity, becomes spacelike inside the ergoregion gives rise to a interesting phenomenon - the Penrose process [146, 148]. The idea is that a particle with 4-momentum $p^a = m\,u^a$, where m is its rest mass and u^a is its 4-velocity, possesses a conserved quantity along its geodesic according to a stationary observer at infinity - namely the energy defined as

$$E = -k \cdot p. \tag{1.44}$$

However, this energy can be negative inside the ergoregion, where k is spacelike. Therefore, one can imagine setting up an experiment in which a particle with negative energy falls through the event horizon, which due to the equivalence principles, allows us to extract energy from the black hole. One way of achieving this is by considering an infalling particle with energy

$$E_0 = -k^a\, p_a^0, \tag{1.45}$$

which we arrange to decay inside the ergosphere into two other particles with 4-momenta p_1 and p_2. The equivalence principle allows us to apply Special Relativity in the local inertial frame of the decaying initial particle, leading to the conservation of the 4-momentum, expressed as

$$p_0^a = p_1^a + p_2^a, \quad \text{hence} \quad E_0 = E_1 + E_2. \tag{1.46}$$

As already mentioned, one of the product particles can be arranged to have negative energy inside the ergosphere

$$E_1 < 0, \tag{1.47}$$

hence provided that the other particle can reach us back at infinity, we will have extracted energy from the black hole

$$E_2 = E_0 + |E_1| > E_0. \tag{1.48}$$

It can, in fact, be shown that indeed the particle with negative energy has to fall inside the black hole, whereas the other one can escape to infinity via geodesic motion.

One can then ask whether it is possible to completely drain the black hole of all its energy this way. To get an intuition about it we look at the horizon generator KVF

$\xi_a = k_a + \Omega_H\, m_a$. It is future-directed, hence one can easily see that

$$0 > p_a\, \xi^a = p_a(k^a + \Omega_H\, m^a) = -E + \Omega_H\, L, \tag{1.49}$$

where $L = p_a\, m^a$ is the angular momentum of the particle along its geodesic and the above inequality results in

$$L < \frac{E}{\Omega_H}. \tag{1.50}$$

For the particle with negative energy that falls inside the black hole, we therefore see that its angular momentum will also be negative, opposite to that of the black hole. As a result the Penrose process will gradually spin down the black hole until it stops rotating, at which point the ergoregion will have vanished, and it will not be possible to carry out the process any more.

If we assume that the black hole settles down to a different member of the Kerr family after the particle with negative energy has been absorbed, then the change in its parameters should be given by

$$\delta M = E, \quad \delta J = L, \tag{1.51}$$

which together with (1.50) results in

$$\delta J < \frac{\delta M}{\Omega_H}. \tag{1.52}$$

Christodolou showed [38] that the above is equivalent to

$$\delta M_{\text{irr}} > 0, \quad \text{with} \quad M_{\text{irr}}^2 = \frac{1}{2}\Big[M^2 + \sqrt{M^4 - J^2}\Big], \tag{1.53}$$

where M_{irr} is the irreducible mass, called so because inverting its definition leads to

$$M^2 = M_{\text{irr}}^2 + \frac{J^2}{4\, M_{\text{irr}}^2} \geq M_{\text{irr}}^2. \tag{1.54}$$

This tells us that the mass of the black hole cannot be reduced below the initial value of M_{irr} via the process described above. The condition $\delta M_{\text{irr}} > 0$ can also be derived from the area theorem, as we will see later. It is then easy to see that the maximum amount of energy we can extract from a Kerr black hole (corresponding to its rotational energy) is simply $M_0 - M_{\text{irr}}(M_0,\, J_0)$. With some algebra, one can show that this is largest for an extremal black hole $M_0 = J_0$ and the extracted amount is $(1 - 1/\sqrt{2}) \approx 29\%$.

In theory, one does not need a black hole horizon to carry out the Penrose process [25] - the presence of an ergoregion is sufficient - and in particular, it is possible for very compact spinning objects, like neutron stars, to also posses an ergoregion. However, as far as our understanding goes [163], we do not expect realistic neutron stars to be able to develop an ergoregion. Even if that was not a problem, the process itself requires timing the decay or a breakdown of a relativistic particle very accurately, thus it is not considered a very practical way of producing energy.

Before proceeding with a discussion of another way of extracting energy from black holes - superradiance, which is also a main ingredient in the later chapters of this thesis, and in fact a large and active field of research, we will present the reason why Kerr black holes are so important to us from a physical and mathematical perspective - namely the uniqueness theorems.

1.2.5 Uniqueness theorems

Kerr black holes are the only stationary, vacuum, black hole solution of the Einstein equation in four, asymptotically flat dimensions that is explicitly known. Moreover, when a black hole forms through gravitational collapse or the merger of two black holes/neutron stars, energy and matter either fall inwards through the event horizon, becoming inaccessible to an outside observer, or get radiated to infinity in the form of gravitational waves. Even if the details of these dynamical processes outside the black hole horizon could be very complicated, we expect that after sufficient amount of time has passed, the exterior of the black hole will reach a stationary state. Therefore, it seems desirable for one to try to explore the phase space of possible stationary, vacuum, black hole solutions to the Einstein equation.

Even though the Kerr black hole represents a two-parameter family of solutions, whose infinite set of multiple moments are unambiguously related to its mass and angular momentum, in a series of remarkable results in the 70s and 80s, it was in fact proven that the Kerr black hole is the unique stationary, vacuum, black hole solution under certain, physically reasonable assumptions that we will detail in what follows [103, 179, 156, 45].

To begin our discussion we will consider spacetimes $(\mathcal{M}, g)$ which are strongly asymptotically predictable with a Cauchy surface Σ for $\bar{V}$, as given in Definition (11), which contain a black hole, and possess an isometry, $\Theta : \mathcal{M} \to \mathcal{M}$, whose KVF, k^a, is timelike in the neighbourhood of $\mathcal{I}^+$ and $\mathcal{I}^-$. Furthermore, we will assume that the spacetime is either empty or the fields within it obey hyperbolic equations and satisfy the dominant energy condition: $-T^a{}_b\, X^b$ is a future-directed causal vector, for

all future-directed timelike vectors X^a. The last condition is necessary since, even if we expect all massive matter, part of the collapse, to eventually fall through the horizon, it is still possible that long range fields - like the electromagnetic field - would still be present in the end. In fact, everything we say here has been generalised to the case of Einstein-Maxwell theory [123, 31, 141], where the Kerr family of solutions extends to the so called Kerr-Newman black holes, which have two more parameters - electric and magnetic charge. As one does not expect large imbalances of charge to be present anywhere in the Universe, here we will concentrate on the more astrophysically relevant Kerr black holes. Two small notes are in order: first, we do not assume at this stage that the solutions are time reversible as there is nothing to indicate otherwise in our setup. We are interested in the final state in the far future, when the system has reached a stationary state. Second, we are looking at the case of a single, connected horizon. The question of multi-horizons is still an open problem [45].

Given a black hole spacetime and an isometry, the former must be invariant under the latter, implying that the corresponding KVF, k^a, must be tangent to the horizon generators, which in turn means that it must be spacelike or null on the horizon. This leaves us with three possible cases.

First, the stationary KVF is causal everywhere, thus forcing it to be null on the horizon. In this case it has been proven that the spacetime must, in fact, be static [103, 171, 172]. This setup was investigated by Israel [122] with the conclusion that the only solution is Schwarzschild [4].

The second possibility is that an ergoregion, where the timelike KVF becomes spacelike, is present, but does not connect to the event horizon, thus making k^a null there once again. This situation can be ruled out by a heuristic argument [103] which we will shortly summarise. As seen in the previous subsection, the existence of an ergoregion allows us to extract energy from the black hole via the Penrose process. However, for an ergoregion disjoint from the black hole (not touching the event horizon), it would not be possible for the negative energy particle to plunge into the horizon and hence it will have to remain inside the ergoregion. Now, one can keep repeating the Penrose process, gradually extracting energy from the black hole. Nevertheless, eventually something has to give - that is, the ergoregion must intersect the horizon or altogether vanish (resulting in a static spacetime), as otherwise we will be able to extract an infinite amount of energy from a finite energy system. This suggests that

[4] This is different form Birkhoff's theorem which starts from spherical symmetry in vacuum and obtains staticity as one of the results.

perhaps the initial setup will be subject to an instability and one should instead begin with an ergoregion that connects to the black hole horizon.

Therefore, the last case to consider is when an ergoregion exist and it intersects the black hole horizon. Then, k^a can be spacelike on the horizon (or a part of it). Assuming, in addition, that $(\mathcal{M}, g)$ is an analytic solution of Einstein's equation, one can prove the *rigidity theorem* [103, 44] - namely the existence of an additional one-parameter group of isometries near the horizon with a corresponding KVF, ξ^a, that commutes with the stationary ones and whose orbits coincides with the null geodesic generators of the event horizon. This construction can be extended to the whole exterior and then used to create a linear combination, together with k^a, which defines another KVF, m^a, with closed, periodic orbits and an axis of rotation - that is, an axisymmetric KVF. This is the point in the chain of arguments presented by the uniqueness theorems where, in a perfect world, one would like to drop the assumption of analyticity, since it is not very realistic, as that would mean the spacetime is fully determined by the neighbourhood of a single point. This has not been achieved yet [45].

At this stage one can either assume analyticity or take axisymmetry for granted, as all the stars we have observed are rotating, and angular momentum cannot just vanish. Thus one arrives at the result established by Carter [30] and Robinson [155]:

Theorem 3 (Axisymmetric uniqueness theorem, Carter, Robinson)**.** *If $(\mathcal{M}, g)$ is a stationary, axisymmetric, asymptotically flat, vacuum spacetime suitably regular on, and outside, a connected event horizon, then $(\mathcal{M}, g)$ is a member of the 2-parameter family of Kerr solutions, characterised by mass M and angular momentum J.*

It should be emphasised that we have only mentioned some of the main results along the way of deriving the above theorem and there is much that we have omitted. Another important ingredient is the topology theorem [103, 46, 92] which establishes that in four, asymptotically flat dimensions the intersection of a stationary black hole with a Cauchy surface must have an S^2 topology. For a detailed review of the history of the uniqueness theorems, references and current and future avenues of exploration on the topic see [156, 45].

We will talk more about the uniqueness theorems at the beginning of chapter (3.1), when we look at ways of avoiding them and what this leads to.

1.2.6 Energy extraction from black holes: Superradiance

The Penrose process is not the only way of extracting energy from a Kerr black hole. One can also resort to superradiant scattering. In black hole physics, one example

of superradiance is exhibited when a scalar, electromagnetic or gravitational wave is incident upon a Kerr black hole with the right condition being met. This is given by

$$0 < \mathrm{Re}\,(\omega) < m\,\Omega_H, \tag{1.55}$$

whereby we have decomposed the field[5] according to the symmetries of the background spacetime

$$\psi(t, r, \theta, \phi) = \mathrm{Re}\left[\tilde{\psi}(r, \theta)\, e^{-i\,\omega\, t}\, e^{i\, m\, \phi}\right], \tag{1.56}$$

where ω is a frequency, possibly complex, and m - an integer - the azimuthal quantum number. In a manner similar to what happens in the Penrose process - part of the incoming wave - the transmitted wave - will be absorbed by the black hole and another part will be reflected back and escape to infinity. Given that the above condition is satisfied, then the transmitted wave will transfer negative energy to the black hole, implying that the wave arriving at infinity will have a higher amplitude than the initial incident one. There are various ways to illustrate this, but for simplicity we will consider the example of a perturbing massless real scalar on a Kerr background. Its stress tensor is given by

$$T_{ab} = \nabla_a\psi\, \nabla_b\psi - \frac{1}{2} g_{ab}\, \nabla^c\psi\, \nabla_c\psi. \tag{1.57}$$

Now, consider two spacelike surfaces Σ and Σ' inside the spacetime, both stretching from i^0 to $\mathcal{H}^+$, with Σ' being entirely to the future of Σ. Furthermore, define H and H' as the intersections of Σ and Σ' with the future event horizon $\mathcal{H}^+$, and take $\mathcal{N}$ to be the part of $\mathcal{H}^+$ from H to H'. Moreover, as Kerr is a stationary spacetime, the total energy of matter on a spacelike hypersurface can be defined naturally as

$$E(\Sigma) = -\int_\Sigma \star J, \tag{1.58}$$

where $J_a = -T_{ab}k^b$ is the conserved energy-momentum 4-vector, and k^b is a timelike KVF. Using this, it can be shown that

$$E(\Sigma') - E(\Sigma) = \int_{\mathcal{N}} \star J, \tag{1.59}$$

which gives an expression for the negative energy flux across the horizon (due to the minus sign in (1.58)), which is the difference between the energies of the two spacelike hypersurfaces.

[5] Here we are assuming a test field, so that the geometry is fixed to leading order in the perturbation.

We adopt the same decomposition for the field as already mentioned (1.56). We want to show that for $0 < \mathrm{Re}\,(\omega) < m\,\Omega_H$ the right hand side of equation (1.59) is positive. To this end, we take the Kerr metric in ingoing coordinates (1.34) and note that $\mathcal{N}$ is a three-dimensional manifold. Hence all that is required is

$$(\star J_{\nu\theta\chi})_{r=r_+} = \sqrt{-\det g}\,\epsilon_{\nu\theta\chi\mu}J^\mu = \sin\theta(r_+^2 + a^2)\xi^a J_a. \tag{1.60}$$

Henceforth, to determine the sign of (1.59), one just needs to look at $\xi^a J_a = -\xi^a T_{ab}k^b = -\xi^a\,\partial_a\psi\,\partial_b\psi\,k^b$, where the second term that would come from the given stress-energy tensor vanishes due to $\xi\cdot k = 0$ on $\mathcal{H}^+$ (ξ is the horizon generator). This leads to

$$\mathrm{Re}\,(\omega)\,(m\,\Omega_H - \mathrm{Re}\,(\omega)) > 0, \tag{1.61}$$

giving the condition $0 < \mathrm{Re}\,(\omega) < m\Omega_H$ for (1.59) to be positive, indicating that energy has been extracted from the Kerr black hole, while negative energy has been deposited.

Superradiance from Hawking's area theorem

A general argument for the existence of superradiant scattering can be derived by using Hawking's area theorem [104, 19] and the laws of black hole mechanics [16]. The first law states that for a rotating black hole

$$\delta M = \frac{\kappa}{8\pi}\delta A_H + \Omega_H\,\delta J, \tag{1.62}$$

which relates the change in mass and angular momentum, due to a linearised perturbation, to the change in the horizon area, δA_H. As before, we will consider the simplest case to work with - a scalar field - but the argument can be generalised to any electromagnetic or gravitational perturbation in a straightforward way. For the latter one can work with the effective stress-tensor for gravitational waves from linearised Gravity. The scalar's stress tensor is given, as before, by (1.57). In a stationary and axisymmetric spacetime, with corresponding Killing vector fields $k = \partial_t$ and $m = \partial_\phi$, one can identify the energy and angular momentum fluxes

$$\epsilon^\mu = -T^\mu{}_\nu\,k^\nu, \quad l^\mu = T^\mu{}_\nu\,m^\nu. \tag{1.63}$$

Therefore, by looking at the $T^r{}_t$ and $T^r{}_\phi$ components of the stress-energy tensor, corresponding to the net radial flux of energy and angular momentum through a spherical surface of fixed radius r, respectively (where we have taken the normal to be

pointing outwards), it is easy to show that the ratio of mass to angular momentum carried in the black hole by the wave results in

$$\frac{\delta M}{\delta J} = \frac{\mathrm{Re}\,(\omega)}{m}, \tag{1.64}$$

where, as before, the scalar field has been decomposed according to the isometries of the spacetime, $\psi(t, r, \theta, \phi) = \psi_0\,(r, \theta)\, e^{-i\,\omega\,t} e^{i\,m\,\phi}$. Plugging this result back in the first law (1.62) leads us to

$$\delta M = \frac{\mathrm{Re}\,(\omega)\,\kappa}{8\,\pi} \frac{\delta A_H}{(\mathrm{Re}\,(\omega) - m\,\Omega_H)}. \tag{1.65}$$

Consequently, referring to the second law of black hole mechanics, which informs us that classically

$$\delta A_H \geq 0, \tag{1.66}$$

for a field scattering off the black hole, given that it obeys the weak energy condition, it is straightforward to derive the fact that energy can be extracted from the black hole under the condition

$$\mathrm{Re}\,(\omega) < m\,\Omega_H. \tag{1.67}$$

Reasoning along exactly the same lines for a charged black hole, where the angular momentum is replaced by the electrostatic potential of the black hole, leads to the analogous conclusion that superradiant scattering appears under the condition that

$$\mathrm{Re}\,(\omega) < q\,\Phi, \tag{1.68}$$

where q is the charge of the scalar field and Φ the electrostatic potential difference between the horizon and infinity.

The above argument relies on the assumptions needed for the first and second laws of black holes mechanics, and in particular, requires that the matter obeys the weak energy condition. We also assumed that the matter waves are initially ingoing. As will be seen shortly, fermions do not scatter superradiantly and indeed their stress-energy tensor does not satisfy the weak energy condition. Moreover, although the above argument tells us that superradiant scattering is possible, it does not imply that it will indeed happen in a given spacetime.

No superradiant scattering for fermions in a Kerr background

An important point is to be made at this stage. All the fields mentioned above are bosonic, and this is not a coincidence. It has been proven that massless [177] and massive [124] (after the separation of the equations was achieved in [32]) Dirac fields do not exhibit superradiance on a Kerr background.

The absence of superradiance for fermions is a consequence of the properties of their stress-energy tensor, as already eluded to in the previous subsection, due to their inability to meet the requirements for the application of Hawking's area theorem, which can be used to argue for the existence of superradiance in certain situations. Proper treatment of the problem requires quantum field theory on a curved background, since fermions are not classical fields. Nevertheless, here we will look at the scattering of spin-$\frac{1}{2}$ waves off a Kerr black hole by working with the relativistic Dirac equation on curved space and treating the fields as classical. We only wish to calculate the reflection and transmission coefficients of the scattering process in order to determine the conditions (if any) for superradiance. To this end, we expand the field as an infinite sum of Fourier modes and carry out a standard mode analysis at infinity and near the event horizon so as to obtain the aforementioned coefficients. We are effectively dealing with infinitely many degrees of freedom - the Fourier coefficients in the mode expansion that have to be specified in an initial value formulation - thus we can motivate our approach as a semiclassical approximation for a large number of fermions. This is similar in spirit to the way one usually introduces quantum field theory of a free scalar by starting from a system of finitely many decoupled harmonic oscillators and extending to the case of infinitely many by writing the scalar field in a basis of plane waves for its Fourier components and eventually promoting the coefficients of its Fourier modes to operators in what is referred to as second quantisation.

We start with the separated equations as their derivation is an algebraically-involved process, but a detailed and rigorous discussion of the problem for both massless and massive fermions can be found in Chandrasekhar's book [33]. As before, we consider the field as a small perturbation to the geometry, which is thus fixed to leading order. The Dirac equation in a curved spacetime is given by

$$\gamma^{\mu}\,\nabla_{\mu}\,\psi + i\,\mu\,\psi = 0, \tag{1.69}$$

where $\left[\gamma^{\mu},\gamma^{\nu}\right] = 2\,g^{\mu\nu}$ are curved space Gamma matrices, constructed from the flat space ones in the Weyl representation (multiplied by i) using a Carter tetrad, and μ is the mass of the field. The covariant derivative is defined with respect to the spinor

affine connection [33]. The ansatz to achieve separability is given by

$$\psi = e^{-i\omega t}e^{im\phi}\left(\frac{S_-(\theta)\,R_-(r)}{\sqrt{2}\,\bar{\rho}},\frac{S_+(\theta)\,R_+(r)}{\sqrt{\Delta}},-\frac{S_-(\theta)\,R_+(r)}{\sqrt{\Delta}},-\frac{S_+(\theta)\,R_-(r)}{\sqrt{2}\,\rho}\right)^T, \quad (1.70)$$

with $\rho = r + i\,a\,\cos\theta$ and Δ as for the Kerr metric. $R_\pm(r)$ and $S_\pm(\theta)$ satisfy a system of second order, ordinary differential equations, coupled via the separation constant λ. These can be written in various forms depending on the notation used. Here we follow Chandrasekhar [33] (accounting for the differences in sign conventions):

$$\left[\Delta\,\mathcal{D}^\dagger_{\frac{1}{2}}\,\mathcal{D}_0 - \frac{i\,\mu\,\Delta}{\lambda + i\,\mu\,r}\mathcal{D}_0 - (\lambda^2 + \mu^2 r^2)\right]R_- = 0, \quad (1.71)$$

$$\left[\mathcal{L}_{\frac{1}{2}}\,\mathcal{L}^\dagger_{\frac{1}{2}} + \frac{a\,\mu\,\sin\theta}{\lambda + a\,\mu\cos\theta}\mathcal{L}^\dagger_{\frac{1}{2}} + (\lambda^2 - a^2\mu^2\cos^2\theta)\right]S_- = 0, \quad (1.72)$$

where the differential operators have been defined as

$$\mathcal{D}_n = \partial_r - \frac{i\,K}{\Delta} + 2\,n\,\frac{r-M}{\Delta}, \quad \mathcal{L}_n = \partial_\phi\theta + Q + n\,\cot\theta, \quad (1.73)$$

$$K = (r^2 + a^2)\omega - a\,m, \quad Q = -a\,\omega\sin\theta + m\,\csc\theta, \quad (1.74)$$

and the dagger operator acts as

$$\mathcal{D}^\dagger_n = \mathcal{D}^*_n, \quad \mathcal{L}^\dagger_n(\theta) = -\mathcal{L}^\dagger_n(\pi - \theta). \quad (1.75)$$

$\Delta^{\frac{1}{2}}R_+$ satisfies the complex-conjugate of the above radial equation, whereas the one for S_+ can be obtained by replacing θ with $\pi - \theta$ in the angular part. For massless Dirac fields one just needs to set $\mu = 0$ above. In order to arrive at the above system of equations, one first goes through an equivalent system of coupled first-order, ordinary differential equations, of which only the radial ones will be presented here. Thus, defining

$$P_+ = \Delta^{\frac{1}{2}}\,R_+, \quad P_- = R_-, \quad (1.76)$$

the radial equations are equivalently given by

$$\Delta^{\frac{1}{2}}\left[\frac{d}{dr} + i\,\frac{r^2+\alpha^2}{\Delta}\omega\right]P_+ = (\lambda - i\,\mu\,r)P_-, \quad (1.77)$$

$$\Delta^{\frac{1}{2}}\left[\frac{d}{dr} - i\,\frac{r^2+\alpha^2}{\Delta}\omega\right]P_- = (\lambda + i\,\mu\,r)P_+, \quad (1.78)$$

with $\alpha^2 = a^2 - (a\,m)/\omega$. From the given equations for $P_\pm$ one can derive that

$$\frac{d}{dr}\Big(|P_+|^2 - |P_-|^2\Big) = 0. \tag{1.79}$$

To see this, we multiply Eq. (1.77) by P_+^* on the right, and simplify the resulting equation with the help of the conjugate of (1.77) multiplied by P_+ on the left. Finally, we perform the equivalent operation for Eq. (1.78) and subtract the two resulting equations from each other. The reason this relation is helpful will become clear when one considers the conserved current associated to the Dirac equation, namely

$$J^\mu = \bar{\psi}\,\gamma^\mu\,\psi, \quad \nabla_\mu\, J^\mu = 0, \tag{1.80}$$

with the usual definition for the adjoint spinor $\bar{\psi} = \psi^\dagger\,\gamma^0$. $\sqrt{-g}\,J^t$ is the 'particle number density' and one can integrate the conservation equation to obtain the following equality, involving the 'particle number'[6] N,

$$\frac{\partial N}{\partial\, t} = -\int_0^{2\,\pi}\int_0^{\pi}\sqrt{-g}\,J^r\,d\theta\,d\phi = 2\,\pi(|P_+|^2 - |P_-|^2)\int_0^{\pi}(|S_+|^2 + |S_-|^2)\sin\theta\,d\theta, \tag{1.81}$$

where we have used $\sqrt{-g} = (r^2 + a^2\cos^2\theta)\sin\theta$, $J^r = -\frac{1}{\rho^2}(|P_+|^2 - |P_-|^2)(|S_+|^2 + |S_-|^2)$, and have taken the normal to the boundary of the $t =$ constant slice to be pointing inwards at the horizon. Since the angular eigenfunctions are orthogonal, without loss of generality, we can normalise them to unity (or sometimes $2\,\pi$, depending on conventions), which means that

$$\frac{\partial N}{\partial\, t} = 2\,\pi(|P_+|^2 - |P_-|^2) = \text{constant}, \tag{1.82}$$

where the second equality follows from (1.79). In fact, looking at the near-horizon behaviour of the $R_\pm$ eigenfunctions in (1.71) we see that

$$R_\pm \to\ A_\pm\,\Delta^{\frac{1\mp1}{4}}\exp\Big[-i(\omega - m\,\Omega_H)r^*\Big], \tag{1.83}$$

[6] There is no natural notion of particles in the context of quantum fields on a curved background (except for some special cases), hence the quotation marks. We are adopting the common labels used in quantum mechanics, but we are not thinking in terms of particles, rather a wave expanded as an infinite sum of Fourier modes, and we make use of the conserved vector quantity present in the system.

with the tortoise coordinate defined in this instance through

$$\frac{dr^*}{dr} = \frac{r^2 + a^2}{\Delta}. \tag{1.84}$$

This can be used to show that $\partial_t N > 0$, as J^r can also be expressed in terms of $R_\pm$, implying that the 'particle current' flowing down, through the horizon, is always positive. Our classical physical intuition would then tells us that superradiance is most likely not possible in this case. We can show this explicitly by considering the reflection and transmission coefficients of a fermionic wave that scatters off the Kerr black hole. In order to carry this out, however, we need to rewrite the radial equations once again, so that they appear in a Schrödinger-like form, which we can subject to the usual analysis. Starting from Eqs. (1.77) and (1.78) we introduce a new tortoise radial variable

$$\frac{d\tilde{r}^*}{dr} = \frac{r^2 + \alpha^2}{\Delta}, \tag{1.85}$$

and then make the first substitution

$$P_\pm = \psi_\pm \, \exp\Big[\mp (1/2) i \, \arctan(\mu \, r/\lambda) \Big], \tag{1.86}$$

followed by a second change of radial variables

$$\hat{r}_* = \tilde{r}^* - \frac{\arctan(\mu \, r/\lambda)}{2 \, \omega}, \tag{1.87}$$

combined with defining

$$Z_\pm = \psi_+ \pm \psi_-. \tag{1.88}$$

All this leads to the very simple-looking equations

$$\left(\frac{d}{d\hat{r}_*} \mp W \right) Z_\pm = -i \, \omega \, Z_\mp, \tag{1.89}$$

which can also be rewritten as

$$\left(\frac{d^2}{d\hat{r}_*^2} + \omega^2 \right) Z_\pm = V_\pm \, Z_\pm, \tag{1.90}$$

where

$$W = \frac{\Delta^{\frac{1}{2}}(\lambda^2 + \mu^2\, r^2)^{3/2}}{(r^2+\alpha^2)(\lambda^2+\mu^2\, r^2) - (\lambda\,\mu\,\Delta)/(2\,\omega)},$$
$$V_\pm = W^2 \pm \frac{d\,W}{d\,\hat{r}_*}. \tag{1.91}$$

Moreover, the tortoise radial coordinate expands the range of the radial variable over the whole real line, that is, $\hat{r}_* \to \infty$ as $r \to \infty$ and $\hat{r}_* \to -\infty$ as $r \to r_+$. Eq. (1.90) is, finally, in a Schrödinger-like form and by analysing its potential we can figure out the asymptotic behaviour of the fields:

$$Z_\pm \to \mathcal{I}_\pm(\omega) e^{\mp i\sqrt{\omega^2-\mu^2}\,\hat{r}_*} \pm \mathcal{R}_\pm(\omega) e^{\pm i\sqrt{\omega^2-\mu^2}\,\hat{r}_*}, \quad \text{as } r \to \infty, \tag{1.92}$$
$$Z_\pm \to \qquad\qquad + \mathcal{T}_\pm(\omega) e^{\mp i\sqrt{\omega^2-\mu^2}\,\hat{r}_*}, \quad \text{as } r \to r_+, \tag{1.93}$$

where $\mathcal{I}_\pm$, $\mathcal{R}_\pm(\omega)$ and $\mathcal{T}_\pm(\omega)$ are the incidence, reflection, and transmission coefficients respectively. Here we can see one of the main differences between massive and massless fields, namely their behaviour near spatial infinity. For massive fields, the potential does not vanish as a power of $1/r$ at infinity, but instead retains a constant value given by the squared mass of the field,

$$V_\pm \to \mu^2 - \frac{2\,M\,\mu^2}{r} + \mathcal{O}(r^{-2}). \tag{1.94}$$

This is a manifestation of the statement that free particles at infinity must have energies exceeding their rest masses, $\omega^2 > \mu^2$,which is the case we are considering. For a massless field the analysis proceeds in a similar way. Setting $\mu = 0$, the fields asymptotically behave as

$$Z_\pm \to \mathcal{I}_\pm(\omega) e^{\mp i\,\omega\,\hat{r}_*} \pm \mathcal{R}_\pm(\omega) e^{\pm i\,\omega\,\hat{r}_*}, \quad \text{as } r \to \infty, \quad \text{(massless)}. \tag{1.95}$$

The last ingredient to complete our analysis can be obtained from Eq. (1.82) by rewriting the relation using the newly defined $Z_\pm$. Some algebra, using (1.89), allows us to obtain

$$\frac{1}{2\,\pi}\frac{\partial\, N}{\partial\, t} = \frac{1}{2\,i\,\omega}\left[Z_+\,\frac{d\,Z_+^*}{d\,\hat{r}_*} - Z_+^*\,\frac{d\,Z_+}{d\,\hat{r}_*}\right] = \frac{1}{2\,i\,\omega}\left[Z_+, Z_+^*\right], \tag{1.96}$$

where $\left[Z_+, Z_+^*\right]$ denotes the Wronskian. The fact that $\partial_t\, N$ does not depend on r over the exterior of the black hole implies that the same holds for the Wronskian. On the

other hand, we can use the asymptotic behaviours of the solutions to evaluate the Wronskian at the horizon and at spatial infinity, leading to

$$\left[Z_+ \frac{d\,Z_+^*}{d\,\hat{r}_*} - Z_+^* \frac{d\,Z_+}{d\,\hat{r}_*}\right]_{r=r_+} = 2\,i\,\omega|\mathcal{T}_+(\omega)|^2, \tag{1.97}$$

$$\left[Z_+ \frac{d\,Z_+^*}{d\,\hat{r}_*} - Z_+^* \frac{d\,Z_+}{d\,\hat{r}_*}\right]_{r\to\infty} = 2\,i\,\sqrt{\omega^2-\mu^2}\Big[|\mathcal{I}_+(\omega)|^2 - |\mathcal{R}_+(\omega)|^2\Big]. \tag{1.98}$$

Equating both expressions above, due to the constancy of the Wronskian, leads us to

$$|\mathcal{I}_+(\omega)|^2 - |\mathcal{R}_+(\omega)|^2 = \frac{\omega}{\sqrt{\omega^2-\mu^2}}|\mathcal{T}_+(\omega)|^2, \tag{1.99}$$

which shows that the reflection coefficient is always less than the incident one, meaning that superradiance is not possible for massive fermions - and, as can be shown in a very similar way [177, 33], for massless fermions - on a Kerr black hole background.

We should also note that superradiance is not exclusive to black holes. It can be shown [189], for example, that scattering of electromagnetic radiation off rotating conducting surfaces results, under certain conditions, in waves with a larger amplitude. It is, in fact, in that context that superradiance was first discovered, even though the term was first used by Dicke [67] in the study of coherent emission in quantum optics.

The final subsection of this introduction will deal with a topic we already mentioned, when we defined what a black hole is - namely the Weak Cosmic Censorship - the idea that singularities, which are a generic feature of General Relativity, should always be hidden behind an event horizon.

1.2.7 Weak Cosmic Censorship Conjecture

We should start by saying that Weak Cosmic Censorship is still just a conjecture and not a proven statement. In addition, there is no universally agreed upon precise formulation. The reason for that is, we do know of counterexamples to the simple statement that singularities are always hidden by event horizons (for example, the negative-mass Schwarzschild solution). Hence, we need to improve on that statement in a way that excludes examples that might be dubbed non-physical for certain reasons - for example, unrealistic matter or behaviour that does not persist once small perturbations are included in the initial data. Furthermore, there are situations where the matter that we consider, although physical, leads to the formation of singularities even in flat space, as our approximate description of its dynamics eventually breaks down (fluids). If that was the case in a curved spacetime as well, it would be hard for us to distinguish

between the appearance of a true gravitational singularity and a bad macroscopic description of a matter system. Hence, we would like to rule out such situations. These considerations have, over the years, led to one possible version for a precise formulation:

Conjecture 1 (Weak Cosmic Censorship Conjecture (WCCC))**.** *Let* (Σ, h_{ab}, K_{ab}) *be a geodesically complete, asymptotically flat, initial data set. Let the matter fields obey hyperbolic equations and satisfy the dominant energy condition* ($-T^a_{\ b}\, V^b$ *is a future-directed causal vector, for all future-directed timelike vectors* V^a*). Then generically the maximal development of this initial data is an asymptotically flat spacetime (in particular it has complete* $\mathcal{I}^+$*) that is strongly asymptotically predictable.*

We will go over all the ingredients of this definition one by one. As stated before, we are working in four spacetime dimensions unless otherwise stated. However, it is important to note that the WCCC is most likely violated in dimensions higher than four. We will briefly remark on that at the end of this section and then talk in more detail about the counterexamples to the conjecture at the beginning of chapter (4.1).

Geodesic completeness is there in order to ensure that we do not start with a solution to Einstein equation that already contains a naked singularity - the negative-mass Schwarzschild solution for example - as that will trivially violate the WCCC. In this way the conjecture protects against the formation of naked singularities, starting from a spacetime without any.

Additionally, asymptotically flat initial data is required so that one is limited to a finite amount of energy, as with infinite energy, it is not hard to imagine ways to break classical physics. However, we are not placing any restrictions on how this finite energy is distributed in the "interior" region (that is, opposite to the asymptotic) of the spacetime. We only require appropriate fall-off conditions at infinity for the gravitational field and matter, so that we have asymptotic flatness.

The case for matter is not so clear. Some authors will just say that the matter should be "suitably" defined. What this encompasses is that the coupled Einstein-matter field equations must have a well posed initial value formulation and should satisfy suitable energy conditions, such as the dominant energy condition. Moreover, as already mentioned above, we would like the included matter to be such that, in a fixed, globally hyperbolic, background spacetime (such as Minkowski), it always leads to globally regular solutions of the Einstein-matter field equations, starting from well-behaved initial data. This way we avoid naked singularities, which are not a product of dynamical gravity (for example pressureless dust [39]). This, of course, rules out fluids, due to developments of shocks and similar phenomena (although one can still try to draw on knowledge from fluid models).

In the end, we want to obtain a spacetime that is asymptotically flat with complete null infinity, $\mathcal{I}^+$. The motivation is that by starting from the above defined initial conditions, it will not be possible for a distant observer to detect the formation of a singularity or any propagating effects thereof. As we saw in the previous sections, $\mathcal{I}^+$ is where null geodesics propagate to, and hence it is also the place where a distant observer will receive any signals from phenomena in the spacetime.

The last word we need to clarify is "generic". As with matter, there is no precise way of achieving this. The idea is that finding a solution that violates the WCCC is not necessarily bad if the initial data required for it is too special in some sense. An example is the evolution of a massless scalar field coupled to gravity within spherical symmetry, as investigated numerically by Choptuik [36] and analytically by Christodoulou [41]. One constructs a one parameter family of solutions, whereby the parameter is linked to the profile/amplitude of the scalar field, and sees that there is a critical value under which the field just disperses to infinity, and above it, it forms a black hole, and it is exactly at the critical value that it leads to the formation of a naked singularity. This is clearly non-generic, as a slight perturbation will either lead to a black hole forming around the singularity or to it vanishing. A more rigorous way of specifying this would be to introduce an appropriate measure on the space of initial data, such that non-generic violations like this example are actually sets of measure zero. On the other hand, for a generic violation one would need to find an open set of counterexamples to the WCCC. Unfortunately, we do not have a clear idea of what such an appropriate measure is.

In closing this section, we will give a brief account of some evidence in favour of the WCCC.

We already mentioned it as an example of a non-generic violation, but in fact, in their work [41], Christodoulou proves that the WCCC holds true in the case of a massless scalar field coupled to Einstein gravity within spherical symmetry. The numerical results in this setup by Choptuik [36] have also been generalised to no symmetry assumptions [58], but only numerically. Furthermore, in recent years, a growing number of fully non-linear numerical simulations of Einstein equation in the strong field regime, like black hole mergers in 4D, have been carried out and no violations of the conjecture have yet been identified.

Another important evidence in support of the WCCC is the study of linear perturbations of the Schwarzschild or Kerr black hole. These investigations are important because we know that the metric perturbation equations on a Cauchy surface Σ for these spacetimes can be written in a form that comprises a well-posed initial value

problem. The latter implies that given smooth initial data on Σ for a globally hyperbolic region $(\bar{V} \cap \mathcal{M}, g)$, we can find a unique solution to the equations throughout $\bar{V} \cap \mathcal{M}$. Moreover, this solution will depend continuously on the initial data in a sense that we are not going to define precisely, but roughly speaking one can construct a linear map from the initial data to the space of solutions, which is continuous and bounded by an appropriate norm of the initial data. One then wants to show that the linearised equations do not have any solutions that "blow-up" or diverge somewhere on $\bar{V} \cap \mathcal{M}$, since otherwise, in the full non-linear regime, it could lead to singular behaviour that might even produce naked singularities. On the other hand, well-behaved perturbations will evolve to a non-singular solution throughout $\bar{V} \cap \mathcal{M}$. In the case of Schwarzschild and Kerr, *linear mode stability* has been established [178, 182, 11, 167, 174] - that is, for a fixed mode, in a Fourier expansion of the perturbing fields, the perturbations always decay. In fact, for Schwarzschild, full linear stability has been proven [51]. Therefore, one expects that starting with initial data sufficiently close to Schwarzschild, the Einstein equation would evolve to a non-singular solution on $\bar{V} \cap \mathcal{M}$. If that were not the case, gravitational collapse might produce singularities not hidden behind an event horizon, providing a generic counterexample to the WCCC.

There are many more results suggesting WCCC might be a working principle in nature, but we will not cover everything here. There are failed attempts at constructing initial data that violates the Penrose inequality [147, 96, 139], which relates the initial area of the apparent horizon to the initial energy contained in the data, and whose derivation assumes the validity of the WCCC. In addition, it also seems impossible to overspin or overcharge an extremal black hole [169] (and references therein).

Moving on from evidence in support of the conjecture, we already mentioned some examples of naked singularities. Due to their specificity, these led to improvements of its formulation. However, in spacetimes which are not asymptotically flat or whose dimensionality is higher than four, some candidates for generic counterexamples to the conjecture have been discovered in recent years. Even if these might not have a direct astrophysical significance for us, Einstein's General Relativity is a mathematical theory which can be formulated in higher dimension or with different asymptotic behaviour. Hence, one should not simply discard these results based on physical intuition as they might be able to teach us something about the mathematical underpinnings of the theory. As already mentioned, we will briefly recap some of these scenarios at the beginning of chapter 4.1 and then we will present our own candidate for a plausible violation of the WCCC in asymptotically flat, four dimensions, which was inspired by some of the aforementioned candidate counterexamples.

Chapter 2

Numerical Methods

2.1 Stationary solutions

An important portion of the work discussed in the chapters after this one has been carried out numerically. We think it is therefore necessary to introduce the reader to the techniques that have been used. There are various ways to solve systems of equations that are of interests to physicists on a computer and we do not claim to have used the best possible method. Nevertheless, we found that the techniques we utilised were effective in dealing with the problems we had, while at the same time not too hard and time-consuming to implement.

In our discussion of the uniqueness theorems we motivated the search for stationary solutions to the Einstein equation as an expected final state of gravitational collapse. Moreover, said theorems showed us that in four, asymptotically flat dimensions the only stationary, vacuum, black hole solution is given by the Kerr family of metrics [30, 155] (or Kerr-Newman for electro-vacuum [141]). Unfortunately, once we alter the setup - increase the number of dimensions or add matter - not only does writing down explicit stationary metrics become increasingly difficult, but generalising uniqueness theorems might not be straightforward [111].

Nevertheless, this does not imply that one is not interested in finding more stationary solutions to the Einstein equation. To the contrary, exploring the phase space of possible solutions can have intriguing consequences, as already in five, asymptotically flat dimensions one finds that black hole horizons are allowed to have a non-spherical topology [76, 74, 73]. In addition, the AdS/CFT correspondence allows one to explore new and interesting phases of conformal field theories by constructing the bulk spacetimes dual to CFTs on curved backgrounds [118–120, 27, 87, 88, 84, 82]. Furthermore, dimensionally reducing from string theory can lead to spacetimes with

extra compact dimensions, which might have interesting new properties and dynamics [98, 28, 137, 186]. On top of this, one can also try to add matter and either search for hairy black hole solutions that avoid some of the assumptions of the established no-hair theorems [109, 35, 108] or look for relativistic star solutions. The latter is a big and active field of research that we will, unfortunately, not touch much more upon, but the interested reader should look at the review [144] and references therein.

On the other hand, over the past few decades we have developed increasingly more and more sophisticated methods to carry out dynamical, numerical simulations of Einstein gravity. These achievements have become even more significant since the gravitational wave detections of the LIGO-Virgo collaboration that we already mentioned in the introduction. Given the level of understanding and effort that has gone into the Numerical Relativity program responsible for these, one might entertain the idea of using its tools to look for stationary solutions to the Einstein equation. For example, dynamical gravitational collapse of matter will settle down to a spacetime of interest to us once the system has equilibrated. While being a valid approach to the problem, it might not be the most practical. Numerical Relativity simulations usually require a lot of resources and time. On top of that, depending on the matter used for the collapse and the type of stationary black hole solution sought, equilibrating to the state we want (for example, vacuum) outside the event horizon might take very long time (for example, Price's law tails for massless fields [151, 152]). Moreover, we are only interested in the very final state of the system. As in the discussion on the uniqueness theorems, where this allowed us to forget the intricacies of gravitational collapse and just focus on the spacetime at very late time, here we hope that there might be an easier and more direct route to obtaining a stationary spacetime of interest. Finally, some of the stationary solutions that we seek might possess unstable modes in certain circumstances, implying that it might not be straightforward to obtain them using a dynamical simulation. An example is the Gregory-Laflamme instability, which has been identified in a number of higher dimensional black hole solutions with horizons that are elongated in at least one direction compared to the rest. It is believed to result in the pinch off of black hole horizons as in the case of the five-dimensional black string [137]. This has lead to discussions about violations of the Weak Cosmic Censorship Conjecture that we will cover in more detail in chapter (4.1), as well as, for example, possibly playing a role in the transition between black funnels and droplets in asymptotically locally AdS solutions [56] with Schwarzschild-AdS boundaries in five bulk dimensions [138]. Nevertheless, this does not mean that such stationary solutions are of no interest. They still form part of the phase space of the problem we are trying

to solve and might give us information about the evolution and some of the phenomena present in the system we are investigating.

The first important thing we need to mention with respect to a direct search for static or stationary solutions to the Einstein equation is that the latter is intrinsically of undefined character - neither elliptic, nor hyperbolic - because of diffeomorphism invariance, as we will see later. Nevertheless, it has been shown that the equations can be posed in a hyperbolic way - namely, starting with initial data on a hypersurface and with an appropriate choice of gauge (picking a coordinate system), it is locally a well-posed Cauchy problem [89, 37, 86, 154] (and a short review in [53]). This allows numerical relativists to carry out time-dependent simulations and obtain reliable answers. On the other hand, finding static and stationary solutions requires an elliptic formulation - that is, a well-posed boundary value problem. Therefore, the first step in our search is to reformulate the Einstein equation in a manifestly elliptic form. Imposing appropriate boundary conditions will then allows us to solve it as the desired elliptic boundary value problem.

There is a class of spacetimes where this has been possible for some time now [129–131, 184, 134–136, 133]. For static or stationary, cohomogeneity-2 problems one can tackle the equations in a type of conformal gauge, where the metric can be written as

$$ds^2 = \Omega(y,z)(dy^2 + dz^2) + h_{ij}(y,z)\, dx^i\, dx^j, \tag{2.1}$$

where $\Omega > 0$, h_{ij} is a Lorentzian metric and the i, j indices run over all coordinates except y and z, which are the ones the system depends on. The presented form comes about due to the fact that any two-dimensional manifold is conformally flat. The Einstein equation yields a system of elliptic equations of motion for Ω and h_{ij} in addition to a set of constraint equations, which are used to specify boundary conditions.

The intuitive ansatz taken above more or less dictates the approach. Unfortunately, it is limited to the setting in which it was pioneered. In general, determining how to solve an equation as an elliptic or hyperbolic problem is not a straightforward task and it is not just a clever ansatz that one needs. Nevertheless, a recently discovered method of rewriting the Einstein equation allows us to recast it as an elliptic boundary-value problem in various situations of interest to us - this is the so called Einstein-DeTurck formulation [105, 9, 185, 82, 84, 88, 158]. We will review it briefly in the following section and discuss its applicability.

2.1.1 Harmonic Einstein equation

The trace-reversed Einstein equation in d-dimensions with cosmological constant and matter is given by

$$R_{\mu\nu} - \frac{2\,\Lambda}{D-2} g_{\mu\nu} = T_{\mu\nu} - \frac{1}{D-2}\, T\, g_{\mu\nu}, \tag{2.2}$$

whereby we have traced the Einstein equation (1.1) so that we can substitute back for the Ricci scalar in order to arrive at the above expression (in this section we are momentarily setting $8\,\pi\,G = 1$, instead of $G = 1$ for convenience). At first, we will deal with the vacuum case, $T_{\mu\nu} = 0$, and comment on the presence of matter later. In order to determine the behaviour of the equation, we linearise it about a background metric $g_{\mu\nu}$ by considering small perturbations around it, $g_{\mu\nu} \to g_{\mu\nu} + h_{\mu\nu}$. This gives us

$$\Delta_R h_{\mu\nu} = \delta R_{\mu\nu} - \frac{2\,\Lambda}{D-2} h_{\mu\nu} = 0, \tag{2.3}$$

where the variation of the Ricci tensor is given by

$$\delta R_{\mu\nu} = \Delta_L h_{\mu\nu} + \nabla_{(\mu}\eta_{\nu)}, \tag{2.4}$$

with Δ_L being the Lichnerowicz operator:

$$\Delta_L h_{\mu\nu} = -\frac{1}{2}\nabla^2 h_{\mu\nu} - R_{\mu\ \nu}^{\ \kappa\ \lambda} h_{\kappa\lambda} + R_{(\mu}{}^{\kappa} h_{\nu)\kappa}, \quad \eta_\mu = \nabla_\sigma h^\sigma{}_\mu - \frac{1}{2}\partial_\mu h, \tag{2.5}$$

and h is the trace of $h_{\mu\nu}$. Indices are raised and lowered with the background metric $g_{\mu\nu}$. We are interested in the highest derivative terms in (2.3), as these dictate the principal symbol, σ_g, of the system of differential equations, and it can be used to determine their character. In our case we have

$$\begin{aligned}\sigma_g h_{\mu\nu} =& \frac{1}{2} g^{\sigma\rho}\Big(- \partial_\sigma\partial_\rho h_{\mu\nu} + 2\,\partial_\sigma \partial_{(\mu} h_{\nu)\rho} - \partial_\mu\partial_\nu h_{\sigma\rho}\Big) \\ =& \frac{1}{2}\Big(- \partial^\rho\partial_\rho h_{\mu\nu} + 2\,\partial^\rho \partial_{(\mu} h_{\nu)\rho} - \partial_\mu\partial_\nu h\Big).\end{aligned} \tag{2.6}$$

Small in our setup means that the wavelength of the perturbations is much less than any curvature scale associated with the fixed background metric $g_{\mu\nu}$. Therefore, their second derivatives will be large, implying that the principal symbol operator governs the short wavelength behaviour of the perturbations.

To study the character of the equation we can do something similar to a Fourier transform - replace the partial derivatives, ∂_μ, in (2.6) with a covector k_μ,

$$\sigma_g(k)h_{\mu\nu} = \frac{1}{2}g^{\sigma\rho}\Big(- k_\sigma k_\rho h_{\mu\nu} + 2\, k_\sigma k_{(\mu} h_{\nu)\rho} - k_\mu k_\nu h_{\sigma\rho}\Big). \tag{2.7}$$

$\sigma_g(k)h_{\mu\nu}$ is then said to be an elliptic operator if and only if $\sigma_g(k)h_{\mu\nu} \neq 0$ for every non-zero k at every point on the manifold under consideration. The physical interpretation of that statement is that there is no point on the manifold where locally the short wavelength perturbations will propagate as waves. A non-linear equation is elliptic if its linearisation about a solution is elliptic. However, it is easy to convince oneself that taking $h_{\mu\nu} = k_{(\mu}\xi_{\nu)}$ (corresponding to $h_{\mu\nu} = \partial_{(\mu}\xi_{\nu)}$) results in $\sigma_g(k)h_{\mu\nu} = 0$ for any ξ. Furthermore, this form of the perturbation resembles that of an infinitesimal diffeomorphism generated by a gauge field ξ - namely $h_{\mu\nu} = \nabla_{(\mu}\xi_{\nu)}$. Moreover, locally the latter reduces exactly to $\nabla_{(\mu}\xi_{\nu)} \sim \partial_{(\mu}\xi_{\nu)}$. This leads us to the realisation that the lack of ellipticity of the Einstein equation is caused by diffeomorphism (gauge) invariance.

This behaviour can be anticipated by counting the degrees of freedom in the Einstein equation. As we mentioned at the very beginning of this work, it represents a system of $D\,(D+1)/2$ equations in D-dimensions. However, the Ricci tensor satisfies the contracted Bianchi identity, $\nabla^\mu R_{\mu\nu} - \frac{1}{2}\nabla_\nu R = 0$, which provides D constraints on its components, reducing the number of non-trivial equations to $D\,(D-1)/2$. Nevertheless, we still need to determine $D\,(D+1)/2$ metric components, implying that there are additional D degrees of freedom to be fixed. Doing that is equivalent to lifting the diffeomorphism invariance of the Einstein equation.

As a small aside - one might ask why is that a problem. Should it not be possible to specify a metric on some numerical grid, such that all its components are smooth functions, and then just solve the equations? If we do not fix the diffeomorphism invariance carefully, it is possible that numerical errors, due to the existence of pure gauge modes, will accumulate leading to loss of precision in our results (whether it is a relaxation scheme, an iterative procedure or some other method we are using), prohibiting us from trusting them. This happens, because arbitrary diffeomorphisms need not preserve the smoothness of the metric components. What is possibly worse, the numerical algorithm we are using will have no way of knowing which solution, out of possibly infinitely many, it should pick. Moreover, even if it somehow arrives at a solution (having selected a gauge in some uncontrolled by us way), it is very unlikely that it will be smooth in the metric components.

It is thus clear that we need to fix this diffeomorphism invariance in order to pose the Einstein equation as an elliptic boundary-value problem. From our General Relativity classes on the linearisation of the Einstein equation we know at least one choice of gauge - the harmonic or de Donder gauge, given by

$$\partial_\nu h^\nu{}_\mu - \frac{1}{2}\partial_\mu h = 0. \tag{2.8}$$

Imposing the above condition reduces the principal symbol (2.6) to

$$\sigma_g h_{\mu\nu} = -\frac{1}{2}\partial^\rho\partial_\rho h_{\mu\nu}. \tag{2.9}$$

The gauge choice represents an additional D local conditions, as needed according to our degree counting, and eliminates the pure gauge modes as desired. For a metric g with Euclidean signature, the operator in (2.9) is elliptic, whereas it is hyperbolic in the Lorentzian case. Noting that static vacuum black holes can be analytically continued to imaginary time, allowing us to treat them as though on a Riemannian manifold, makes the former statement in the previous sentence exactly what we seek. However, in general, with the above gauge choice we have merely restated the fact that the Einstein equation can be formulated as an initial value problem. Nevertheless, we can recover ellipticity by imposing certain symmetries of interest to us, as we will discuss soon.

One way of imposing the above gauge condition is to find a one-form, ξ_μ, whose variation results in $\partial_\nu h^\nu{}_\mu - \frac{1}{2}\partial_\mu h$, so that when we set the gauge - that is fix ξ_μ - the resulting $\delta\xi_\mu = 0$ will enforce our gauge choice. One possibility is to take

$$\xi_\mu = g^{\tau\sigma}\Big(\partial_\tau g_{\sigma\mu} - \frac{1}{2}\partial_\mu g_{\tau\sigma}\Big), \quad \text{with} \quad \xi^\mu = g^{\tau\sigma}\Gamma^\mu_{\tau\sigma} = -\nabla^2 x^\mu, \tag{2.10}$$

whereby $\Gamma^\mu_{\tau\sigma}$ is the Levi-Civita connection with respect to the metric g, ∇^2 is the scalar Laplacian and x^μ corresponds to a choice of coordinate chart (in terms of scalar functions), which has been given so we can make an observation shortly.

While the above gauge fixing does indeed break the diffeomorphism invariance, it is a local statement, thus not covariant, hence will make applications difficult. However, its vector formulation is suggestive of a resolution, as the difference between two connections is a tensor, implying that we can simply take, as a global definition,

$$\xi^\mu = g^{\tau\sigma}\Big(\Gamma^\mu_{\tau\sigma} - \bar{\Gamma}^\mu_{\tau\sigma}\Big) \quad \Longleftrightarrow \quad \xi_\mu = g^{\tau\sigma}\Big(\bar{\nabla}_\tau g_{\sigma\mu} - \frac{1}{2}\bar{\nabla}_\mu g_{\tau\sigma}\Big), \tag{2.11}$$

where $\bar{\Gamma}^{\mu}_{\tau\sigma}$ is the Levi-Civita connection associated to an arbitrary, fixed metric $\bar{g}$ on the manifold, with $\bar{\nabla}$ being its corresponding covariant derivative. $\bar{g}$ is usually called the reference metric, with ξ in the above form known as the DeTurck vector [101, 59], first introduced in Riemannian geometry to demonstrate that weakly parabolic Ricci flow is diffeomorphic to strongly parabolic Ricci-DeTurck flow.

In order to implement the above considerations we need to add an additional term, built out of ξ, to the Einstein equation, so that its linearisation will lead to (2.9). The form of the gauge condition (2.8) together with the terms in (2.6) easily suggest that we need to subtract the covariant derivative of the DeTurck covector, $\nabla_{(\mu}\xi_{\nu)}$, which leads us to the Einstein-DeTurck or Harmonic Einstein equation (currently in vacuum),

$$R_{\mu\nu} - \nabla_{(\mu}\xi_{\nu)} - \frac{2\,\Lambda}{D-2}g_{\mu\nu} = 0, \quad \xi^{\mu} = g^{\tau\sigma}\left(\Gamma^{\mu}_{\tau\sigma} - \bar{\Gamma}^{\mu}_{\tau\sigma}\right). \tag{2.12}$$

Considering small fluctuations about a fixed background as before, $g_{\mu\nu} \to g_{\mu\nu} + h_{\mu\nu}$, produces

$$\Delta_H h_{\mu\nu} = \delta R_{\mu\nu} - \frac{1}{2}\pounds_{\xi} h_{\mu\nu} - \frac{2\,\Lambda}{D-2}h_{\mu\nu} = 0, \tag{2.13}$$

with the new term being the Lie derivative of the metric perturbations with respect to the DeTurck vector, ξ^{μ}. By construction the principal symbol of the Einstein-DeTurck equation is given by

$$\sigma^{H}_{g} h_{\mu\nu} = -\frac{1}{2}\partial^{\rho}\partial_{\rho} h_{\mu\nu}. \tag{2.14}$$

However, one important issue immediately arises - solutions to (2.12) will be solutions to the Einstein equation only if $\xi^{\mu} = 0$. On the other hand, requiring the vanishing of the DeTurck vector effectively determines the gauge, as fixing ξ leads to $\delta\xi = 0$, which enforces our gauge choice, as we explained earlier. Moreover, $\xi^{\mu} = 0$ corresponds to D additional equations, providing the constraints we need to fix all the gauge modes, as inferred earlier when counting degrees of freedom. However, this is not an algebraic gauge fixing procedure, as usually is the case, rather we are solving a differential equation for the metric g, given a certain reference metric $\bar{g}$. This implies that the gauge condition, $\xi^{\mu} = 0$, is affected only after the Harmonic Einstein equation has been fully solved. Therefore, our reformulation consists in simultaneously solving the gauge fixing condition $\xi^{\mu} = 0$ together with the Einstein equation.

Importantly though, the Harmonic Einstein equation also exhibits solutions that have a non-trivial DeTurck vector, $\xi^{\mu} \neq 0$. These are called Ricci solitons and, fortunately for us, are not that troublesome when constructing solutions numerically.

We will comment on them shortly, but in the worst case scenario, one can always check numerically whether $\xi^\mu = 0$ on a solution.

Prior to proceeding with a discussion on how to obtain stationary solutions in Lorentzian signature, we will make a final comment about the gauge-fixing mechanism.

Before writing the DeTurck vector covariantly we said that in a coordinate chart it takes on the form $\nabla^2 x^\mu$. Demanding its vanishing might be recognised by readers familiar with time-dependent Numerical Relativity problems as the widely used harmonic gauge, $\nabla^2 x^\mu = 0$. It is a special case of the generalised harmonic gauge, defined locally in a coordinate chart as $\nabla^2 x^\mu = H^\mu$, for some H^μ. Setting $H^\mu = -g^{\tau\sigma}\bar{\Gamma}^\mu_{\tau\sigma}$ appears to make our covariant gauge fixing condition, $\xi^\mu = 0$, and the generalised harmonic gauge equivalent, however, there is a small caveat. ξ^μ is a global vector field, dependent on our choice of reference metric, whereas H^μ is defined only locally (it does not transform as a vector field). Furthermore, the relation between H and $\bar{\Gamma}$ involves the metric g, which we want to solve for, hence specifying one will not determine the other unambiguously in a numerical scheme.

Additionally, we should also check whether there is any more freedom for gauge transformations after setting $\xi^\mu = 0$. To this end, gauge transform ξ itself

$$\xi^\mu \to \xi^\mu + \frac{1}{2}\nabla^\nu\nabla_\nu\zeta^\mu + \frac{1}{2}R^\mu{}_\nu\zeta^\nu - \left(\Gamma^\mu_{\sigma\nu} - \bar{\Gamma}^\mu_{\sigma\nu}\right)\nabla^\sigma\zeta^\nu, \tag{2.15}$$

where ζ is the generator of the new small diffeomorphism. We want to set the above terms involving ζ equal to zero and solve for ζ. This will guarantee that our gauge choice remains fixed, while possibly giving us some residual gauge freedom in the form of choosing ζ, given the expression vanishes for non-trivial values of ζ. It can be easily checked that the operator acting on ζ is elliptic, implying that at least locally we should be able to obtain a unique solution for ζ^μ. Unfortunately, global properties like existence and uniqueness have not been established yet.

2.1.2 Obtaining solutions to the Harmonic Einstein equation

As explained, we are looking for solutions to (2.12) with $\xi^\mu = 0$. The most intuitive approach to achieving this would actually be in the hyperbolic context. By replacing $R_{\mu\nu}$ in the contracted Bianchi identity, $\nabla^\mu R_{\mu\nu} - \frac{1}{2}\nabla_\nu R = 0$, with $R_{\mu\nu} - \nabla_{(\mu}\xi_{\nu)}$ we can obtain the following equation for the DeTurck vector

$$\nabla^\nu\nabla_\nu\xi_\mu + R_\mu{}^\nu\xi_\nu = 0. \tag{2.16}$$

If we were to prescribe initial data on a Cauchy surface with ξ^μ and its normal derivative to the hypersurface vanishing, then because (2.16) is a wave equation which can be posed as a well defined initial value problem, we know that ξ^μ will remain zero throughout an evolution of the metric g. Therefore, one can evolve the Harmonic Einstein equation starting form initial data for the metric on a Cauchy surface together with vanishing constraints on ξ^μ and its time derivative and obtain a solution to the unmodified Einstein equation in a coordinate system that has been determined by the $\xi^\mu = 0$ condition.

While intuitive, the above approach is dynamical, whereas, as already elucidated, here we are interested in deriving static and stationary spacetimes from an elliptic boundary-value problem perspective.

Let us begin with a slightly more formal definition of these terms. A spacetime is stationary if it admits a timelike Killing vector field. It is static if in addition there exists a spacelike hypersurface that is orthogonal to the orbits of the isometry (a time translation symmetry) associated to the timelike Killing vector[1]. Therefore, the latter type of spacetimes form a subclass of the former. When discussing the uniqueness of stationary, black hole spacetimes in four, asymptotically flat, vacuum dimensions, we referenced the rigidity theorems. These state that under the assumption of analyticity, the presence of a stationary Killing vector field that is not everywhere normal to an non-extremal event horizon ensures the existence of at least one additional rotational Killing field in the spacetime. Moreover, one can use the latter (be it a single one or many) to form a linear combination together with the timelike Killing vector that will be a horizon generator for the black hole. This result has actually been generalised to higher dimensions [112] and suggests an approach.

Assume that we have a black hole spacetime which admits a stationary Killing field, $T = \partial_t$, together with a set of N rotational Killing vectors, $R_{(a)} = \partial_{z^a}$, $a \in \{1, ..., N\}$, all of which commute with T. The $R_{(a)}$ are taken to have closed, periodic orbits normalised to $2\,\pi$. The Killing horizon generators can then be formed as

$$K = T + \Omega_H^{(a)}\, R_{(a)}, \tag{2.17}$$

with $\Omega_H^{(a)}$ being constants, representing the horizon angular velocity, with respect to each rotational Killing vector, as perceived by stationary observers at infinity. This construction can also be generalised to a spacetime with more than one disconnected Killing horizon, but we will omit the details. We can then write a line element for a

[1] This is equivalent to the spacetime also possessing a time reflection symmetry, $t \to -t$.

spacetime with the above properties in the following general form,

$$g = G_{AB}(x)\Big[dy^A + Y_i^A(x)\,dx^i\Big]\Big[dy^B + Y_j^B(x)\,dx^j\Big] + h_{ij}(x)\,dx^i\,dx^j, \tag{2.18}$$

where $y^A = \{t, z^a\}$, x^i represents the rest of the coordinates, G_{ab} is Lorentzian, h_{ij} Euclidean and $\partial_{y^A} g_{\mu\nu} = 0$ due to the isometries. Here the index ranges are given by: $A \in \{0, ..., N\}$ and $i \in \{N+1, ..., D\}$. h_{ij} is the metric of the manifold formed from the full Lorentzian spacetime as the orbit space under the isometries corresponding to the Killing vectors T and $R_{(a)}$. The reader familiar with stationary black hole solutions in General Relativity will notice that all explicitly known spacetimes[2] that fit the above profile do in fact have $Y_i^A(x) = 0$. Nevertheless, in the most general scenario there is no a priori reason for that to happen.

Before looking at the resulting Harmonic Einstein equation, we need to choose a reference metric, $\bar{g}$. At first it might seem that we are free to choose any metric as such, but that is not the case. For the cases that have received more attention up to now - asymptotically flat, Kaluza-Klein, or locally AdS black holes [105, 9, 185], the reference metric, $\bar{g}$, needs to possess the same symmetries as the metric g we seek, otherwise the boundary conditions on g will not be consistent with vanishing DeTurck vector, $\xi^\mu = 0$. This also implies that the Harmonic Einstein operator, $R_{\mu\nu} - \nabla_{(\mu}\xi_{\nu)}$, will share the same isometries. Moreover, the surface gravity and each of the horizon's angular velocities (i.e. with respect to each rotational KVF) of the reference metric need to match the corresponding quantities of the stationary solution we are trying to find.

With that comment in mind our choice for reference metric should be clear - it will have the same form as (2.18), hence

$$\bar{g} = \bar{G}_{AB}(x)\Big[dy^A + \bar{Y}_i^A(x)\,dx^i\Big]\Big[dy^B + \bar{Y}_j^B(x)\,dx^j\Big] + \bar{h}_{ij}(x)\,dx^i\,dx^j. \tag{2.19}$$

We can then look at the second order derivative terms in the Einstein-DeTurck equation, which dictate its character. To this end, define

$$R^H_{\mu\nu} = R_{\mu\nu} - \nabla_{(\mu}\xi_{\nu)}, \tag{2.20}$$

[2] In Kerr this is due to the so called "t-ϕ" reflection symmetry, which leaves the spacetime metric invariant under the simultaneous change of $t \to -t$ and $\phi \to -\phi$. This is equivalent to reversing the flow of time and the sense of rotation of the black hole.

whereby we can safely omit the cosmological constant terms as these will not contribute to the derivatives. Then

$$\begin{aligned} R^H_{AB} &= -\frac{1}{2} h^{lm}\, \partial_l\, \partial_m\, G_{AB} + \dots, \\ R^H_{Ai} &= -\frac{1}{2} h^{lm}\, \partial_l\, \partial_m \Big(G_{AB}\, Y_i^B \Big) + \dots, \\ R^H_{ij} &= -\frac{1}{2} h^{lm}\, \partial_l\, \partial_m \Big(h_{ij} + G_{AB}\, Y_i^A\, Y_j^B \Big) + \dots, \end{aligned} \tag{2.21}$$

demonstrating that the character of the equations is governed entirely by h_{ij}, which we said is Euclidean and thus positive definite, implying the above expressions cannot be zero, unless the metric vanishes, leading to the conclusion that the Harmonic Einstein equation is elliptic in this scenario.

Another setup of interest for us pertains to spacetimes with a Killing horizon which are invariant under a single KVF only that generates the said horizon [61, 62, 95]. They avoid the already mentioned rigidity theorems. The latter assume the existence of a stationary KVF that is not the horizon generator, but they do not prohibit the existence of a single Killing field $K = \partial_t + \Omega_H\, \partial_\phi$ which is null at the horizon and thus also generates it. That type of KVF is not necessarily timelike at infinity, hence the spacetime might not be stationary in the usual sense, as in the case of the solutions found with AdS asymptotics [61, 62], where one can instead talk about time-periodicity.

Unfortunately, for these spacetimes it has not been possible yet to prove that the Einstein-DeTurck system constitutes an elliptic boundary-value problem. Nevertheless, the equations can be solved numerically and it has been determined *a posteriori* that they are elliptic for the solutions that have been found, confirming the validity of utilising the DeTurck approach.

We should mention that the Einstein-DeTurck method has also been successfully employed in the case of spacetimes whose horizon is not Killing [88, 84, 158]. This setup is outside the scope of this work, thus we will not cover it. More details can also be found in the excellent article on numerical techniques for stationary solutions to the Einstein equation in [66].

2.1.3 Addition of matter

Everything we have said up to now applies to vacuum spacetimes, but the Harmonic-Einstein equation can also be utilised in the presence of matter. Depending on the choice of matter fields present, the extension can either be straightforward or require some more work. We already gave the trace-reversed Einstein equation in (2.2). Its

principal symbol about linearisations of the metric is not affected by the addition of the stress-energy tensor for matter, therefore we can apply the same reasoning as before and add the DeTurck term,

$$R_{\mu\nu} - \nabla_{(\mu}\xi_{\nu)} - \frac{2\,\Lambda}{D-2} g_{\mu\nu} = T_{\mu\nu} - \frac{1}{d-2}\,T\,g_{\mu\nu}. \tag{2.22}$$

However, in order to be able to solve the whole Einstein coupled to matter system we need to ensure that the equations of motion for the latter can also be posed as an elliptic boundary-value problem.

The case of a minimally coupled scalar field[3], which is of most relevance for this work, corresponds to a stress tensor of the form

$$T_{ab} = 2\,\nabla_a\psi\,\nabla_b\psi - g_{ab}\Big[\nabla^c\psi\,\nabla_c\psi - 2\,V(\psi)\Big], \tag{2.23}$$

with the scalar equation of motion given by

$$\Box\,\psi = V'(\psi). \tag{2.24}$$

This is a wave equation, and as is well known, can be solved as a boundary value problem, thus requiring no further modifications from us. Another way of seeing that is by recalling that scalar fields do not exhibit gauge freedom.

On the other hand, if one were to look at an Einstein-Maxwell system, then the matter fields do possess gauge degrees of freedom that need to be fixed. We will not deal with such systems, as we will be working exclusively with scalars, nevertheless we will sketch the idea, whereas more details can be found in [157, 66]. The approach is similar to what we did for the Einstein equation - one needs to add a covariant gauge-fixing term to the Maxwell equation that will depend on a choice of a reference one-form field that will satisfy the same boundary conditions (asymptotically and wherever else needed - for example at the event horizon) as the Maxwell field that one is solving for. The Einstein part of the equations is modified as before.

The above procedure can, in principal, be generalised to other minimally coupled matter fields by the addition of a corresponding covariant gauge fixing term that is linear in whatever gauge transformation is rendering the principal symbol under question of unfavourable character.

[3]We are working with a real field here, though all we say applies equally well to a complex scalar - the type we are dealing with in chapter (3.1).

With all that we have said up to now, we have shown that we can rewrite the Einstein equation in a way, (2.12) or (2.22), that will allow us to solve it as an elliptic boundary value problem in the case of stationary, axisymmetric spacetimes, possibly with the addition of a minimally coupled scalar field. The last piece of the puzzle that remains is to consider whether this will allows us to satisfactorily obtain solutions to the unmodified equations, meaning we have to look into the existence of Ricci solitons - solutions with non-vanishing DeTurck vector. There are no general results on that yet, but there is enough that we know to have the situation under our control.

Most importantly, since the equations are elliptic, local uniqueness theorems guarantee us, given suitable boundary conditions on the metric (and fields if any), that a solution with $\xi^\mu = 0$ cannot, in general, be arbitrarily close to one with $\xi^\mu \neq 0$. In practice, numerically Ricci solitons should be easily distinguishable from the solutions one is after. A straightforward way of determining this is by looking at the norm of ξ, given by $\xi^\mu \xi_\mu$ and verifying that it indeed vanishes everywhere in the spacetime. Numerically this is achieved by monitoring the convergence of $\xi^\mu \xi_\mu$ to zero.

Interestingly, there are situations in which it has been shown that Ricci solitons cannot exist at all. One such setting is for static Lorentzian spacetimes which are asymptotically flat, Kaluza-Klein or locally AdS [82]. Another set of systems of interest is for stationary, axisymmetric spacetimes with zero or negative cosmological constant, possessing a $t \to -t$ and $\phi \to -\phi$ reflection symmetry [85]. It should be mentioned that these results are for vacuum spacetimes and in the presence of matter the strategy outlined in the previous paragraph is the only option at the moment.

2.1.4 Boundary conditions

Before we can proceed with solving the Harmonic Einstein equation, we need to impose appropriate boundary conditions so that it becomes a well-posed elliptic boundary-value problem. The numbers and types of boundaries will depend on the spacetime we are working with. In general, one utilizes coordinates in a neighbourhood of a boundary such that the metric takes the form

$$ds^2 = \alpha^2 \, d\eta^2 + \gamma_{ij}(dx^i + \beta^i \, d\eta)(dx^j + \beta^j \, d\eta), \tag{2.25}$$

where the boundary corresponds to the hypersurface $\eta = 0$ and $\gamma_{ij}|_{\eta=0}$ is the induced metric there. As we already mentioned earlier, the full metric $g_{\mu\nu}$ has $D(D+1)/2$ independent components. One the other hand, fixing geometric quantities on the hypersurface $\eta = 0$ - that is, imposing conditions on the induced metric $\gamma_{ij}|_{\eta=0}$ or on

the extrinsic curvature (corresponding to Neumann and Dirichlet data, respectively), will only provide us with $D(D-1)/2$ boundary conditions. Hence, we are missing D constraints. However, as we already saw when counting degrees of freedom, it is only logical that the remaining boundary conditions should come from the DeTurck gauge-fixing condition, $\xi^\mu = 0$, which guarantees us that solutions to the Einstein-DeTurck equation will also solve the original Einstein equation. Nonetheless, our approach to dealing with diffeomorphism invariance is affected at the level of the full Harmonic Einstein equation - that is we are simultaneously solving the Einstein equation for the metric g and the condition $\xi^\mu = 0$. Therefore, when imposing boundary conditions, we need to make sure that these are not only consistent with the behaviour of the spacetime we are looking to find, but that they also ensure the vanishing of the DeTurck vector on the boundary hypersurface, $\xi^\mu|_{\eta=0} = 0$. It should be clear that enforcing boundary conditions which do not allow for $\xi^\mu|_{\eta=0} = 0$, while still possibly giving us a well-defined boundary value problem, will lead us to finding Ricci solitons.

Looking back at (2.16), we see that acquiring a solution to the Einstein-DeTurck equation with $\xi^\mu = 0$ means that we need to impose boundary conditions such that (2.16) is a well-defined elliptic problem that admits the trivial solution $\xi = 0$. In certain cases like static, asymptotically flat or Kaluza-Klein spacetimes it is fairly straightforward to see that this is the case [105, 185]. However, in practice one might need to check explicitly this is the case by expanding the relevant equations around the boundaries in question.

There are two types of boundaries we are interested in for this work - asymptotic and fictitious ones. More generally, there are other types as well - like extremal horizons - but these will not be touched upon, as we will not be constructing extremal solutions.

Asymptotic boundaries are an infinite proper distance away from any other point in the spacetime - like spatial infinity in asymptotically flat spacetimes, or the timelike boundary of AdS. There one usually imposes boundary conditions that preserve the asymptotic character of the spacetime - for example, asymptotic flatness. In the case of asymptotically locally AdS spaces and the AdS/CFT correspondence, the boundary conditions might also determine certain properties of the dual conformal field theory (CFT).

On the other hand, fictitious boundaries are a finite proper distance away from other points in the spacetime. In Lorentzian signature they can correspond to a non-extremal

horizon[4] or an axis of symmetry. One needs to ensure regularity at these places via the boundary conditions imposed there.

When determining the behaviour in a neighbourhood of a boundary in Einstein gravity, one will be dealing with second-order differential equations, which require two pieces of information to fully determine the expansion off the hypersurface, $\eta = 0$. Imposing a boundary condition will fix one of these coefficients and this is what some authors call a defining boundary condition. This can be used together with the equations of motion to work out the other unknown piece as well. This is usually referred to as a derived boundary condition and is not necessary for the well-posedness of the boundary value problem. Moreover, with a good choice of coordinates and function definitions, imposition of defining boundary conditions might lead to the derived ones being a direct result of the equations of motion holding true. Nevertheless, this is not always convenient or straightforward, and sometimes it might prove beneficial from a numerical efficiency point of view to impose derived conditions as well.

2.1.5 Numerical implementation and the Newton-Raphson method

Having formulated the Einstein equation for stationary and axisymmetric spacetimes as an elliptic boundary value problem we actually need to integrate it numerically. One of the most common approaches to solving such problems goes under the name of the Newton-Raphson method, which is what we have used for the work in this thesis. Before explaining its implementation for our system of equations, we will quickly illustrate the idea behind it using a simple one-dimensional root-finding problem.

Consider a continuously differentiable, real valued function f, such that x^* is a zero of the function, $f(x^*) = 0$. We want to determine x^*. To this end, we start with a guess, x_0, which we try to improve on iteratively. As f is differentiable, we can expand it in a Taylor series around x_0, thus

$$f(x) = f(x_0) + f'(x_0)(x - x_0) + \mathcal{O}\Big[(x - x_0)^2\Big]. \tag{2.26}$$

Assuming that x_0 is close enough (which we will comment on below) to the root we are seeking, we can refine our guess by finding the root of the above linear approximation

[4] In Euclidean signature, technically, there is no boundary there, rather the static KVF, which generates a $U(1)$ isometry, vanishes. In Cartesian coordinates one can easily show that the metric components are smooth there, however, if one were to adapt a chart to the symmetry, the horizon might appear as a fictitious boundary, analogous to how spherical coordinates do not cover the origin.

to f, and using the result as our next guess-point, around which we expand the function to linear order again. Namely,

$$x_1 = x_0 - \frac{f(x_0)}{f'(x_0)}, \tag{2.27}$$

followed by $f(x) = f(x_1) + f'(x_1)(x - x_1) + \mathcal{O}\Big[(x - x_1)^2\Big]$, which, given the right conditions, should be a better approximation than the expansion around x_0. We can then repeat the procedure again for $x_2 = x_1 - \frac{f(x_1)}{f'(x_1)}$ and so on, generalising to

$$x_{n+1} = x_n - \frac{f(x_n)}{f'(x_n)}. \tag{2.28}$$

Geometrically, at each step we are finding the point at which the tangent line to the curve $y = f(x)$ at $x = x_n$ intercepts the x-axis.

We can try to estimate how efficient our procedure is in getting closer to the true root with each successive step. Assume the function has a continuous second derivative. We can then Taylor expand it around a point x_n that is close to the root x^* as

$$0 = f(x^*) = f(x_n) + f'(x_n)(x^* - x_n) + \frac{1}{2}f''(x_n)(x^* - x_n)^2 + \mathcal{O}\Big[(x^* - x_n)^3\Big]. \tag{2.29}$$

Dividing the above equation by $f'(x_n)$ (assuming it is non-zero) and rearranging leads to

$$\frac{f(x_n)}{f'(x_n)} = -(x^* - x_n) - \frac{f''(x_n)}{2\,f'(x_n)}(x^* - x_n)^2 + \mathcal{O}\Big[(x^* - x_n)^3\Big]. \tag{2.30}$$

Replacing the left hand side with the help of (2.28) and simplifying leaves us with

$$\underbrace{x^* - x_{n+1}}_{\epsilon_{n+1}} = -\frac{f''(x_n)}{2\,f'(x_n)}(\underbrace{x^* - x_n}_{\epsilon_n})^2 + \mathcal{O}\Big[(x^* - x_n)^3\Big], \tag{2.31}$$

where $\epsilon_n = x^* - x_n$ denotes the error in our approximation to the root after n iterative steps of the scheme. The above expression shows that, given certain assumptions, the Newton-Raphson method converges at least quadratically. More precisely, we assumed a non-vanishing first and a continuous second derivative in a neighbourhood of the root we are seeking to determine, as well as an initial guess that is close enough to the true root, in the sense that we can trust the Taylor series expansion around it. Given that some of the above conditions are not met, then the convergence can be slower - for example, if the first derivative vanishes at the root, as for $f(x) = x^2$.

Importantly, this method does not always converge. It is possible that the successive points will move further and further away from the root or that the algorithm will start oscillating between points. In general, the closer the initial guess to the root one is seeking the better, but even that is not always true, especially for generalisations of the method to higher dimensions.

After the brief recap above, we can discuss the way the Newton-Raphson method works for us - in the case of a system of partial differential equations. Take the latter to be given by

$$E_i\Big[x, F_1(x), \ldots, F_N(x)\Big] = 0, \tag{2.32}$$

where $i \in \{1, \ldots, N\}$, x represents all the coordinates that the system depends on and $F_i(x)$ are functions of these that we wish to solve for. The equations E_i depend on the functions $F_i(x)$ as well as their derivatives. We linearise by expanding about a particular set of functions, $\Big\{F_1^{(0)}(x), \ldots, F_N^{(0)}(x)\Big\}$, which are assumed to be close to a solution of the equations, $E_i\Big[x, F_1(x), \ldots, F_N(x)\Big] = 0$,

$$F_i(x) = F_i^{(0)}(x) + \delta F_i^{(0)}(x). \tag{2.33}$$

The resulting expansion is

$$\begin{aligned} E_i\Big[x, F_1(x), \ldots, F_N(x)\Big] =& E_i\Big[x, F_1^{(0)}(x), \ldots, F_N^{(0)}(x)\Big] \\ &+ \frac{\delta E_i}{\delta F_j^{(0)}}\Big[x, F_1^{(0)}(x), \ldots, F_N^{(0)}(x)\Big]\, \delta F_j^{(0)}(x) + \mathcal{O}\Big(\delta F^2\Big), \end{aligned} \tag{2.34}$$

with $\frac{\delta E_i}{\delta F_j^{(0)}}$ a differential operator acting on $\delta F_j^{(0)}(x)$ that can be represented as a matrix. As before, we truncate to leading order and rearrange, so that

$$\frac{\delta E_i}{\delta F_j^{(0)}}\Big[x, F_1^{(0)}(x), \ldots, F_N^{(0)}(x)\Big]\, \delta F_j^{(0)}(x) = E_i\Big[x, F_1^{(0)}(x), \ldots, F_N^{(0)}(x)\Big]. \tag{2.35}$$

Given an initial guess, $\Big\{F_1^{(0)}(x), \ldots, F_N^{(0)}(x)\Big\}$, approximating the solution to the full equation, $E_i\Big[x, F_1(x), \ldots, F_N(x)\Big] = 0$, the above is a linear system of equations that can be solved numerically using standard techniques in order to determine the $\delta F_j^{(0)}$'s. Setting $F_i^{(1)}(x) = F_i^{(0)}(x) + \delta F_i^{(0)}(x)$, we can continue repeating the above procedure as before, so that

$$F_i^{(n+1)}(x) = F_i^{(n)}(x) + \delta F_i^{(n)}(x), \tag{2.36}$$

until we find a solution to the equations to the desired precision.

It is important to mention that starting with a good initial guess, the Newton-Raphson method will return a single solution to the system of equations that we are solving. Exploring the phase space of solutions might, therefore, require a bit of ingenuity. Nonetheless, there are situations where one can do more than guessing. In this work we will construct hairy black hole solutions that branch off from Kerr at the onset of superradiance, meaning that there is a parameter that continuously connects the two. Varying the latter slightly from a known solution, that is Kerr, can provide us with a reasonable initial seed suitable for finding a hairy black hole using the Newton-Raphson method.

An additional strategy, which might improve our chances of finding a solution with a guess that is not sufficiently close to it, is by damping the Newton-Raphson method. Instead of taking $\delta F_i^{(n)}(x)$ as a step size for the next iteration, one can multiply it by a parameter - for example, $\lambda\,\delta F_i^{(n)}(x)$, with $0 < \lambda < 1$ - so that our next guess does not fly away from the basin of attraction of the solution. One can either use a constant parameter λ, or employ some short algorithm to improve convergence by choosing a more optimal value for λ at each step - for example, minimisation of the residue. The latter would, of course, lead to a decrease in performance and not necessarily compensate for the lack of a better initial guess.

We now move on to discuss our particular implementation of the methods and techniques described above.

At each step of the Newton-Raphson method, we need to solve a linear equation - that is (2.35), which is of the form $A\,x = b$, with $A = \frac{\delta E_i}{\delta F_j^{(0)}}\Big[x, F_1^{(0)}(x), \ldots, F_N^{(0)}(x)\Big]$ being the matrix that represents the linearised Einstein-DeTurck equation, $b = E_i\Big[x, F_1^{(0)}(x), \ldots, F_N^{(0)}(x)\Big]$ is our guess and $x = \delta F_j^{(0)}(x)$ is the iterative step we are solving for. To do this numerically, we need to discretise it - that is, put it on a grid of points. For example, $x_0, x_1, \ldots, x_N$, in one dimension, with $N \in \mathbb{N}$. We can then evaluate functions and their derivatives on the grid. Here, we use pseudospectral collocation methods, and work with a non-uniform grid, and in particular, we utilise the Chebyshev-Gauss-Lobatto (CGL) collocation points, defined by:

$$x_k = \frac{x_L + x_R}{2} + \frac{x_R - x_L}{2}\cos\left(\frac{k\,\pi}{N}\right), \quad k = 0, 1, \ldots, N, \tag{2.37}$$

where x_L and x_R define the endpoints of our domain, $x \in [x_L, x_R]$. Near its edges the CGL grid increases in density, which, amongst all, prevents the appearance of the so called Runge phenomenon. The latter is the problem of spurious oscillations at the

edges of an interval when one uses polynomial interpolation of high degree over a set of equispaced interpolation points, and it happens even for smooth functions with no oscillatory behaviour anywhere. The value of a function at a point is simply given by $f_k = f(x_k)$. To calculate derivatives we need to also introduce differentiation matrices - that is, on our grid derivatives are evaluated as $f_i^{(n)} = D_{ij}^{(n)} f_j$, where summation over j is assumed and $D^{(n)}$ represents an n-th order differentiation matrix. For spectral methods, numerical derivatives of a function are computed using all points on the grid. This is in contrast to the simple and popular method of finite differences for example, where, depending on its order, only the closest two, four and so on neighbours are used to determine the derivative value at a point. If implemented correctly, in computations, spectral methods can yield exponential convergence with increasing grid size. Using a finite differences method, on the other hand, offers only polynomial convergence. However, for very large grids, the matrices of the latter will be very sparse, in comparison to the always dense differentiation matrices associated to spectral approaches. Furthermore, achieving exponential convergence requires smoothness of the functions that are being evaluated. Although, in this work we will always be able to setup the problem in a way so that we deal with such functions only, there are situations where that might not be the case. In particular, the nature of gauge-fixing when using the Einstein-DeTurck formulation can sometimes lead to undesirable gauge modes appearing in the series expansion off the conformal boundary, when trying to construct spacetimes that are asymptotically locally AdS.

We define the differentiation matrices numerically as

$$D_{kj}^{(1)} = \frac{c_k}{c_j} \frac{1}{x_k - x_j}, \quad k \neq j, \tag{2.38}$$

where

$$c_i = \prod_{k=0,\, k\neq i}^{k=N} (x_k - x_i), \tag{2.39}$$

and the diagonal terms can be computed via the relation

$$D_{jj}^{(p)} = - \sum_{k=0,\, k\neq j}^{k=N} D_{jk}^{(p)}, \quad p = 1, 2, \ldots. \tag{2.40}$$

Higher order derivatives can either be found by taking powers of $D^{(1)}$ or using the general formula

$$D_{kj}^{(p+1)} = \frac{p+1}{x_k - x_j} \Big(\frac{c_k}{c_j} D_{kk}^{(p)} - D_{kj}^{(p)} \Big), \quad p = 1, 2, \ldots, \tag{2.41}$$

which we found was faster with our code.

2.1.6 Preconditioning

The form of the spectral differentiation matrices can, depending on the system we are investigating, lead to situations in which the matrix form of $\frac{\delta E_i}{\delta F_j^{(0)}}\left[x, F_1^{(0)}(x), \ldots, F_N^{(0)}(x)\right]$ in (2.35) is badly *conditioned* - that is it will have a very large *condition number*. The latter is a concept in numerical analysis.

Condition number characterises by how much the output of a function changes based on a change in its input. Solving a linear system of the form $A\,x = b$ numerically necessarily involves some form of approximation[5], no matter what algorithm is used. The condition number is a property of the matrix - it is independent of rounding errors due to finite precision in carrying out computations during the execution of the numerical method. It, roughly speaking, measures how does an error in b affect the accuracy with which we determine the solution of the linear system, x, using our approximate numerical methods. In particular, a large condition number means that even a small error in b can lead to a significant error in determining x numerically. On the other hand, a small condition number bounds the error in x to be not much larger than the one in b.

In practical terms, this means that the individual steps of our Newton-Raphson scheme to iteratively solve the Einstein-DeTurck equation - that is, solving the linear system (2.35), might be drastically slowed down. In our numerical approach, badly conditioned matrices come about mainly due to the use of spectral methods. The spectral differentiation matrices compute derivatives using all the points on the grid, implying that they can capture the behaviour of long wavelength modes. This is in contrast to methods that rely only on points in the neighbourhood of where the derivative is evaluated, which inherently limits the ability of the latter to effectively detect low energy excitations. This added sensitivity to long wavelength modes for spectral methods translates into a higher condition number, as there are more distinct eigenvalues to be determined by the solver.

Fortunately, there is a way to deal with badly conditioned matrices in numerical analysis and it involves the application of a preconditioner. The latter is a matrix P^{-1} (or P - both are used, depending on notation conventions) which is applied to the operator A in our linear problem with the aim of reducing its condition number. The

[5] If we did not need to approximate that would mean we knew the exact answer, hence we would not be trying to solve the problem numerically in the first place.

idea is that solving $A\,x = b$ is equivalent to solving

$$A\,P^{-1}\,P\,x = b, \tag{2.42}$$

which can also be written as

$$\Big(A\,P^{-1}\Big)y = b, \quad y = P\,x. \tag{2.43}$$

This is referred to as right preconditioning. Its left counterpart is simply defined as

$$P^{-1}\Big(A\,x - b\Big) = 0. \tag{2.44}$$

As long as P is a non-singular matrix, the solutions to both systems above also solve the original linear equation $A\,x = b$. The choice of P is ours, and we want to make it in a way so that $P^{-1}\,A$ or $A\,P^{-1}$ has a smaller condition number than A by itself. Naturally, its implementation comes with a cost associated to it, since we have to carry out an additional operation at each step of the iterative procedure - the Newton-Raphson method for us. Therefore, one would like to choose a preconditioner that is easier to evaluate than A, but at the same time leads to a noticeable decrease in its condition number. The two extremes in this choice are the identity matrix - which does not help us in any way, but is very cheap to construct - and in the opposite end of the spectrum - taking $P^{-1} = A^{-1}$, which is equivalent to solving our original problem. Numerical packages and libraries rarely explicitly form the product matrix $P^{-1}\,A$ or $A\,P^{-1}$, in the same way routines for solving systems of linear equations numerically almost never actually calculate the matrix inverse A^{-1}, and instead use LU decomposition or any another similar method better suited to the type of matrix that A is.

In our work, we used the software *Mathematica* whose function for solving linear equation - that is, *LinearSolve* - has an option for the specification of a preconditioner that requires nothing more than providing the matrix for it. We found that in the case of spectral collocation methods the choice of preconditioner depends on whether one is carrying out the computations with machine or arbitrary precision. In the former case a good approach is to pass the solver as a preconditioner the linear operator $A = \frac{\delta E_i}{\delta F_j^{(0)}}\Big[x, F_1^{(0)}(x), \ldots, F_N^{(0)}(x)\Big]$, still constructed on a CGL grid but utilising finite differences differentiation matrices instead of spectral ones - that is, we are using a low order polynomial approximation, but not with the usual uniform grid, as usually done for finite differences, but rather with our non-uniform CGL grid. The former are much sparser and will most often lead to well-conditioned operators.

When arbitrary precision calculations are required, the above strategy is still valid, but it is sometimes worth checking whether using a "machine precision" version of A (still formed with spectral derivatives) for preconditioning will not offer better results. Implementations using arbitrary float arithmetic are, in general, much slower than calculations using machine precision. Hence, even if the condition number of the preconditioner is not much lower than that of the original operator A, its determination will be much quicker. This is almost equivalent to solving the machine precision version of the problem, whose solution should technically be close to the answer we are seeking. Therefore, applying it should lead to a well-conditioned operator.

That concludes the chapter and we will next use the numerical techniques just discussed to construct and investigate the linear mode stability of scalar hairy Kerr black holes in asymptotically flat, four dimensions.

Chapter 3

Scalar Hairy Black Holes in Four Dimensions are Unstable

3.1 Introduction

With the advent of gravitational wave astronomy by the LIGO Collaboration, now also joined by Virgo, [2, 1, 5–8, 3, 4], the understanding of asymptotically flat black holes (BHs) in four spacetime dimensions has taken a novel central role in theoretical physics. The study of BHs can be broadly divided into two complementary categories: (a) the search for stationary solutions and their concomitant stability analysis and (b) strong field dynamics. While the latter is an active topic of research, the former was thought to have been understood during the seventies [30, 155] and led to the formulation of the so-called no-hair or uniqueness theorems, which we already covered in the introductory chapter. As a quick reminder - these state that if $(\mathcal{M}, g)$ is a stationary, axisymmetric, four-dimensional asymptotically flat vacuum spacetime that is suitably regular on and in the vicinity of a connected event horizon, then it is isometric to a member of the Kerr family [127]. Combining these with the assumption of axisymmetry and the expectation that a newly formed black hole will eventually settle down to an equilibrium, implies that most black holes in the current day Universe should be representatives of this family.

For spacetimes with positive or negative cosmological constant, however, such theorems have not been proven to the same extent and hairy black hole (HBH) solutions have been found - that is, black holes characterised by more than the usual mass, angular momentum and charge parameters, which are covered by the uniqueness theorems in flat 4D. The few exceptions are: Static, spherically symmetric black holes with $\Lambda > 0$ cannot possess scalar or Proca hair [21], and static solutions with

$\Lambda < 0$ - the negative mass AdS soliton [93, 94], which is asymptotically toroidal, and Schwarzschild-AdS and the standard AdS metric in asymptotically hyperbolic setting [10] - also do not such support hair.

On the other hand, one can couple a massive scalar field conformally, including quartic self-interactions, to a de Sitter black hole [140] and the resultant HBHs satisfy the dominant and strong energy conditions. Furthermore, for $\Lambda < 0$, hairy solutions have been discovered in Einstein-Yang-Mills theory [183], and in [100], where Einstein gravity with negative Λ is coupled to an Abelian Higgs field in four dimensions, paving the way for the discovery of the holographic superconductor [102].

Accomplishing the same for vanishing cosmological constant was attempted successfully for the first time by Gubser [99] - hairy analogues of the Reissner-Nordström black hole in four dimensions were obtained by introducing a real massive scalar field, coupled in a non-renormalisable way to the gauge field. The solutions satisfy the dominant energy condition, but fail the positivity of energy theorem [161, 162, 115, 97] due to the existence of negative regions in the potential, overstepping the assumptions of the uniqueness theorems (a generalisation of which to include that case was made in [110]).

Nevertheless, the uniqueness theorems do possess assumptions not all of which are physically well motivated. Most notably, they assume the existence of a stationary Killing vector field which is not the horizon generator. In [61], the first example of a hairy black hole (HBH) violating this assumption was constructed - a five dimensional black hole with scalar hair and anti de-Sitter (AdS) boundary conditions. These solutions are time-dependent and not axisymmetric from the matter perspective, but the gravitational sector does preserve axisymmetry and stationarity. They were generalised in [65], where purely gravitational, four-dimensional, black holes solutions with a single Killing vector field were constructed (the metric itself has a single Killing field only).

Three key ingredients for constructing scalar hair were identified in the first work above [61]: (1) a confined scalar field so that bound states exist, (2) the presence of superradiant scattering, and (3) the existence of a single Killing vector field, which happens to coincide with the horizon generator. A few years later, Herdeiro and Radu noticed that such a construction could be carried out in asymptotically flat spacetimes [109] if a complex massive scalar field is minimally coupled to gravity. The idea being that the confining nature of AdS is replaced by the presence of the mass term. They did this numerically, whereas the authors of [35] achieved that in a mathematically rigorous way. Building on this generalisation to asymptotically flat spacetimes, BHs

with Proca hair have been recently constructed in [108]. In all of these cases (the exception being the five-dimensional case studied in [23]), the HBHs branch from the onset of the superradiant instability [17, 170, 54, 60, 190, 68, 166, 188, 24, 25] and extend into regions of moduli space where Kerr BHs do not exist.

It is then interesting to investigate whether these HBHs are themselves unstable, since their stability analysis could have important consequences for whether they might be of astrophysical interest. This looks like a daunting task with little chance of success, since no Teukolsky equation has been found for the system at hand. It would seem one would have to perturb the full Einstein-Klein-Gordon (EKG) system and thus solve a complicated set of coupled linear partial differential equations. What is worse is that, since the background scalar field exhibits explicit time dependence, it would seem unlikely that the concept of quasinormal mode (QNM) could be useful, since the time dependence of the fields would not factorise - that is, no useful Laplace transform can be taken to study stability using Sturm-Liouville type methods. In order to bypass these issues, we will prove the existence of a new gauge where the scalar field perturbations decouple from the metric perturbations. Furthermore, we investigate the issue of residual gauge freedom, showing that our main results cannot be gauged away, thus rendering them physical.

This work is organised as follows. We first reconstruct the solutions of [109] and recover their results, then in the second subsection we perturb the equations of motion and prove the existence of a particular gauge where the matter sector plays a pivotal role, followed by a discussion of our results in subsection three, with the final section dedicated to conclusions.

3.2 Einstein-Klein-Gordon system

We start with Einstein-Hilbert gravity minimally coupled to a complex massive scalar field

$$S = \int_{\mathcal{M}} d^4x\sqrt{-g}\left(\frac{R}{16\,\pi\,G} - \nabla_a\psi^*\nabla^a\psi - \mu^2|\psi|^2\right) . \tag{3.1}$$

As stated in the beginning, we work in units with $G = c = 1$. Thus, the corresponding equations of motion are given by

$$R_{ab} = 8\pi\Big[2\nabla_{(a}\psi^*\nabla_{b)}\psi + g_{ab}\,\mu^2\psi^*\psi\Big] , \tag{3.2a}$$

$$\Box\psi = \mu^2\psi\,. \tag{3.2b}$$

A well-known solution to the above system of partial differential equations (PDEs) is the Kerr family of BHs, where the scalar field ψ vanishes identically and

$$ds^2 = -\frac{\Delta}{\Sigma^2}\left(dt - a\sin^2\theta d\phi\right)^2 + \frac{\sin^2\theta}{\Sigma^2}[a\,dt - (r^2+a^2)d\phi]^2 + \Sigma\left(d\theta^2 + \frac{dr^2}{\Delta}\right), \quad (3.3)$$

with $\Delta = r^2 + a^2 - 2\,M\,r$ and $\Sigma^2 = r^2 + a^2\cos^2\theta$. The BH event horizon is a null hypersurface with $r = r_+ \equiv M + \sqrt{M^2 - a^2}$, angular velocity $\Omega_K = a/(a^2 + r_+^2)$ and temperature $T_K = (r_+^2 - a^2)/[4\pi r_+(r_+^2 + a^2)]$. The constant M is the BH mass and a parametrises its angular momentum via $J = Ma$. The absence of naked singularities demands $|a| \leq M$ with the inequality saturating at extremality, when the Kerr BH event horizon becomes degenerate with $T_K = 0$.

In [109, 35] it was shown that HBHs can coexist with Kerr BHs in certain regions of the solutions' space. Their existence in the phase diagram of (3.2) can be understood via a linearised analysis of scalar perturbations on a fixed Kerr background. In such a spacetime scalar perturbations can be studied by taking $\psi = \hat{\psi}(r,\theta)e^{-i\,\omega\,t + i\,m\,\phi}$, with ω the frequency we wish to determine and $m \in \mathbb{Z}$ an azimuthal quantum number. If $\mathrm{Im}(\omega) > 0$, the system exhibits a linear mode instability. The resulting equation for $\hat{\psi}(r,\theta)$ is separable into two ordinary differential equations (ODEs) that couple via their respective eigenvalues: one equation along the angular direction θ and one along the radial direction r.

The presence of an ergoregion can be used to extract energy from the BH and source superradiant *scattering* [18, 54, 170, 19, 166], so long as $0 < \omega \leq m\Omega_K$. Since the scalar field is massive, these waves can be trapped and thus source an instability. This is the so-called superradiant instability first uncovered in the late seventies and early eighties by Zouros and Eardley [190] and Detweiller [60]. From the onset of this instability, novel hairy BHs bifurcate [65] with $\omega = m\Omega_K$, thus preserving a single Killing vector field $\Xi = \partial/\partial_t + \Omega_K\partial/\partial_\phi$ only. Since the scalar field is complex, it yields a stress energy tensor that is axisymmetric and stationary, thus preserving as many isometries as those possessed by the Kerr line element (3.3). These BHs were constructed at the nonlinear level in [109, 35] and shown to coexist with the Kerr BH for certain regions of the (M, J) plane, thus violating the uniqueness of the Kerr family of solutions.

As mentioned earlier, in order to assess their linear stability, we want to know whether these BHs are also susceptible to superradiance. To this end, we perturb them and solve the resulting equations numerically, whereby a suitable choice of gauge reduces the system of equations to a Klein-Gordon (KG) equation for the scalar

perturbation in a fixed HBH background. We therefore first construct these BHs to a very high accuracy using the DeTurck method, which was first presented in [106] and recently reviewed in [66].

3.3 Hairy Black holes

3.3.1 DeTurck method

Employing the DeTurck method in order to create HBHs amounts to solving the following system of PDEs:

$$R_{ab} - \nabla_{(a}\xi_{b)} = 8\pi\left[2\nabla_{(a}\psi^{*}\nabla_{b)}\psi + g_{ab}\,\mu^{2}\psi^{*}\psi\right], \tag{3.4}$$

where $\xi^{a} = g^{bc}\left[\Gamma^{a}_{bc}(g) - \Gamma^{a}_{bc}(\mathfrak{g})\right]$ is the DeTurck vector and $\Gamma^{a}_{bc}(\mathfrak{g})$ is the Levi-Civita connection for a reference metric $\mathfrak{g}$. The only restriction on $\mathfrak{g}$ is that it obeys the same boundary conditions (with matching surface gravity and angular velocity as discussed earlier) as the metric we wish to find.

Recall that we wish to solve (3.2a), meaning we need to ensure $\xi = 0$ on solutions of (3.4). We are interested in stationary, axisymmetric spacetimes with a $t - \phi$ reflection symmetry which, according to [106, 83], give a second order system of elliptic PDEs. Furthermore, it has been shown that, when $\psi = 0$, solutions with $\xi^{a} \neq 0$ cannot exist [85]. For the case at hand though, due to the presence of a scalar field, we have to verify *a posteriori* that this is the case. Since the equations are elliptic, local existence theorems imply that a solution with $\xi \neq 0$ cannot be arbitrarily close to one with vanishing ξ.

The most generic ansatz for such a spacetime is

$$\begin{aligned} ds^{2} = -F(x,z)x^{2}dt^{2} + r_{0}^{2}\Bigg[&\frac{A(x,z)(1-z^{2})^{2}}{(1-x^{2})^{2}}\left(d\phi - (1-x^{2})^{2}W(x,z)\frac{dt}{r_{0}}\right)^{2} \\ &+ \frac{4C(x,z)}{(1-x^{2})^{4}}dx^{2} + \frac{4D(x,z)}{(1-x^{2})^{2}(2-z^{2})}\left[dz + B(x,z)dx\right]^{2}\Bigg], \end{aligned} \tag{3.5}$$

where r_0 is the BH radius. Here, $x \in (0,1)$ plays the role of a radial coordinate with $x = 0$ being the horizon and $x = 1$ asymptotic spatial infinity. $z \in (-1,1)$ is an angular coordinate, with $z = -1$ being the south pole of the horizon and $z = 1$ the north. There is also a $\mathbb{Z}_2$ reflection symmetry $z \to -z$, so we will take $z \in (0,1)$ and impose reflection symmetry at $z = 0$.

3.3.2 Metric ansatz and boundary conditions

Appropriate boundary conditions have to be imposed at the edges of our domain. At the horizon ($x = 0$), requiring regularity, we set

$$\partial_x A = \partial_x D = \partial_x C = \partial_x \psi = 0,\ F = C,\ W = \Omega_{HBH},\ B = 0\,. \tag{3.6}$$

At asymptotic infinity ($x = 1$), where the metric has to approach Minkowski spacetime, we have

$$A = C = D = F = 1,\ W = B = \psi = 0\,. \tag{3.7}$$

At the north pole ($z = 1$), also demanding regularity, we get

$$\partial_z F = \partial_z D = \partial_z C = \partial_z W = \partial_z \psi = 0,\ A = D,\ B = 0\,. \tag{3.8}$$

And finally at the axis of the polar angle reflection symmetry ($z = 0$), insisting on smoothness, we require

$$\partial_z A = \partial_z F = \partial_z D = \partial_z C = \partial_z W = \partial_z \psi = 0,\ B = 0\,. \tag{3.9}$$

Our choice of reference metric is based on obtaining the Kerr metric asymptotically, which amounts to $A = F = C = D = 1$, $B = 0$ and $W = \widehat{\Omega}(1 - x^2)$, so that its angular velocity vanishes at infinity and is fixed at the horizon to $\Omega_H = \widehat{\Omega}/r_0$. Using the boundary conditions at the horizon, one can show that the temperature of the hairy solution is $T_H = 1/(4\pi\, r_0)$. We will measure all physical quantities in temperature (or equivalently surface gravity) units.

3.3.3 Scalar field boundary conditions

Finally, for the scalar field we take

$$\psi(t, x, z, \phi) = e^{-i\,\tilde{m}\,\Omega_H\, t} e^{i\,\tilde{m}\,\phi} (1 - z^2)^{\tilde{m}}\, \tilde{\psi}(x, z)\,, \tag{3.10}$$

where $(1 - z^2)^{\tilde{m}}$ ensures the regularity of the scalar field at the south and north poles. This is easy to see by looking near the poles of the squashed sphere, $z = \pm 1$, where spherical symmetry is almost perfectly recovered, hence the angular part of the metric

to lowest order in $(1-z)$ can be written as

$$\begin{aligned} ds^2_{z=\pm 1} &\approx \frac{A(x,z)}{(1-x^2)^2}\left(dz^2+(1\pm z)^2 d\phi^2\right) \\ &= \frac{A(x,\tilde{z})}{(1-x^2)^2}\left(d\tilde{z}^2+\tilde{z}^2 d\phi^2\right)\,, \end{aligned} \tag{3.11}$$

where in the second line we have applied a shift $1\pm z\to\tilde{z}$. In this way we see that the metric takes the familiar form of 2D flat space in polar coordinates. The latter are, however, not regular at the origin (which after the shift in z corresponds to the pole of the sphere), thus forcing us to change to Cartesian coordinates, so as to investigate the behaviour of the scalar field there. This is easily achieved by the following transformation

$$(\tilde{x},\tilde{y}) = (\tilde{z}\,\cos\phi\,,\tilde{z}\,\sin\phi)\,, \tag{3.12}$$

which takes the $d\tilde{z}^2+\tilde{z}^2 d\phi^2$ part of the metric to $d\tilde{x}^2+d\tilde{y}^2$. The scalar field, has the general form

$$\psi(t,x,\tilde{z},\phi) = e^{-i\,\omega\,t}e^{i\,\tilde{m}\,\phi}f(x,\tilde{z})\,, \tag{3.13}$$

whose $e^{i\,\tilde{m}\,\phi}$ part can be rationalised under the change of variables (3.12), depending on the value of $\tilde{m}$. Computing the first two cases – $\tilde{m}=1$ and $\tilde{m}=2$ – illustrates a simple general relation, which can be straightforwardly verified with the help of trigonometric identities - namely

$$e^{i\,\tilde{m}\,\phi} = \left(\frac{\tilde{x}+i\tilde{y}}{\sqrt{\tilde{x}^2+\tilde{y}^2}}\right)^{\tilde{m}}\,. \tag{3.14}$$

Therefore, regularity at the poles fixes the polar angular dependence of the scalar field ψ at least as $(1\pm z)^{\tilde{m}}$, in order to compensate for the denominator in (3.14). Furthermore, at asymptotic infinity we demand that $\tilde{\psi}=0$ and at the horizon we require regularity, which is enforced via $\partial\tilde{\psi}/\partial x\big|_{x=0}=0$.

The moduli space of HBH solutions is then generated by varying Ω_H and the integer $\tilde{m}$. In the actual code we treat Ω_H as an unknown number and provide an additional equation in the form of a very small normalisation condition $\tilde{\psi}(0,1)=\epsilon$ on the scalar field at the horizon ($x=0$, $z=1$). The moduli space of solutions is then generated by varying ϵ at fixed integer $\tilde{m}$. Our numerical findings for the background are consistent with those in [109].

3.4 Perturbing the HBHs

In order to investigate the stability of the HBHs, we have to perturb (3.2). We consider small changes in both the metric and scalar field:

$$g_{ab} = g^{(0)}_{ab} + h_{ab}\,, \tag{3.15a}$$
$$\psi = \psi^{(0)} + \eta\,, \tag{3.15b}$$

where $^{(0)}$ represents background quantities. These give rise to the following equation for the perturbed scalar:

$$\Box^{(0)}\eta - \mu^2\eta - \hat{L}^{(0)}\psi^{(0)} = 0 \tag{3.16a}$$
$$\hat{L}^{(0)} = \bar{h}^{ab}\nabla^{(0)}_a\nabla^{(0)}_b - \nabla^{(0)}_a\bar{h}^{ad}\nabla^{(0)}_d - \frac{1}{2}\mu^2\bar{h}, \tag{3.16b}$$

where we have also defined the trace-reversed metric perturbation $\bar{h}_{ab} \equiv h_{ab} - \frac{1}{2}h\, g^{(0)}_{ab}$ and $h \equiv g^{(0)}_{ab}h^{ab}$.

Next, we have to choose a way to fix the gauge freedom induced by the following transformations

$$h_{ab} \to h_{ab} + \mathcal{L}_\chi g^{(0)}\,, \tag{3.17a}$$
$$\eta \to \eta + \mathcal{L}_\chi\psi^{(0)}\,, \tag{3.17b}$$

where χ is assumed to be the same order as h_{ab} and η.

Even though, one would like to completely separate the scalar from the gravitational perturbations in the EKG Eqs. (3.2), this does not seem possible in our case.

The most we can achieve is to choose a gauge in such a way as to decouple the perturbed Klein-Gordon equation from the metric perturbations h_{ab}, while still leaving the perturbed Einstein equation sourced by the scalar perturbation η. One way of doing this is by first setting:

$$\nabla^{(0)}_a\bar{h}^{ad} = P^d(\bar{h}, \bar{h}_{ab})\,. \tag{3.18}$$

It is essential for our proof that P_d can only depend on h_{ab}, but not its derivatives. In order to prove that such a gauge can be achieved, independently of our choice of P, we transform Eq. (3.18) using Eqs. (3.17):

$$\Box^{(0)}\chi_d + R^{(0)}_{da}\chi^a + \nabla^{(0)}_a\bar{h}^a{}_d - P_d - P^{(\chi)}_d = 0\,, \tag{3.19}$$

where $P_d^{(\chi)}$ is the gauge transformed version of P_d, which again depends only on $\bar{h}_{ab}$ but not on its first derivatives.

Moreover, (3.17) tells us that $P_d^{(\chi)}$ also can only depend on first order derivatives of χ_d, implying that the principal symbol of Eq. (3.19) is governed by $\Box^{(0)}$. We can then use Theorem 10.1.2 of [179] to show that χ can be chosen in such a way, as to have the above Eq. (3.19) uniquely satisfied for each component of χ.

Theorem 10.1.2 (Robert M. Wald, *General Relativity*, Chicago Univ. Pr., 1984)**.** *Let (M, g_{ab}) be a globally hyperbolic spacetime(or a globally hyperbolic region of an arbitrary spacetime) and let ∇_a be any derivative operator. Let Σ be a smooth Cauchy surface. Consider the system of n linear equations for n unknown functions $\phi_1, \ldots, \phi_n$ of the form*

$$\Box\phi_i + \sum_j (A_{ij})^a \nabla_a \phi_j + \sum_j B_{ij}\phi_j + C_i = 0.$$

Then the equation has a well posed initial value formulation on Σ. More precisely, given arbitrary smooth initial data, $(\phi_i, n^a\nabla_a\phi_i)$ for $i = 1, \ldots, n$ on Σ there exists a unique solution of the equation throughout M. Furthermore, the map from intial data on Σ to solutions in any fixed compact region of spacetime is continuous for the norms defined on the solutions and on the initial data. Finally, a variation of the initial data outside of a closed subset, S, of Σ does not affect the solution in $D(S)$.

This confirms that we can set $\nabla_a^{(0)}\bar{h}^{ad} = P^d$ for any choice of P^d that can depend at most on h_{ab}, but not on its derivatives.

With this gauge choice, we would like to set $\hat{L}^{(0)}\psi = 0$ in (3.16a), which will decouple the perturbed KG equation from the metric perturbations $\bar{h}_{ab}$. This translates to being able to uniquely solve

$$\bar{h}^{ab}\nabla_a\nabla_b\psi^{(0)} - P^d\nabla_d^{(0)}\psi^{(0)} - \frac{1}{2}\mu^2\bar{h}\psi^{(0)} = 0. \tag{3.20}$$

A P^d can be chosen, such that the above equation is satisfied, and noting again that, as desired, it turns out to be a function of $\bar{h}_{ab}$ only. However, one should point out that it might be singular at certain points of the spacetime, where $\nabla_d^{(0)}\psi^{(0)}$ vanishes (such points will most likely exist). This is not an issue in our case, as we only wish to solve for the scalar perturbations. On the other hand, were we to obtain the metric ones as well, then, after determining η, we would have to switch to a different gauge, where the singularities introduced in the perturbed Einstein equation due to P^d will not be present. Going back to the scalar perturbation, the final equation to be solved

for them is then

$$\Box^{(0)}\eta - \mu^2\eta = 0\,. \tag{3.21}$$

The gravitational sector, on the other hand, does not allow for an obvious decoupling strategy. Trace-reversing the perturbed Einstein equations and utilising the Ricci identity

$$2\nabla^{(0)}_{[c}\nabla^{(0)}_{d]}V_{ab} = R^{(0)}_{becd}V_a{}^e - R^{(0)}_{eacd}V^e_b \tag{3.22}$$

one can obtain

$$R^{(0)}_{c(a}\bar{h}_{b)}{}^c + R^{(0)}_{dbac}\bar{h}^{dc} + \nabla^{(0)}_{(a|}\nabla^{(0)}_c\bar{h}^c_{|b)} - \nabla^{(0)}_a\nabla^{(0)}_b\bar{h} - \frac{1}{2}\Box^{(0)}\bar{h}_{ab} + \frac{1}{4}g^{(0)}_{ab}\Box^{(0)}\bar{h} = 8\pi\left[2\nabla^{(0)}_{(a}\eta^*\nabla^{(0)}_{b)}\psi^{(0)} + 2\nabla^{(0)}_{(a}\left(\psi^{(0)}\right)^*\nabla^{(0)}_{b)}\eta + g_{ab}\mu^2\left(\eta^*\psi^{(0)} + \left(\psi^{(0)}\right)^*\eta\right)\right]. \tag{3.23}$$

Unfortunately, due to the presence of matter, the equations cannot be simplified any further, unlike in the vacuum case, where the Ricci tensor vanishes and tracing the above equation leads to $\Box^{(0)}\bar{h} = 0$. Fortunately, due to the decoupling of the KG equation for η from the metric perturbations, we do not need to know the form of h_{ab} in order to assess the linear stability of the HBHs.

3.4.1 Residual gauge freedom

Finally, we come to the thorny issue of residual gauge transformations $\hat{\chi}$, i.e. gauge transformations that leave the gauge condition (3.18) invariant. One can show that such residual gauge transformations necessarily satisfy

$$\Box^{(0)}\hat{\chi}_d + R^{(0)}_{da}\hat{\chi}^a - P^{(\chi)}_d = 0\,, \tag{3.24}$$

We have to show that such gauge perturbations *cannot* be used to set all solutions of (3.21) to zero using Eq. (3.17b) with $\chi = \hat{\chi}$. We devise a test to distinguish pure gauge from physical modes based on the fact that the former necessarily produce a metric perturbation that diverges exponentially at large distances, thus becoming incompatible with the requirement of asymptotic flatness.

By performing a Frobenius analysis close to $x = 1$ (asymptotic infinity) it can be shown that

$$\eta = e^{-\frac{\Gamma}{1-x}}(1-x)^\kappa\tilde{\eta}(t,x,\theta,\phi) \tag{3.25}$$

where $\tilde{\eta}(t,x,\theta,\phi)$ is a polynomial in $(1-x)$ and $\Gamma\,,\kappa\in\mathbb{C}$. A similar analysis can be repeated for $\psi^{(0)}$ and gives

$$\psi^{(0)}=e^{-\frac{\tilde{\Gamma}}{1-x}}(1-x)^{\tilde{\kappa}}\tilde{\psi}^{(0)}(t,x,\theta,\phi)\,, \tag{3.26}$$

with $\tilde{\psi}^{(0)}(t,x,\theta,\phi)$ polynomial in $(1-x)$ and $\tilde{\Gamma}\,,\tilde{\kappa}\in\mathbb{R}$.

Assume momentarily $\tilde{\Gamma}>\mathrm{Re}(\Gamma)$. If η is pure gauge, then from (3.17b) with $\chi=\hat{\chi}$, the residual gauge perturbation $\hat{\chi}$ has to blow up exponentially as $x\to 1^-$. However, this generates a metric perturbation, via Eq. (3.17a), that necessarily diverges exponentially as $x\to 1^-$, thus becoming inconsistent with the assumption of asymptotic flatness [12, 14, 15]. Therefore, by comparing the behaviour of the numerically computed perturbations at asymptotic infinity to the decay of the scalar hair in our background solutions, we can say whether the mode has a chance of being pure gauge. Crucially, the above argument shows that modes with $\tilde{\Gamma}>\mathrm{Re}(\Gamma)$ are necessarily physical. For $\tilde{\Gamma}<\mathrm{Re}(\Gamma)$ we cannot say anything for certain.

3.5 Obtaining superradiant modes numerically

In order to solve Eq. (3.21) (Klein-Gordon equation on a fixed Kerr or hairy background) we take advantage of the fact that the background metric $g^{(0)}_{ab}$ is stationary and axisymmetric and as such we can decompose the scalar field perturbation as

$$\eta=\hat{\eta}(x,z)e^{-i\,\omega\,t+i\,m\,\phi}, \tag{3.27}$$

and solve for $(\hat{\eta},\omega)$ given a value of m (recall that $\tilde{m}$ denotes the azimuthal quantum number of the background solution, and m the quantum number of the corresponding perturbations). We focus on the fundamental mode ($n=0$), as it is the fastest growing one. To solve the resulting eigenvalue problem, we will use Newton's method [29]. For the numerical simulations we use spectral collocation methods on a Chebyshev grid and impose appropriate boundary conditions. The BH radius drops out of the equations, hence, without loss of generality, we set $r_0=1$. Apart from imposing boundary conditions it is also necessary to factor out the asymptotic behaviour of the scalar field at the boundaries of the coordinate grid, so that numerically we are solving for smooth functions. The required factors can be inferred by performing a Frobenius analysis about the locations of interest. Near asymptotic infinity ($x=1$), we have a wave-like equation in the radial direction, with the constant term coming at a different order in the expansion, suggesting a factor of the form $e^{\frac{\alpha}{1-x^2}}$. Furthermore,

the z-derivatives show up earlier in the series than the radial ones, requiring a further $(1-x^2)^\beta$ to be taken out. α and β are determined by the series expanded equations and the requirement for a finite energy solution. The boundary condition itself turns out to be of Robin type.

$$\begin{aligned}
\hat{\eta}(x,z) &= e^{\frac{\alpha}{1-x^2}}(1-x^2)^\beta f(x,z)\,,\\
\alpha = -\sqrt{\mu^2-\omega^2},\ \beta &= 1+\frac{2\mu^2-4\omega^2+(\mu^2-\omega^2)\partial_x C(1,z)+\omega^2\partial_x F(1,z)}{4\sqrt{\mu^2-\omega^2}}\,,\\
(1-z)\partial_x f(x,z)\big|_{x=1} &= \hat{U} f(x,z)\big|_{x=1}\,,\\
\hat{U}(x,z) &= \left[G_1(z)\partial_{zz}+G_2(z)\partial_z+G_3(x,z)\right]\,,
\end{aligned} \tag{3.28}$$

with

$$G_1(z) = -\frac{(1-z)(2-z^2)}{4\sqrt{\mu^2-\omega^2}},\ G_2(z) = -\frac{z(3z^2-4m(2-z^2)-5)}{4(1+z)\sqrt{\mu^2-\omega^2}}\,, \tag{3.29}$$

$$\begin{aligned}
G_3(x,z) = &-\frac{(1-z)}{4}\left(\partial_x A(x,z)+\partial_x D(x,z)\right)+\frac{(1-z)(3\mu^2-5\omega^2)}{8\sqrt{\mu^2-\omega^2}}\,\partial_x C(x,z)\\
&-\frac{1}{16}(1-z)\sqrt{\mu^2-\omega^2}\,\left(\partial_x C(x,z)\right)^2+\frac{(1-z)\sqrt{\mu^2-\omega^2}}{4}\,\partial_{xx}C(x,z)\\
&+\frac{(1-z)\omega^2}{8\sqrt{\mu^2-\omega^2}}\,\partial_x C(x,z)\,\partial_x F(x,z)-\frac{(1-z)(5\omega^2-\mu^2(7\omega^2-2\sqrt{\mu^2-\omega^2}))}{8\left(\mu^2-\omega^2\right)^{3/2}}\,\partial_x F(x,z)\\
&-\frac{(1-z)\omega^2(4\mu^2-3\omega^2)}{16\left(\mu^2-\omega^2\right)^{3/2}}\,\left(\partial_x F(x,z)\right)^2+\frac{(1-z)\omega^2}{4\sqrt{\mu^2-\omega^2}}\,\partial_{xx}F(x,z)\\
&+\frac{1-z}{4\left(\mu^2-\omega^2\right)^{3/2}}\left[3\mu^4+8\omega^4+4m(1+m)(\mu^2-\omega^2)-2\mu^2\left(6\omega^2-\sqrt{\mu^2-\omega^2}\right)\right]
\end{aligned}$$

Close to the horizon ($x=0$), the power series indicate the presence of a regular singularity, forcing us to pull out x^γ in front, whereby the constant is determined by the expanded equations and the restriction to ingoing waves only at the horizon. We impose Neumann boundary conditions

$$\begin{aligned}
\hat{\eta}(x,z) &= x^\gamma f(x,z)\,,\\
\gamma &= -2i(\omega-m\Omega_H)\,,\\
\partial_x f(x,z)|_{x=0} &= 0\,.
\end{aligned} \tag{3.30}$$

At the north pole of the squashed sphere ($z = 1$), the series expansion again signals for a regular singularity, necessitating a prefactor of $(1 - z^2)^\delta$, with δ determined by the equations. The boundary conditions are Neumann again

$$\begin{aligned} \hat{\eta}(x, z) &= (1 - z^2)^\delta f(x, z)\,, \\ \delta &= m\,, \\ \partial_z f(x, z)|_{z=1} &= 0\,. \end{aligned} \tag{3.31}$$

In the neighbourhood of the symmetry axis $z = 0$, we do not expect any singular behaviour, as this is not a true boundary (had we stuck with the original range of the coordinates, the $z = -1$ boundary would have required the same treatment as $z = 1$), and the series expanded KG equation confirms that. The reflection symmetry in the polar coordinate separates the physical states of the scalar field into two equivalent subsets and the choice of Neumann or Dirichlet boundary conditions, which we are free to make, selects one of the two. We choose the former

$$\partial_z \hat{\eta}(x, z)|_{z=0} = 0\,. \tag{3.32}$$

3.6 Results

We have computed the quasinormal mode spectrum of HBHs with $\tilde{m} = 1$, close to the superradiance onset in Kerr (see Fig.1 in [57]), for perturbations with $m = 1$ and $m = 2$. The former turns out to be pure gauge ($\tilde{\Gamma} = \mathrm{Re}(\Gamma)$), corresponding to shifts in the phase space of HBHs - altering the mass and angular momentum of the scalar cloud around the BH. The modes with $m = 2$, however, are physical and *always* unstable in the regions where the $\tilde{m} = 1$ HBHs exist.

This is summarised in Fig. 3.1, where we plot $\varpi \equiv \omega/\mu$ as a function of $M\mu$ (recall that μ is the mass of the scalar field). Each curve represents a different constant value of μ/T for the background Kerr BHs (or μ_H/T_H for the HBHs - it is the same quantity, but in our numerics we had separate parameters). In order to compare the growth rate of the instability with that of a Kerr BH with the *same* dimensionless angular momentum $J\mu^2$ and dimensionless mass $M\mu$, we plot in Fig. 3.2 the ratio $\mathrm{Im}\,\varpi_H/\varpi_K$, with ϖ_H being computed using the HBHs and ϖ_K with a Kerr BH with the same $J\mu^2$ and $M\mu$. The fact that this ratio is always below unity, indicates that the HBHs are less unstable than Kerr BHs at fixed mass, angular momentum and scalar mass, as argued in [57].

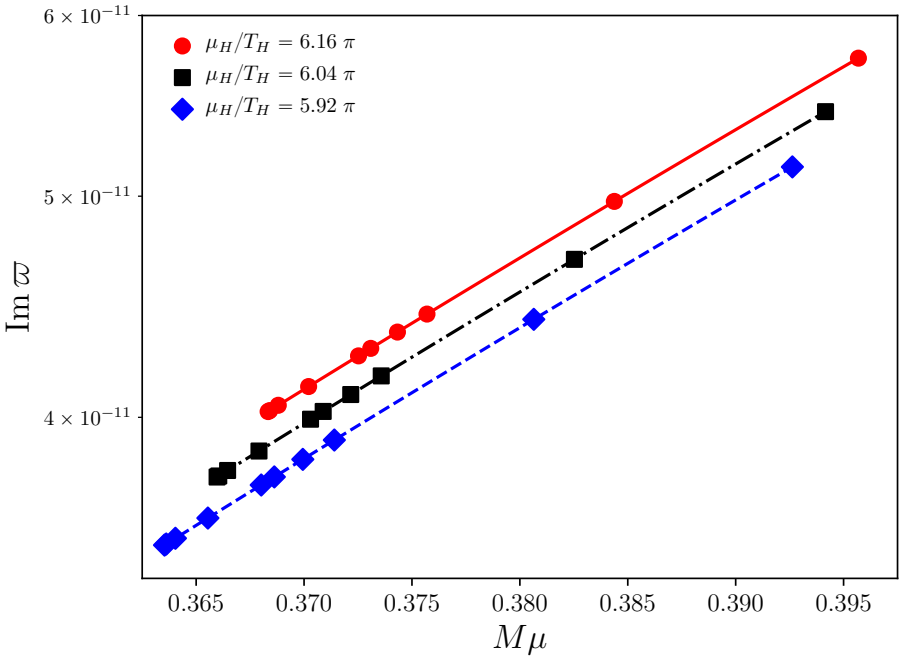

Figure 3.1 The imaginary part of ϖ around HBHs, computed with $m = 2$, as a function of μM - each curve contains a family of HBHs with a fixed value of μ_H/T_H.

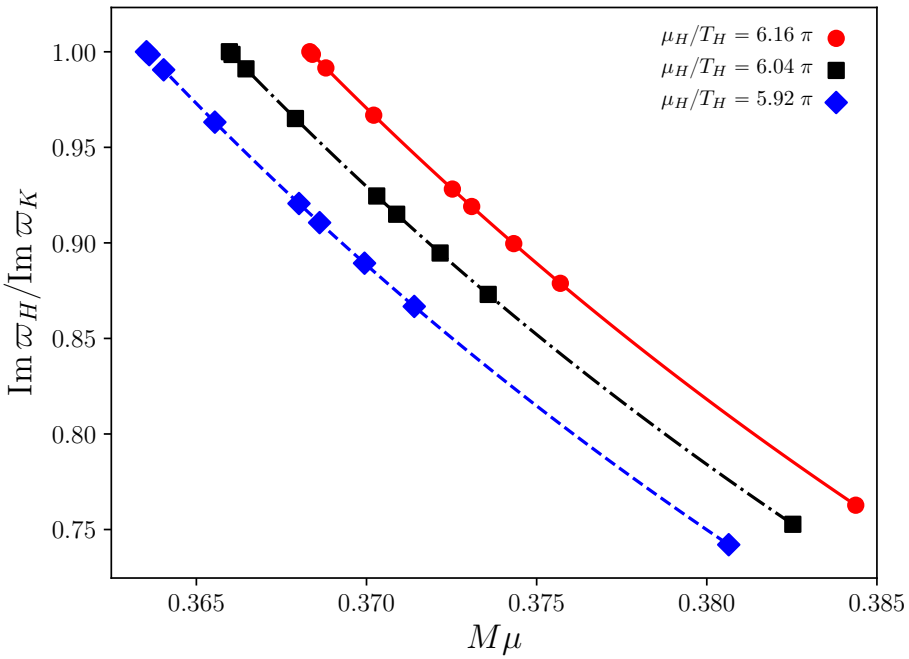

Figure 3.2 The ratio ϖ_H/ϖ_K, as a function of μM - each curve contains a family of HBHs with a fixed value of μ_H/T_H and Kerr BHs with the same $J\mu^2$ and $M\mu$ as the HBHs.

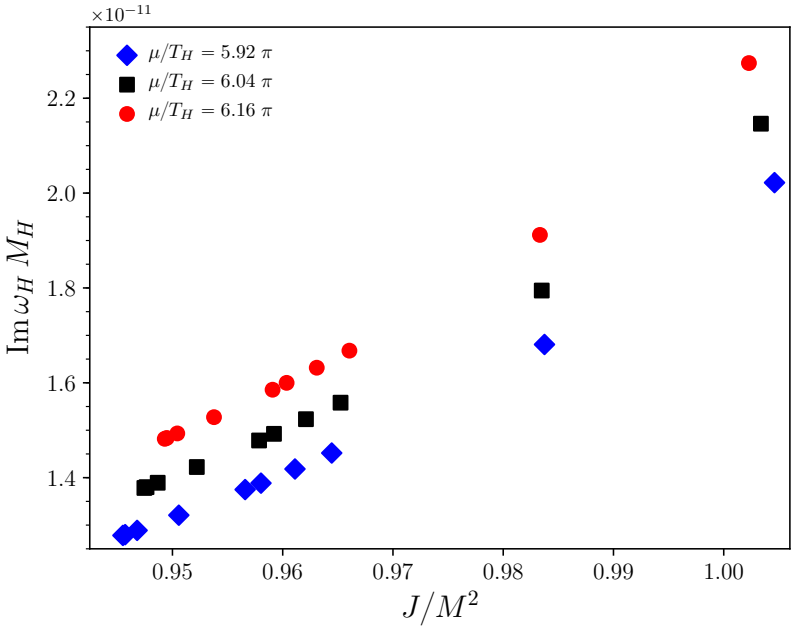

Figure 3.3 The imaginary parts of the QNM spectra of massive scalar field perturbations, $m = 2$, around hairy (ω_H) BHs for several values of μ_H/T_H and J/M^2. M_H is the mass of the respective HBH background. The rightmost point of each constant μ_H/T_H curve is in the superextremal region $J/M^2 > 1$, where Kerr black holes do not exist.

The imaginary parts of the above presented QNM spectra are also separately plotted against J/M^2 in Fig. 3.3 and Fig. 3.4, demonstrating their positivity for the range of parameters considered and clearly showing that the rightmost point on each curve in Fig. 3.2 lies in the region of superextremality $J/M^2 > 1$, where Kerr BHs do not exist. We anticipate similar results for higher m modes.

The real parts of the QNM spectra for perturbations around HBHs are shown in Fig. 3.5.

3.6.1 Numerical convergence tests

In order to verify that solving (3.4) numerically gives us HBHs, we compute the norm of the DeTurck vector ξ^2 for each of the solutions. We should mention that all our calculations were done with arbitrary precision of minimum 30 digits. Here we will exhibit its convergence properties for three of the solutions, which we think should pose the biggest numerical challenges as they are the ones that stretch furthest into the corners of the HBH phase space that we have explored. This includes a solution with the highest value of the scalar field amplitude at the horizon which we have constructed, as well as the fastest and slowest spinning HBHs that we have managed

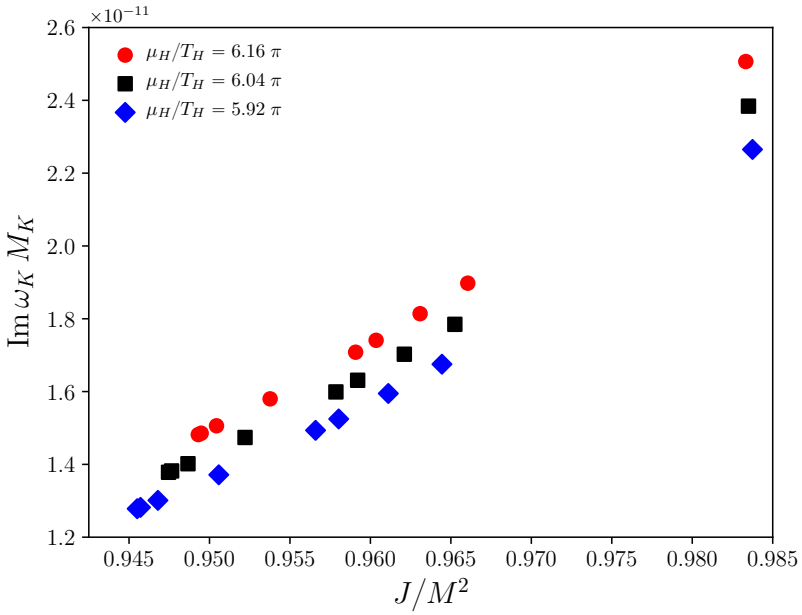

Figure 3.4 The imaginary parts of the QNM spectra of massive scalar field perturbations, $m = 2$, around Kerr (ω_K) as a function of J/M^2. Each background solution has the same $J\mu^2$ and $M\mu$ as the matching HBH point in Fig. 3.3. M_K is the mass of the respective Kerr BH.

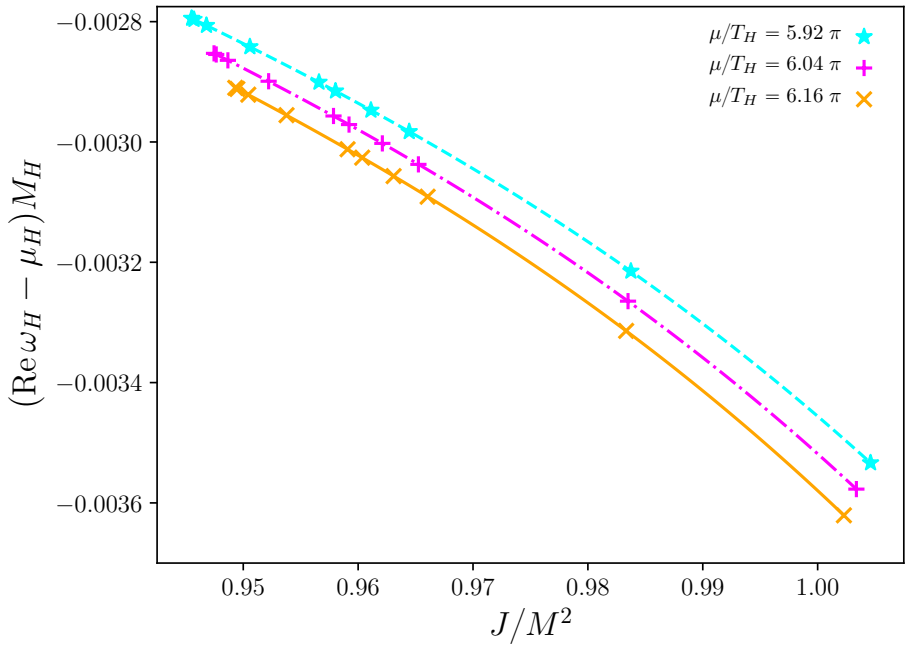

Figure 3.5 Real part of the QNM spectra of massive scalar field perturbations, $m = 2$, around HBHs (ω_H) subtracted by the scalar mass (μ) for several values of μ_H/T_H and J/M^2. M_H - mass of the hairy background.

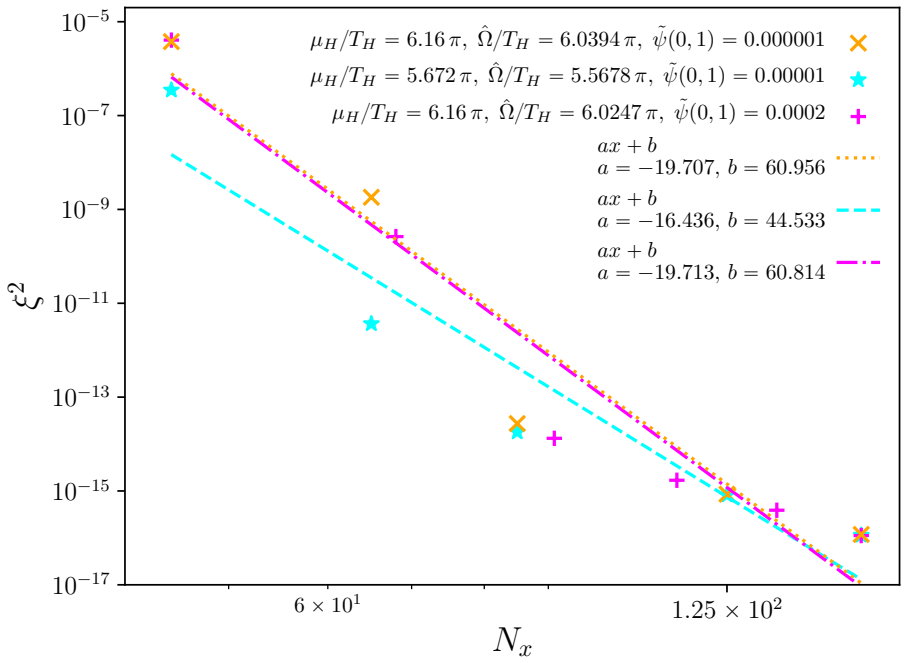

Figure 3.6 The maximum value of ξ^2 for the HBH solutions of (3.4) as a function of radial grid size N_x on a Log-Log plot

to obtain. The results are shown in Fig. 3.6 where we present the maximum value of ξ^2 for different radial grid sizes on a Log-Log plot. In the angular direction we are fixed at $N_z = 35$, as this was found to be sufficient. Only the lowest angular velocity solution (the first to be found) has been obtained at $N_x = 125$. The maximum resolution in the radial direction is $N_x = 160$. The closer to extremality, the harder it is to resolve the AdS_2-like throat appearing near the horizon, thus the worse accuracy for smaller grids.

To check that the superradiant modes that we compute can be trusted, we plot the ratio of the imaginary frequencies of solutions obtained at successive radial resolutions (the angular resolution is fixed at $N_z = 35$)

$$\left| 1 - \frac{\mathrm{Im}\,\omega_{K,N_x}}{\mathrm{Im}\,\omega_{K,N_x+\Delta}} \right| , \tag{3.33}$$

where Δ is the increase in the grid size - Fig. 3.8. We show results for a HBH background, as well as for the three fastest spininng Kerr BHs, due to their proximity to extremality, making them numerically challenging. The data in Fig. 3.7 is obtained in the background of the HBH with the highest scalar field amplitude at the horizon from the solutions that we have found (the hardest one to work with from the HBHs), whereas Fig. 3.8 represents the results in the three Kerr backgrounds discussed above.

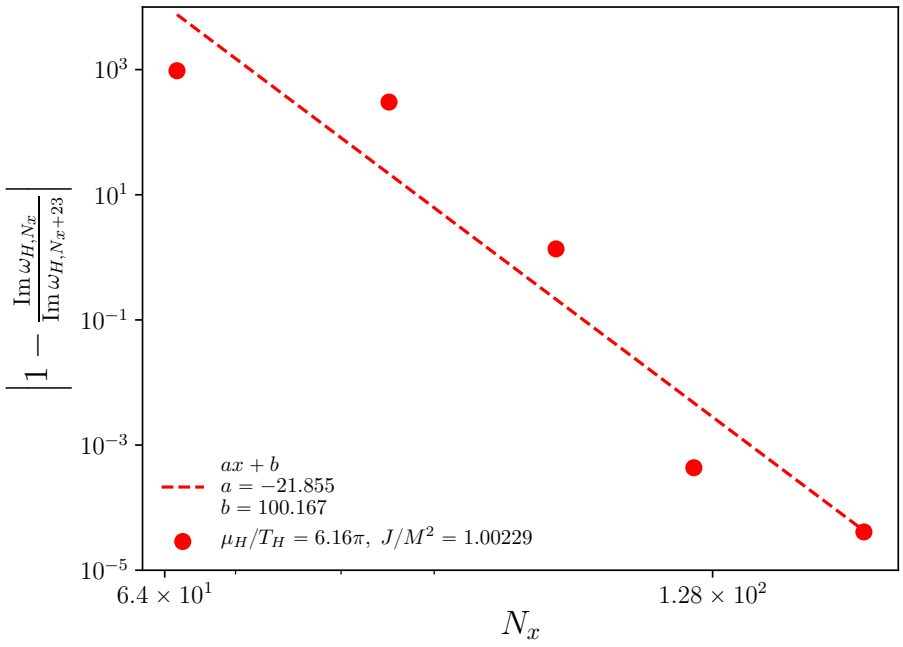

Figure 3.7 Numerical convergence of the imaginary part of the superradiant frequency of the scalar field with $m = 2$ in a fixed HBH background for the highest scalar field amplitude at the horizon that we have considered in our studies.

The decays are not exponential because of the non-analytic behaviour of the scalar field near asymptotic infinity, $(x = 1)$, and the horizon, $(x = 0)$. All results presented in the main section have been obtained at the highest resolution available for the respective spacetime - from 160×35 to 260×35, where we can safely trust the first four digits of the results.

3.7 Conclusions

We have perturbed the HBHs of [109] and we have shown that they are unstable to linear mode perturbations. For the range of parameters that we have analysed, these BHs are uniquely identified by an integer $\tilde{m}$ and by the ratios μ/T_H and J/M^2 (or Ω_H/T_H). All unstable modes we found have $m > \tilde{m}$. Furthermore, for small amplitudes of the scalar hair around the BH, the growth rate of the instability is comparable to that of a massive scalar field around a member of the Kerr family, whereas ,for large scalar hair amplitudes, the HBHs are a few times less unstable than their nonhairy counterparts.

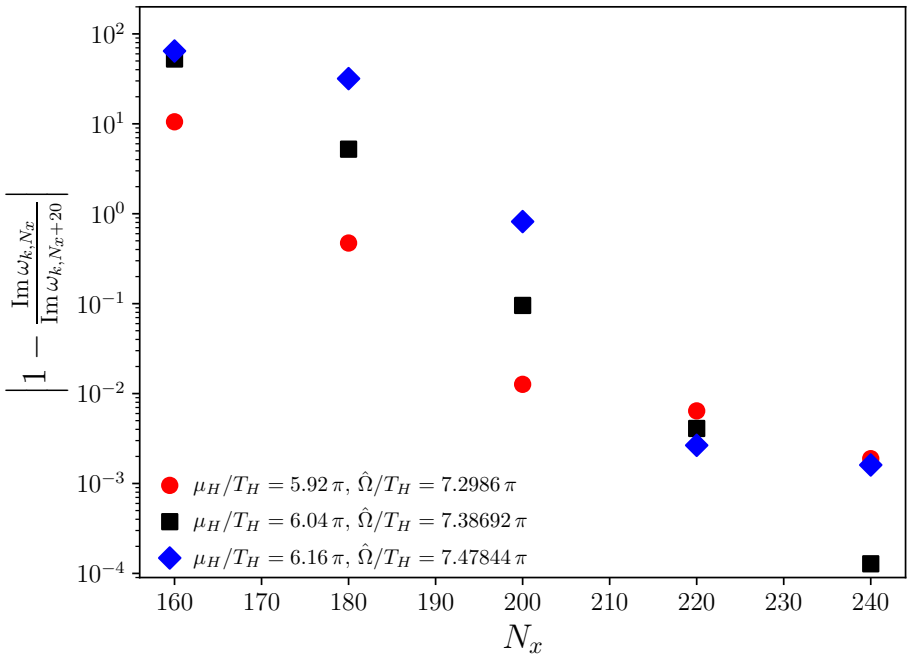

Figure 3.8 Numerical convergence of the imaginary part of the superradiant frequency of the scalar field with $m = 2$ in a fixed Kerr background for the three fastest spinning BHs that we have considered in our studies.

By comparing the growth rates of the fastest and slowest growing $m = 1$ modes around Kerr, with their equivalent $m = 2$ modes around a HBH at the same J/M^2 and fixed gravitational coupling $M\mu$, we can assess the astrophysical significance of the portion of the moduli space of HBHs of [109] that we studied. In this comparison we are neglecting the energy radiated during the formation of the HBH, which is a reasonable approximation [24, 26, 71, 70]. We take a HBH with $J/M^2 = 0.983$ and $M\mu = 0.3844$, where the fastest decay is observed and another one with $J/M^2 = 0.946$ and $M\mu = 0.3635$, where the instability is the weakest. Our data imply that the former undergoes an instability, due to the $m = 2$ mode, evolving on timescales between $\tau \sim 4.8 \times 10^6$ s and $\tau \sim 1.7 \times 10^7$ s for the smallest and largest final mass BHs as detected by LIGO-VIRGO and $\tau \sim 2.7 \times 10^{15}$ s for supermassive BHs ($10^{10}\,M_\odot$). For the corresponding Kerr BH, the $m = 1$ superradiant mode extracts energy efficiently [24, 26, 71, 70], exhibiting e folding times between $\tau \sim 795$ s and $\tau \sim 2740$ s, for the same intermediate masses as above, and $\tau \sim 4.4 \times 10^{11}$ s in the case of supermassive BHs. The second HBH is subject to instabilities with lifetimes of the order of $\tau \sim 6.9 \times 10^6$ s, $\tau \times 2.4 \times 10^7$ s and $\tau \times 3.8 \times 10^{15}$ s for the three cases of BH masses. The complementary unstable Kerr solution experiences similar rates - $\tau \sim 1.1 \times 10^7$ s, $\tau \sim 3.7 \times 10^7$ s and

$\tau \sim 6.0 \times 10^{15}$ s accordingly. This implies that in the explored region of parameter space HBHs may suffer from superradiance on the same scale as their nonhairy counterparts, but they can also be distinctly more robust to its effects. Nevertheless, the timescales involved in both processes are at least two orders of magnitude smaller than the age of the Universe for the HBH solutions we analysed.

We should note that some regions of the moduli space of the HBHs are not excluded by our analysis [57]. In particular, it has been predicted in [132, 107] that starting from the onset of superradiance in Kerr, and continuing along a line of constant $M\mu$, the instability growth rate for HBHs decreases towards zero as the corresponding ergoregionless-boson star is approached. Thus, it is conceivable that the region not excluded by our analysis is actually larger than the excluded region.

Chapter 4

Plausible scenario for a generic violation of the WCCC in asymptotically flat 4D

4.1 Introduction

In the first chapter we introduced the concept of the Weak Cosmic Censorship Conjecture (WCCC) - singularities in General Relativity should be hidden behind event horizons. We gave as precise a formulation as we could and listed evidence in its support. However, we also mentioned potential counterexamples to the WCCC that have appeared in the literature in recent years. We will now quickly review some of these.

We start with likely violations in dimensions more than four [77], and more precisely, with the famous simulation of Luis Lehner and Frans Pretorius of five-dimensional black strings [117], which shows that subject to the so-called Gregory-Laflamme (GL) instability [98], they develop a self-similar structure suggestive of a pinch-off of the apparent horizon in finite asymptotic time, which will reveal the singularity inside to an outside observer [137]. The GL instability is present for black holes whose horizons are extended in at least one direction compared to the rest. It is a result of long-wavelength perturbations and settles in for wavelengths larger than a certain threshold, which for black strings depends on the dimensionality (black strings exist in any dimension larger than four) and the radius of the string's horizon, which has the topology of a cylinder in five dimensions. The behaviour of black strings under the GL instability resembles that of fluids with surface tension subject to a classical membrane instability,

named after Rayleigh and Plateau[1], which, depending on the conditions, can eventually lead to the breakup of the liquid jet. In fact, many key features of the black string instability can be reproduced using this analogy [28]. Depending on the viscosity of the fluid, the breakup is foreran by the formation of spherical bulges along the jet, separated by thin necks. This process keeps on repeating with newer bulges appearing, connected by even thinner necks, until eventually the fluid breaks up. At this point the Navier-Stokes equations of fluid mechanics break down, indicating a singularity. However, we know from experiments that it is molecular dynamics that resolves it [72]. The black string undergoes a very similar evolution, whereby its intermediate state is characterised by a series of three-dimensional spherical black holes connected by thin black string segments. In the simulation of [137], the breakup of the string is not actually observed, as it is not possible to run the numerics for so long, however, the authors give convincing arguments for it happening, based on the self-similarity of the process. There are two points that should be pointed out about this result. The authors track the evolution of the apparent horizon, as that is much easier to do than for the event horizon. It is a result of General Relativity that apparent horizons are always contained within event horizons, thus it is theoretically possible to imagine a situation in which the apparent horizon pinches off, but the event horizon does not. Nevertheless, it is believed that this is not the case. In addition, the simulation starts with an unstable solution and it is not known whether one can actually arrive at it starting from initial data, as one needs to do for a true violation of the WCCC.

The above example is not actually in an asymptotically flat setting, as the transverse direction of the spacetime, along which the event horizon extends, is periodically identified (black strings extend infinitely). However, there are also plausible counterexamples in higher dimensions, which are asymptotically flat - black rings in five dimensions [81], and Myers-Perry (MP) black holes in six [80]. One can intuitively see this by noting that making the rings very thin, leads to them locally resembling black strings, and hence, they undergo an analogous evolution to the black strings, with the same conclusion. Similarly in the MP case, for high enough angular momenta, they thin out and start looking like a black brane, which is also subject to the GL instability, and thus, again a similar behaviour as for the strings is observed.

The last two counterexamples that we will discuss are with AdS asymptotics. The first work is in Einstein gravity with negative cosmological constant in four dimensions, coupled to a Maxwell field [116, 48, 47]. The latter lives at the boundary, which is flat, as the authors work in the Poincaré patch of AdS, and has only a time component whose

[1]These are not the only similarities between gravity and fluids - for more information [22, 75].

amplitude can be time-dependent. The proposal is based on the idea that for a constant amplitude vector potential one can construct static, zero temperature bulk solutions, which represent self-gravitating electric fields, but only up to a certain threshold value for the amplitude [114]. Above these maximum values, the authors found that naked singularities form in the bulk. Therefore, the setup for a violation consists in starting from a vanishing potential and gradually increasing its amplitude at the boundary with time, until it goes past the threshold value. Performing time evolution of the system numerically shows that, past the critical amplitude value, $F_{\mu\nu}F^{\mu\nu}$ starts growing unboundedly in time along the whole Poincaré horizon. From the Einstein equation one can show that this is equivalent to curvature growing unboundedly as well. However, the authors do not form a singularity in their simulations, which means that they do not violate a precise formulation of the WCCC, similar to the one we gave in the introductory chapter, but with AdS asymptotics. To clarify in a few words - the generalisation to asymptotically AdS spacetimes will involve starting from a well-behaved initial data, with corresponding well-defined boundary conditions, and prohibit the formation of singularities observable from the boundary. The authors instead motivate a more "physical" in intuition formulation of the conjecture. One way of thinking about the WCCC is: It tells us that regions where new physics is expected to start becoming important and classical theory breaks down will be inaccessible to us behind an event horizon. New physics are associated with an energy scale, thus one can attempt to rephrase the WCCC in terms of an energy scale, which should be unattainable if one starts from well-behaved initial data with appropriate boundary conditions. The authors then claim that whatever that scale is, if an observer is ready to wait long enough, then the curvature along the Poincaré horizon in their system will eventually reach it, and hence, the WCCC will be violated. We should point out that, in contrast to the previous counterexamples that we presented, whereby the violation happens at an infinitesimally small event in spacetime, here curvatures grow unboundedly in a large region. Moreover, the authors try different profiles for the vector potential at the boundary and show that the violating behaviour is generic.

If one accepts the "physical" version of the WCCC, then the above scenario provides a valid counterexample to the conjecture in classical Einstein-Maxwell gravity in four dimensions with a negative cosmological constant. More interestingly though, we also know how to resolve this violation. The idea how to achieve this comes from the so called Weak Gravity Conjecture, which is a statement about quantum gravity. In simple terms, it states that elementary particles, with a certain charge to mass ratio, must be present in the theory, in order to allow extremal charged black holes to decay.

Formulating a classical version of the aforementioned statement [47] inclines the authors to add charged scalar fields to the system. The presence of these particles makes the static solutions susceptible to charged superradiance, which leads to the branching off of new type of hairy solutions in the system, as long as the charge of the particles is large enough. The value required coincides with what one gets from the Weak Gravity conjecture, and the new hairy solutions are regular past the critical threshold value of the amplitude from before. Hence, no naked singularities are expected to appear in the time evolution anymore.

The second setup for violation of the WCCC in AdS comes from the superradiant instability of Kerr-AdS [142]. We will discuss the case of gravitational perturbations [29, 63], decomposed in Fourier modes, similar to previous chapters. As we mentioned briefly before, the timelike nature of the AdS boundary provides a natural confining mechanism, which allows superradiant modes to repeatedly bounce back and forth between the event horizon and the boundary, extracting energy and angular momentum from the black hole in the process, until eventually the backreaction of the waves becomes significant enough so that it cannot be neglected, resulting in the the superradiant instability. In our case the waves accumulate gravitational energy in a "condensate" around the black hole, leading to the formation of a *black resonator* [61, 65] - a representative of a new family of stationary black hole solutions in the system, invariant only under a single helical KVF. They branch off at the onset of superradiance for a specific superradiant mode in Kerr-AdS - that is, for a certain ℓ and m in the harmonic decomposition of the perturbations, and thus select out its particular frequency. A given black resonator is stable towards superradiance from the mode that it branched off from (and lower m modes), but is unstable towards higher m superradiant modes. Moreover, for the same asymptotic charges, E and J, the black resonators have higher entropy than Kerr-AdS and are thus favoured thermodynamically. In addition, their entropy is an increasing function of m, therefore progression towards superradiant modes with higher azimuthal numbers is preferred.

On top of that, in a generic setup the initial data will have support on more than a single perturbation mode (in addition, the non-linearities of the Einstein equation will excite further modes), implying that the above finite m black resonator cannot be the endpoint of the superradiant instability. One can imagine then that the system will continue evolving towards configurations with higher and higher m, until it reaches a limiting black resonator with $m \to \infty$, which will be stable against all other modes. Nevertheless, the authors argue [142], based on supersymmetry and energetic arguments, combined with the fact that in their zero-size limit the black resonators connect to

geons - smooth and horizonless, blobs of gravitational energy with harmonic time dependence in pure AdS - that if such a black resonator exists, it would not be regular. They claim afterwards that due to the lack of any other known stationary solutions, the system either settles down to a singularity in a finite time - violating the weak cosmic censorship - or it continues to evolve indefinitely towards configurations with even higher azimuthal number m and entropy, necessitating the consideration of physics on smaller and smaller scales. Eventually though, one will reach a regime where the effects of quantum theory might become important, thus again violating the WCCC, though its physically motivated version this time.

As we saw in the previous chapter, the confining nature of the AdS boundary can be simulated in an asymptotically flat setting by considering massive perturbations, and it is exactly that we will do in this chapter, however, with real (not complex as in the case investigated before) scalars. We propose a four-dimensional, asymptotically flat counterexample to the WCCC motivated by the superradiant instability [17, 170, 55, 190, 60, 68, 188, 24, 25, 166], afflicting real, massive scalar perturbations around Kerr black holes (BHs) [127] - rotating, with spherical topology and considered the most general BH solutions of the vacuum Einstein equation [156].

The angular dependence of such perturbations around Kerr is parametrised by two integers $\{m, \ell\}$: m counts the number of nodes in the azimuthal direction and $\ell - |m|$ the number of zeros in the polar direction. We show that for *any* scalar field of mass μ and *any* nonzero value of the BH spin, for sufficiently large values of $\ell = m$, these perturbations herald instabilities around the BH, extracting energy and angular momentum. Furthermore, the timescales associated to these instabilities grow parametrically as $e^{4\,\ell\,\log\ell}$, indicating that each of the ℓ modes decouples from the rest, evolving independently.

As time progresses, modes with smaller values of ℓ stabilise one by one, forming scalar clouds around the BH, similar to those in [35, 109]. However, these BHs were shown to be unstable to higher m-modes [95], giving rise to the expectation of a cascade towards larger values of ℓ. This corresponds to a transfer of energy from lower ℓ-modes to higher ones, indicating an evolution towards smaller scales - a phenomenon akin to turbulence in nonrelativistic $3+1$ fluids.

A possible stabilising mechanism is the emission of gravitational waves (GWs) by the scalar clouds [159, 26]. We are working with a real field this time, hence the stress-tensor will not be stationary and axisymmetric, implying that gravitational radiation will not be suppressed. Moreover, the massive scalar is minimally coupled and no other matter is present in the system, hence there is no scalar radiation to

be concerned about, as the superradiant growth and quasinormal decay are already accounted for at the linear level. So, were the gravitational waves to dissipate the clouds' energy faster than superradiance creates them, the above scenario would not be possible. We numerically compute the GW emission for fixed gravitational coupling, $M\,\mu$, and spin parameter, J/M^2, as a function of $\ell = m$ and find that it leads to energy and angular momentum dispersion that would not be able to counter the efficiency of superradiance.

This chapter is organised as follows: first we present our setup and provide analytic and numerical data for the instability timescales at large ℓ. We then compute, numerically, the energy radiated towards future null infinity in this process as well as the backreaction of the scalar on one of the components of the Weyl tensor. We see that modes with higher ℓ radiate less, implying that energy is accumulated at small scales more efficiently for larger values of ℓ. Finally we end with discussion of the results.

4.2 Setup

We work with the Einstein-Hilbert action minimally coupled to a real massive scalar field ψ

$$S = \int_{\mathcal{M}} \mathrm{d}^4x\sqrt{-g}\left(\frac{R}{16\,\pi\,G} - \nabla_a\psi\nabla^a\psi - \mu^2\psi^2\right), \tag{4.1}$$

where μ is the scalar field mass, g_{ab} the spacetime metric and R its Ricci scalar. The equations of motion are

$$R_{ab} - \frac{R}{2}g_{ab} = 8\pi\,G\,T_{ab}, \tag{4.2a}$$

where R_{ab} is the Ricci tensor of g_{ab},

$$\Box\psi = \mu^2\psi\,, \tag{4.2b}$$

and

$$T_{ab} = 2\nabla_a\psi\nabla_b\psi - g_{ab}\nabla^c\psi\nabla_c\psi - \mu^2\psi^2 g_{ab}\,. \tag{4.2c}$$

An important solution to these equations is the Kerr BH [127], with $\psi = 0$ and

$$\mathrm{d}s^2 = -\frac{\Delta}{\Sigma^2}\left(\mathrm{d}t - a\sin^2\theta\mathrm{d}\phi\right)^2 + \Sigma\left(\mathrm{d}\theta^2 + \frac{\mathrm{d}r^2}{\Delta}\right) + \frac{\sin^2\theta}{\Sigma^2}[a\,\mathrm{d}t - (r^2+a^2)\mathrm{d}\phi]^2\,, \tag{4.3}$$

where $\Delta = r^2 + a^2 - 2\,M\,r$, $\Sigma^2 = r^2 + a^2\cos^2\theta$, $\phi \in (0, 2\pi)$ is a periodic coordinate and $\theta \in (0, \pi)$ is a polar coordinate. The BH event horizon is a null hypersurface

with $r = r_+ \equiv M + \sqrt{M^2 - a^2}$, angular velocity $\Omega_K = a/(a^2 + r_+^2)$ and surface gravity $\kappa_K = (r_+^2 - a^2)/[2r_+(r_+^2 + a^2)]$. The constant M is the BH mass and a parametrises its angular momentum via $J = M\,a$. The absence of naked singularities demands $|a| \leq M$, with the inequality being saturated at extremality, when the Kerr BH event horizon becomes degenerate with $\kappa_K = 0$.

We study Eq. (4.2b) on a fixed Kerr background (4.3), which is stationary and axisymmetric with respect to the Killing fields $\partial/\partial t$ and $\partial/\partial\phi$, respectively. We consider perturbations of the form

$$\psi(t, r, \theta, \phi) = e^{-i\,\omega\, t + i\, m\, \phi}\widehat{\psi}_{\omega m}(r, \theta), \tag{4.4}$$

and assume that $\widehat{\psi}_{\omega m}(r, \theta)$ is separable, $\widehat{\psi}_{\omega m}(r, \theta) = R_{\omega\ell m}(r)S_{\omega\ell m}(\theta)$, with the label ℓ anticipating that the separation constant will be parametrised by an integer ℓ. Not all solutions to Eq. (4.2b) are separable, but we are interested in those composed of the sum (possibly infinite) of such separable solutions. $\omega \in \mathbb{C}$ is a complex frequency, determined by imposing appropriate boundary conditions. We are interested in finding unstable mode solutions for which $\mathrm{Im}(\omega) > 0$.

Inserting the *ansatz* (4.4) into Eq. (4.2b) yields a system of two second order ordinary differential equations (ODEs), coupled via the separation constant Λ,

$$\Delta\left[\Delta\, R_{\omega\ell m,r}\right]_{,r} + V(r)R_{\omega\ell m} = 0, \tag{4.5a}$$

$$\frac{1}{\sin\theta}\left[\sin\theta\, S_{\omega\ell m,\theta}\right]_{,\theta} - \left[a^2\, k^2\cos^2\theta + \frac{m^2}{\sin^2\theta} - \Lambda\right] S_{\omega\ell m} = 0, \tag{4.5b}$$

where

$$V(r) = -k^2r^4 + 2M\mu^2r^3 - (\Lambda + a^2k^2)r^2 + (2M\Lambda - 4amM\omega + 2Ma^2\omega^2)r - a^2(\Lambda - m^2)\,, \tag{4.5c}$$

with $k \equiv \sqrt{\mu^2 - \omega^2}$. Finding bound states amounts to finding the values of ω for which ψ has ingoing boundary conditions at the event horizon (consistent with the equivalence principle), and finite energy on a partial Cauchy surface $t = \text{const}$.

This problem can be tackled numerically (for any values of the parameters) and analytically (in certain regions of moduli space), with the same method as in [79], which combines a matched asymptotic and WKB type approach. We will first compute the modes using a WKB expansion in m, which we detail next.

4.3 WKB Expansion and Numerical Validation

Our WKB expansion is valid for any spin parameter $|a| < M$, and only assumes m to be large. For small values of a and μ, it reproduces the results in [60] (up to an infamous factor of 2, see [91]). It should be noted that the large m limit does not commute with the extremal limit. It can be shown that at any finite value of m, $\mathrm{Im}(\omega) = 0$ at extremality. However, the region of the black hole moduli space where this behaviour occurs scales inversely with m, and is thus absent in the strict $m \to +\infty$ limit. The behaviour in this region could be investigated by switching the order of limits.

We work with $l - m = n$, where $n \sim \mathcal{O}(1)$, $n \in \mathbb{N}_0$. To this end, we rewrite the Klein-Gordon equation in the following way

$$\frac{r - r_+}{r_+}\left[\Delta\, R'_{\omega\ell m}(r)\right]_{,r} + V(r)\, R_{\omega\ell m}(r) = 0, \tag{4.6a}$$

$$\frac{\left[\sin\theta\, S'_{\omega\ell m}(\theta)\right]_{,\theta}}{\sin\theta} - \left[\tilde{a}^2\,\tilde{k}\,\cos^2\theta + \frac{m^2}{\sin^2\theta} - \Lambda\right] S_{\omega\ell m}(\theta) = 0, \tag{4.6b}$$

$$\begin{aligned} V(r) &= a_1 + a_2\,\frac{r}{r_+} + a_3\,\frac{r^2}{r_+^2} - \tilde{k}\,\frac{r^3}{r_+^3} + \frac{a_4}{r/r_+ - \tilde{a}^2}, \\ a_1 &= \Lambda + \tilde{a}\,\tilde{\omega}\left(1+\tilde{a}^2\right)\left[\tilde{a}\,\tilde{\omega}\left(1+\tilde{a}^2\right) - 2\,m\right], \\ a_2 &= \tilde{a}^2\,\tilde{\omega}^2\left(1+\tilde{a}^2\right) - \Lambda, \quad a_3 = \tilde{\mu}^2 + \tilde{a}^2\,\tilde{\omega}^2, \\ a_4 &= \tilde{a}^2\left[m - \tilde{a}\,\tilde{\omega}\left(1+\tilde{a}^2\right)\right]^2, \end{aligned} \tag{4.6c}$$

where $\tilde{k} = \tilde{\mu}^2 - \tilde{\omega}^2$, Λ is the angular separation constant and we have introduced dimensionsless variables

$$\tilde{a} = \frac{a}{r_+},\ \tilde{M} = \frac{M}{r_+},\ \tilde{\omega} = \omega\, r_+,\ \tilde{\mu} = \mu\, r_+. \tag{4.7}$$

In the eikonal limit $\ell \gg 1$ the spheroidal eigenvalue is $\Lambda = \ell(\ell+1) + O(\ell^{-1})$; this can easily be verified by a series expansion of the angular equation after prefactoring $(\sin\theta)^m$ from $S(\theta)$. In order to determine $\tilde{\omega}$ we divide the domain in two intersecting regions, solve (4.6a) in each of them, and then match the solutions in the overlap. To

this end we introduce the new variable $x = r/r_+ - (1+\tilde{a}^2)$

$$
\begin{gathered}
(x+\tilde{a}^2)\Big[\tilde{\Delta}\, R'_{\omega\ell m}(x)\Big]_{,x} + \tilde{V}(x) R_{\omega\ell m}(x) = 0, \qquad (4.8)\\
V(x) = b_1 + b_2\, x + b_3\, x^2 - \tilde{k}\, x^3 + \frac{a_4}{1+x},\\
b_1 = \tilde{\omega}^2\left(1+\tilde{a}^2\right)^2\left(1+4\,\tilde{a}^2\right) - 2\,m\,\tilde{a}\,\tilde{\omega}\left(1+\tilde{a}^2\right) - \tilde{a}^2\Big[\ell(\ell+1) + \left(1+\tilde{a}^2\right)^2\tilde{\mu}^2\Big],\\
b_2 = -\left(1+\tilde{a}^2\right)\Big[\left(1+3\,\tilde{a}^2\right)\tilde{\mu}^2 - 3\left(1+2\,\tilde{a}^2\right)\tilde{\omega}^2\Big] - \ell(\ell+1),\\
b_3 = \left(3+4\,\tilde{a}^2\right)\tilde{\omega}^2 - \left(2+3\,\tilde{a}^2\right)\tilde{\mu}^2,
\end{gathered}
$$

with $\tilde{\Delta} = (1+x)(x+\tilde{a}^2)$.

4.3.1 Near-horizon region

Using quasimodes [113, 125], one can show that $\tilde{k} = \mathcal{O}(\ell^{-2})$. We thus take the near-horizon region to be defined by $x \ll \ell^2$ and see that

$$
\tilde{k}\, x^3 \ll x\, m^2, \quad b_3\, x^2 \ll x\, m^2, \qquad (4.9)
$$

implying that we can drop the cubic and quadratic terms inside $V(x)$, leaving us with

$$
(x+\tilde{a}^2)\Big[\tilde{\Delta}\, R'_H(x)\Big]_{,x} + \left[b_1 + b_2\, x + \frac{a_4}{1+x}\right] R_H = 0. \qquad (4.10)
$$

We then multiply the equation by $(1+x)$ and change variables to $u = (x+\tilde{a}^2)/(1-\tilde{a}^2)$, leading us to a solution as a linear combination of Gauss hypergeometric functions

$$
\begin{aligned}
R_H(x) = A_{in}(-u)^{\delta}(1+u)^{\phi}\,{}_2F_1\Big[c_-, c_+; c; -u\Big]\\
+ A_{out}(-1)^{-2\,\delta}(-u)^{-\delta}(1+u)^{\phi}\,{}_2F_1\Big[\lambda_-, \lambda_+; 2-c; -u\Big],
\end{aligned}
$$

where $u = (x+\tilde{a}^2)/(1-\tilde{a}^2)$, $A_{in/out}$ are constants and

$$
\begin{gathered}
\delta = \frac{i\,\Omega_0}{1-\tilde{a}^2}\left[1 + \frac{\tilde{a}^4(1-\tilde{a}^4)(2\,\tilde{\mu}^2 - 3\,\tilde{\omega}^2)}{\Omega_0^2}\right]^{\frac{1}{2}}, \quad \phi = -i\,\frac{m - \tilde{a}\,\tilde{\omega}\,(1+\tilde{a}^2)}{1-\tilde{a}^2},\\
\Omega_0 = m\,\tilde{a} - \tilde{\omega}\,(1+\tilde{a}^2)\\
c_\pm = \frac{1}{2} \pm \frac{\sqrt{1-4\,b_2}}{2} + \phi + \delta, \quad c = 1+2\,\delta, \quad \lambda_\pm = c_\pm - c + 1. \qquad (4.11)
\end{gathered}
$$

Demanding ingoing waves only at the horizon, $x = 0$, requires setting $A_{out} = 0$. To see this, note that in the limit $x \to 0$ the hypergeometric functions take on a constant value to leading order, hence one just needs to know which of $(-u)^{\pm\delta}$ gives the correct behaviour there. This can most easily be deduced by performing a transformation from BL to Kerr coordinates

$$\mathrm{d}v = \mathrm{d}t + \frac{r^2 + a^2}{\Delta}\mathrm{d}r, \quad \mathrm{d}\chi = \mathrm{d}\phi + \frac{a}{\Delta}\mathrm{d}r. \tag{4.12}$$

Looking at the near-horizon limit allows us to obtain

$$e^{-i\,\omega\,t}e^{i\,m\,\phi} = e^{-i\,\omega\,v}e^{i\,m\,\chi}(r - r_+)^{i\left(\tilde{\omega}\frac{1+\tilde{a}^2}{1-\tilde{a}^2} - \frac{m\,\tilde{a}}{1-\tilde{a}^2}\right)}, \tag{4.13}$$

which has opposite sign to what we expect at the horizon, as the transformation eliminates any singular behaviour.

4.3.2 Far away region

Before zooming into spatial infinity, we first multiply (4.8) by $(1 + x)$, and then make the following transformation, in order to ensure that we will get the correct asymptotic behaviour,

$$\begin{gathered}\mathcal{R}_{\omega\ell m}(x) = h(x)\,Q_\infty(x), \quad h(x) = \frac{\sqrt{4\,\tilde{k}^2\,x^2 + 4\,\tilde{k}\,x\,d_2 + d_1^2}}{2\,\tilde{k}\,x + d_1}, \\ d_1 = \left(1 + 2\,\tilde{a}^2\right)\left(2\,\tilde{\mu}^2 - 3\,\tilde{\omega}^2\right), \quad d_2 = \left(1 + 3\,\tilde{a}^2\right)\tilde{\mu}^2 - \left(2 + 5\,\tilde{a}^2\right)\tilde{\omega}^2.\end{gathered} \tag{4.14}$$

We also have to divide the resulting equation by

$$\frac{(1+x)(x+\tilde{a}^2)(t_0 + t_1\,x + t_2\,x^2 + t_3\,x^3 + 2\,x^4)}{2\,x\,(x+i_0)^2\sqrt{x(x+i_1) + i_0^2}}, \tag{4.15}$$

where we have defined

$$\begin{gathered}t_0 = i_0^3(1+\tilde{a}^2) + \tilde{a}^2(i_0\,i_1 - 2\,i_0^2),\ t_1 = i_0(2\,i_1(1+\tilde{a}^2) + 2\,\tilde{a}^2) - i_0^2(1+\tilde{a}^2) + 2\,i_0^3 - \tilde{a}^2\,i_1, \\ t_2 = 3\,i_0(1+\tilde{a}^2+i_1), \quad t_3 = 1 + \tilde{a}^2 + 4\,i_0 + i_1, \quad i_0 = d_1/(2\,\tilde{k}), \quad i_1 = d_2/\tilde{k}.\end{gathered} \tag{4.16}$$

We are now ready to expand near spatial infinity. We work with $x \gg 1$, which leaves us with

$$\begin{aligned} x^2\, Q''_\infty(x) + 2\, x\, Q'_\infty(x) - (\tilde{k}\, x^2 + e_1\, x - b_2) Q_\infty(x) = 0, \\ e_1 = (1+\tilde{a}^2)(\tilde{\mu}^2 - 2\,\tilde{\omega}^2), \end{aligned} \tag{4.17}$$

to solve. The above can be transformed into Whittaker's differential equation with the help of

$$x = \frac{z}{2\sqrt{\tilde{k}}},\ j(z) = \frac{Q_\infty(z)}{z}, \tag{4.18}$$

resulting in

$$j''(z) + \left(-\frac{1}{4} - \frac{e_1}{2\sqrt{\tilde{k}}\, z} + \frac{b_2}{z^2} \right) j(z) = 0. \tag{4.19}$$

The general solution to (4.19) is then a linear combination of the Whittaker functions $W_{\kappa,\nu}(z)$ and $W_{-\kappa,\nu}(-z)$, thus

$$\begin{aligned} R_\infty = B_1\, v(z)\, W_{-\kappa,\nu}(-z) + B_2\, v(z)\, W_{\kappa,\nu}(z), \\ \kappa = -\frac{e_1}{2\sqrt{\tilde{k}}}, \quad \nu = \frac{1}{2}\sqrt{1 - 4\, b_2}, \quad v(z) = h(z)/z, \end{aligned} \tag{4.20}$$

with $B_{1/2}$ constants. Expanding for large z, and using

$$z = 2\sqrt{\tilde{k}}\left[\frac{r}{r_+} - (1+\tilde{a}^2) \right] \xrightarrow[r\to\infty]{} 2\sqrt{\tilde{k}}\frac{r}{r_+}, \tag{4.21}$$

we see that

$$\lim_{r\to\infty} \left[B_1\, v(z)\, W_{-\kappa,\nu}(-z) + B_2\, v(z)\, W_{\kappa,\nu}(z) \right] = B_1\, e^{\sqrt{\tilde{k}}\, r/r_+} r^{-1-\kappa} + B_2\, e^{-\sqrt{\tilde{k}}\, r/r_+} r^{-1+\kappa}. \tag{4.22}$$

Imposing that the solution decays at infinity sets $B_1 = 0$.

4.3.3 Matching

We now perform the matching procedure in the overlapping region $1 \ll x \ll \ell^2$. To this end, we take $x \sim \ell^{\frac{3}{2}}$ and expand the near-horizon and far-away solutions for large and small variables respectively.

Looking at the near-horizon region first, we can straightforwardly use the standard asymptotic series of the Hypergeometric function, as all the parameters grow slower than the variable of the function, leaving us with

$$\lim_{x\to\infty} R_H = A_{in}\frac{(-1)^\delta\,\Gamma[c_+-c_-]\,\Gamma[c]}{\Gamma[c_+]\,\Gamma[c-c_-]}\left[\frac{x}{(1-\tilde{a}^2)}\right]^{\nu-\frac{1}{2}} + A_{in}\frac{(-1)^\delta\,\Gamma[c_--c_+]\,\Gamma[c]}{\Gamma[c_-]\,\Gamma[c-c_+]}\left[\frac{x}{(1-\tilde{a}^2)}\right]^{-\nu-\frac{1}{2}}. \tag{4.23}$$

Next we consider the expansion of the far-away solution for small variable and again we can use the standard series in the literature to do so, as the parameters outgrow the argument of the Whittaker function, thus

$$\lim_{x\to 0} R_\infty = -B_2\frac{(2\sqrt{\tilde{k}})^{\nu-\frac{1}{2}}\Gamma[-2\,\nu]}{\Gamma[\frac{1}{2}-\nu-\kappa]}x^{\nu-\frac{1}{2}} - B_2\frac{(2\sqrt{\tilde{k}})^{-\nu-\frac{1}{2}}\Gamma[2\,\nu]}{\Gamma[\frac{1}{2}+\nu-\kappa]}x^{-\nu-\frac{1}{2}}. \tag{4.24}$$

Afterwards we equate the coefficients in front of the equivalent terms in (4.23) and (4.24) in order to derive

$$\begin{aligned}\frac{\Gamma[\frac{1}{2}-\nu-\kappa]}{\Gamma[\frac{1}{2}+\nu-\kappa]} &= \left(2\,(1-\tilde{a}^2)\sqrt{\tilde{k}}\right)^{2\,\nu}G(\ell),\\ G(\ell) &= \frac{\Gamma[c_--c_+]\,\Gamma[-2\,\nu]\,\Gamma[c_+]\,\Gamma[c-c_-]}{\Gamma[2\,\nu]\,\Gamma[c_+-c_-]\,\Gamma[c_-]\,\Gamma[c-c_+]}.\end{aligned} \tag{4.25}$$

Furthermore, in the limit $l\to\infty$ the RHS above has very small real and imaginary parts, implying that $\Gamma[\frac{1}{2}+\nu-\kappa]$ in the denominator on the LHS must have a pole, thus

$$\frac{1}{2}+\nu-\kappa = -N, \tag{4.26}$$

with $N\in\mathbb{N}_0$, corresponding to the radial node of the scalar field. This allows us to deduce the real part of $\sqrt{\tilde{k}}$

$$\mathrm{Re}\left(\sqrt{\tilde{k}}\right) = -\frac{e_1}{2N+2\,\nu+1}. \tag{4.27}$$

Next, with $|\tilde{\omega}_R| \gg |\tilde{\omega}_I|$ [187, 69], implying $|\tilde{k}_R| \gg |\tilde{k}_I|$, we can expand (4.27) for large ℓ to obtain the real part of $\tilde{\omega}$

$$\tilde{\omega}_R = \tilde{\mu} - \frac{(1+\tilde{a}^2)^2\,\tilde{\mu}^3}{8\,\ell^2} + \mathcal{O}(\ell^{-3}), \tag{4.28}$$

confirming our expectations. Moreover, our calculation is accurate to $\mathcal{O}(1)$ only, hence we can replace $\tilde{\omega}$ with $\tilde{\mu}$ everywhere except inside $\tilde{k}$, where the leading order term cancels. This reduces (4.25) to

$$\begin{aligned}
\frac{\Gamma[\frac{1}{2}-\nu-\kappa]}{\Gamma[\frac{1}{2}+\nu-\kappa]} &= \left[\frac{\tilde{\mu}^2(1-\tilde{a}^4)}{N+\frac{1+\hat{\nu}}{2}}\right]^{\hat{\nu}} \hat{G}(\ell), \\
\hat{G}(\ell) &= \frac{\Gamma[-\hat{\nu}]^2\,\Gamma[\sigma_+ + \hat{\phi}_+]\,\Gamma[\sigma_+ + \hat{\phi}_-]}{\Gamma[\hat{\nu}]^2\,\Gamma[\sigma_- + \hat{\phi}_+]\,\Gamma[\sigma_- + \hat{\phi}_-]}, \\
\hat{\nu} = \sqrt{(1+2\,\ell)^2 - 4(1+\tilde{a}^2)(2+3\,\tilde{a}^2)\tilde{\mu}^2}, &\quad \hat{\phi}_\pm = \pm\frac{i\,\tilde{a}\,\tilde{\mu}\,(m-\tilde{a}(1+\tilde{a}^2))}{1-\tilde{a}^2} \\
\sigma_\pm = \frac{1\pm\hat{\nu}}{2} + \hat{\delta}, \quad ,\hat{\delta} = \frac{i\,\xi}{1-\tilde{a}^2}&\left[1-\frac{\tilde{a}^4\,\tilde{\mu}^2\,(1-\tilde{a}^4)}{\xi^2}\right]^{\frac{1}{2}}, \quad \xi = \tilde{a}\,m - (1+\tilde{a}^2)\tilde{\mu},
\end{aligned} \tag{4.29}$$

For the imaginary part of $\tilde{\omega}$ we allow (4.26) to be complex

$$\frac{1}{2} + \nu - \kappa = -N + \epsilon, \tag{4.30}$$

with $\epsilon \ll 1$, $\epsilon \in \mathbb{C}$. We can look at the $\epsilon \to 0$ limit of (4.30), using (4.27), to derive

$$\mathrm{Im}\left(\sqrt{\tilde{k}}\right) = \epsilon\frac{2\,i\,e_1}{(1+2\,N+2\,\nu)^2}, \tag{4.31}$$

which also enables us to find, in the limit $\ell \to \infty$,

$$\tilde{\omega}_I = i\ \mathrm{Im}(\epsilon)\frac{(1+\tilde{a}^2)^2\,\tilde{\mu}^3}{4\,\ell^3}. \tag{4.32}$$

Next, we look at (4.29) for $\epsilon \to 0$ and obtain

$$(-1)^N\,N!\,\epsilon = \left[\frac{\tilde{\mu}^2(1-\tilde{a}^4)}{N+\frac{1+\hat{\nu}}{2}}\right]^{\hat{\nu}} \frac{\hat{G}(\ell)}{\Gamma[-N-\hat{\nu}]}. \tag{4.33}$$

Taking ℓ large, we can rearrange for ϵ, which allows us to derive an expression for $\tilde{\omega}_I$ via (4.32). It is valid for any spin parameter $|a| < M$ and scalar field mass μ,

$$\tilde{\omega}_I = \frac{(1+\tilde{a}^2)^{3+2\,\ell}\Big((1-\tilde{a}^2)^2\ell^2+4\,\tilde{a}^2\,m^2\Big)^{\frac{1}{2}+\ell}\,\tilde{\mu}^{5+4\,\ell}}{2^{-N+5+6\,\ell}\sqrt{\pi}\,N!\,\ell^{-N+\frac{11}{2}+6\,\ell}}\,\sinh\left[\frac{2\,\pi\Big(\tilde{a}\,m-(1+\tilde{a}^2)\tilde{\mu}\Big)}{1-\tilde{a}^2}\right]\times$$
$$\exp\left[2\,\ell-2(N+1)+\frac{2\,\tilde{\mu}\,(1+\tilde{a}^2)^2\arctan\left[\frac{2\,\tilde{a}\,m}{\ell(1-\tilde{a}^2)}\right]}{1-\tilde{a}^2}-\frac{4\,\tilde{a}\,m\,\arctan\left[\frac{2\,\tilde{a}\,m}{\ell(1-\tilde{a}^2)}\right]}{1-\tilde{a}^2}\right]. \tag{4.34}$$

Setting $\ell = m$ $(n = 0)$ we get the growth rate of the dominant modes in the spectrum

$$\tilde{\omega}_{I,\ell=m} = \frac{2^{N-5-6\,\ell}(1+\tilde{a}^2)^{4+4\,\ell}\tilde{\mu}^{5+4\,\ell}}{\sqrt{\pi}\,N!\,\ell^{-N+\frac{9}{2}+4\,\ell}}\sinh[\frac{2\,\pi(\tilde{a}\,\ell-\tilde{\mu}(1+\tilde{a}^2))}{1-\tilde{a}^2}]\times$$
$$\exp\left[-2\left(N+1+\frac{\tilde{\mu}\,(1+\tilde{a}^2)^2\arctan\left[\frac{-2\,\tilde{a}}{1-\tilde{a}^2}\right]}{1-\tilde{a}^2}\right)+\ell\left(2+\frac{4\,\tilde{a}\,\arctan\left[\frac{-2\,\tilde{a}}{1-\tilde{a}^2}\right]}{1-\tilde{a}^2}\right)\right], \tag{4.35}$$

which can also be rewritten in a way that will make the usual condition for superradiance more apparent, namely:

$$\mathrm{Re}(\omega M) = \hat{\mu}\left(1-\frac{\hat{\mu}^2}{2\ell^2}\right)+\mathcal{O}(\ell^{-3})\,, \tag{4.36a}$$

$$\mathrm{Im}(\omega M) = \frac{\ell^{-4\,\ell-\frac{9}{2}+N}}{2^{2\,\ell+1-N}\sqrt{\pi}N!}\hat{\mu}^{4\,\ell+5}\sinh\left[\frac{\pi\,(\ell\,\Omega_K-\mu)}{\kappa_K}\right]\times$$
$$\exp\left[-\frac{2}{\kappa_K}\left(\ell\,\Omega_K-\frac{\hat{\mu}}{r_+}\right)\arctan\left(\frac{\Omega_K}{\kappa_K}\right)-2(1-\ell+N)\right]\times\left[1+\mathcal{O}(\ell^{-1})\right]\,, \tag{4.36b}$$

where $\hat{\mu}\equiv\mu M$ and we identify $N\in\mathbb{N}_0$ as a radial overtone. Note that for $\tilde{a}=0$ the sinh changes sign and we reproduce the correct behaviour for Schwarzschild [64], where the instability disappears,

$$\tilde{\omega}_{I,\tilde{a}=0} = -\frac{2^{N-5-6\,\ell}e^{-2(N+1)+2\,\ell}\tilde{\mu}^{5+4\,\ell}}{\sqrt{\pi}\,N!\,\ell^{-N+\frac{9}{2}+4\,\ell}}\sinh[2\,\pi\,\tilde{\mu}]. \tag{4.37}$$

Furthermore, its onset sits precisely at the onset of superradiance, namely $\ell\Omega_K = \mathrm{Re}(\omega)$. More importantly for our purposes, in the limit $\ell\to+\infty$, the growth rate of the instability scales as $e^{-4\ell\log\ell}$, and no matter what the value of μ or a, one can always

find a value of $\ell = \ell_\star \equiv \lceil \mu/\Omega_K \rceil$ above which the instability sets in. This shows that *all* Kerr black holes are unstable to massive scalar field perturbations, irrespective of their initial spin $|J| < M^2$ and of the mass μ of the scalar perturbation.

4.3.4 Klein-Gordon equation numerically

One can test the regime of validity of our approximation by comparing with data obtained by solving numerically, without approximations, the full equations. We apply spectral collocation methods on a discretised Chebyshev grid with

$$z = \frac{1+\cos\theta}{2}, \quad x = 1 - \frac{r_+}{r}, \tag{4.38}$$

where $x = 0$ and $x = 1$ correspond to the event horizon and spatial infinity, and $z = 0$ and $z = 1$ to the north and south poles of the squashed sphere, respectively. We use dimensionless variables (4.7), and factor out the singular behaviour at the boundaries so that we only solve for smooth functions in their integration domain. This necessarily involves a choice of normalisation, which we describe next. We define:

$$\begin{aligned}
&R_{\omega\ell m}(x) = (1-x)^\beta\, e^{\frac{\alpha}{1-x}}\, x^\gamma\, \mathcal{R}_{\omega\ell m}(x),\\
&S_{\omega\ell m}(z) = z^{m/2}(1-z)^{m/2}\, \mathcal{S}_{\omega\ell m}(z),\\
&\alpha = -\sqrt{\tilde\mu^2 - \tilde\omega^2}, \quad \beta = 1 + \frac{(1+\tilde a^2)(\tilde\mu^2 - 2\tilde\omega^2)}{2\sqrt{\tilde\mu^2-\tilde\omega^2}},\\
&\gamma = -i\left(\tilde\omega\frac{1+\tilde a^2}{1-\tilde a^2} - \frac{m\,\tilde a}{1-\tilde a^2}\right),
\end{aligned} \tag{4.39}$$

with $\mathcal{R}_{\omega\ell m}(0) = \mathcal{S}_{\omega\ell m}(1) = 1$. No additional boundary conditions are needed as (4.39) force the system to pick the right solution. We then use the methods of [66] to solve for the eigenpair $(\tilde\omega, \Lambda)$ using a Newton-Raphson routine (the only additional complication is that we are searching for extremely small growth rates when m increases, so using extended precision is mandatory).

As seen in Fig. 4.1, our numerical data agrees excellently with (4.36b). Furthermore, one can measure deviations of our WKB expression to the exact numerical result, and it agrees with the error given in Eq. (4.36b).

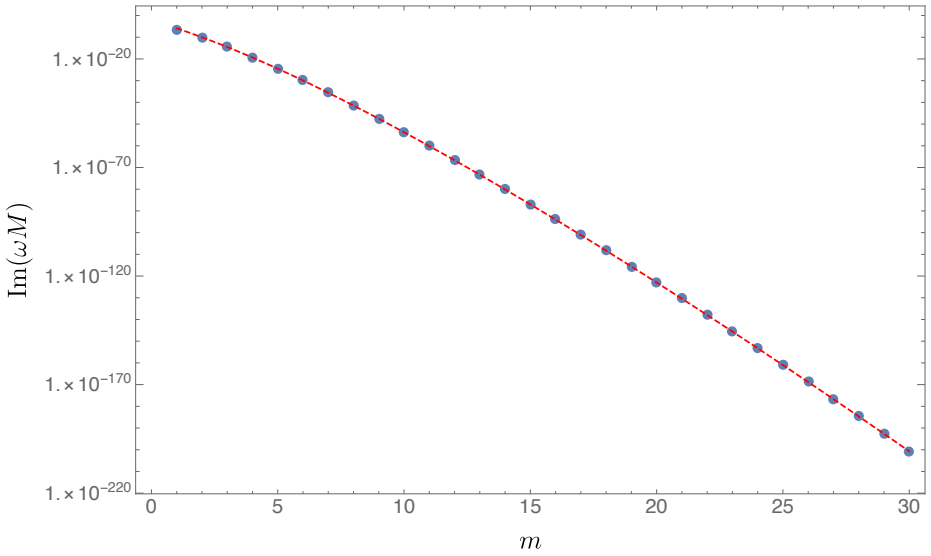

Figure 4.1 The superradiant modes of a massive scalar around Kerr with $M\,\mu = 0.42$ and $J/M^2 = 0.99$, as a function of m. The dashed red curve shows the analytic expression (4.36b) and the blue disks our exact numerical data.

4.4 Backreaction

We want the GWs emitted by a scalar cloud around a Kerr BH and its leading order backreaction on the geometry. In the vector field case [71, 70], it has been shown that the system evolves adiabatically; the emergence of the cloud due to superradiance, and the consecutive saturation of the vector mode responsible, due to the spinning down of the BH, proceed on a much faster timescale than the dispersion of energy and angular momentum due to GW emission from the cloud.

We proceed using nonlinear perturbation theory and declare

$$\psi = \sum_{i=0}^{+\infty} \psi^{(2i+1)} \varepsilon^{2i+1} \,, \quad \text{and} \quad g = g_K + \sum_{i=1}^{+\infty} g^{(2i)} \varepsilon^{2i} \,, \tag{4.40}$$

where g_K is given by the Kerr metric (4.3). We expand the equations of motion (4.2) in a power series in ε. To first order in ε we solve eq. (4.2b) subject to a choice of initial data. For the case at hand, we choose ψ to be given by the real part of one of the unstable modes we have determined above. These are labelled by a given value of m. Furthermore, since $\mathrm{Im}(\omega M) \ll \mathrm{Re}(\omega M)$, we take ω to be purely real. We then proceed to second order and attempt to compute the leading order backreaction on the metric, $g^{(2)}$, and its associated curvature. The standard approach to the linearised Einstein equation presents us with a daunting task. However, Kerr BHs are algebraically special,

allowing us to bypass computing $g^{(2)}$, and directly calculate certain gauge invariant scalars built out of the Weyl tensor. These do not couple amongst themselves and we focus on the Newman-Penrose scalar, ψ_4, since it also allows us to efficiently compute the GWs emitted by the scalar cloud, which we treat as a perturbing source. ψ_4 obeys the Teukolsky equation [175, 150, 176]

$$\Big[\big(\Delta + 3\gamma - \bar{\gamma} + 4\mu + \bar{\mu}\big)\big(D + 4\epsilon - \rho\big) - 3\psi_2 - \big(\bar{\delta} + 3\alpha + \bar{\beta} + 4\pi - \bar{\tau}\big)\big(\delta + 4\beta - \tau\big)\Big]\psi_4 = 4\pi\, T_4, \quad (4.41)$$

whereby the source term T_4 is reconstructed directly from Eq. (4.2c), and thus depends on the scalar field and its gradient only.

$$T_4 = \big(\Delta + 3\gamma - \bar{\gamma} + 4\mu + \bar{\mu}\big) \times \Big[\big(\bar{\delta} - 2\bar{\tau} + 2\alpha\big)T_{n\bar{m}} - \big(\Delta + 2\gamma - 2\bar{\gamma} + \bar{\mu}\big)T_{\bar{m}\bar{m}}\Big] + \big(\bar{\delta} - \bar{\tau} + \bar{\beta} + 3\alpha + 4\pi\big) \times \Big[\big(\Delta + 2\gamma + 2\bar{\mu}\big)T_{n\bar{m}} - \big(\bar{\delta} - \bar{\tau} + 2\bar{\beta} + 2\alpha\big)T_{nn}\Big]. \quad (4.42)$$

Our sign convention is $(-,+,+,+)$, opposite to Teukolsky's. Nevertheless, the equation in terms of NP variables is unchanged. For their definitions, in our convention, we use [90].

The tetrad projections we need in T_4 are T_{nn}, $T_{n\bar{m}}$ and $T_{\bar{m}\bar{m}}$. Moreover using a null tetrad implies we can ignore the $g_{\mu\nu}$ term in $T_{\mu\nu}$. In a Kinnersley tetrad [128], we have

$$T_{nn} = \frac{e^{-2\,i\,\omega\,t}e^{2\,i\,m\,\phi}}{8\,\Sigma^2}\Big[i\,K\,R^{(re)}_{\omega\ell m} + \Delta_k\,R^{(re)}_{\omega\ell m,r}\Big]^2 S^{(re)\,2}_{\omega\ell m},$$

$$T_{n\bar{m}} = \frac{e^{-2\,i\,\omega\,t}e^{2\,i\,m\,\phi}}{4\sqrt{2}\,\Sigma\,(r - i\,a\,\cos\theta)}\Big[i\,K\,R^{(re)}_{\omega\ell m} + \Delta_k\,R^{(re)}_{\omega\ell m,r}\Big]\times \Big[S^{(re)}_{\omega\ell m,\theta} - \Big(a\,\omega\,\sin\theta - \frac{m}{\sin\theta}\Big)\,S^{(re)}_{\omega\ell m}\Big]R^{(re)}_{\omega\ell m}\,S^{(re)}_{\omega\ell m},$$

$$T_{\bar{m}\bar{m}} = \frac{e^{-2\,i\,\omega\,t}e^{2\,i\,m\,\phi}}{4\,(r - i\,a\,\cos\theta)^2}\,R^{(re)\,2}_{\omega\ell m} \times \Big[S^{(re)}_{\omega\ell m,\theta} - \Big(a\,\omega\,\sin\theta - \frac{m}{\sin\theta}\Big)\,S^{(re)}_{\omega\ell m}\Big]^2, \quad (4.43)$$

with $R^{(re)}_{\omega\ell m} = \Re\big(R_{\omega\ell m}\big)$ and $S^{(re)}_{\omega\ell m} = \Re\big(S_{\omega\ell m}\big)$, as we are taking the real part of an unstable mode as the perturbing source.

The GW frequency and mode number are related to the scalar field ones by $\hat{\omega} = 2\,\omega$, $\hat{m} = 2\,m$. The easiest way to see this is by using our ansatz for the scalar field 4.4 (with $\widehat{\psi}_{\omega m}(r,\theta) = R_{\omega\ell m}(r)S_{\omega\ell m}(\theta)$) and a generalised definition for the stress tensor of

a scalar as

$$T_{\mu\nu}\Big(\Upsilon,\Psi\Big) = 2\nabla_\mu\Upsilon\nabla_\nu\Psi - g_{\mu\nu}\Big(\nabla_\sigma\Upsilon\nabla^\sigma\Psi + \mu^2\Upsilon\Psi\Big). \tag{4.44}$$

Plugging in $\psi^{(re)} = 1/2(\psi + \bar{\psi})$ for Υ and Ψ, leads us to

$$T_{\mu\nu}\Big(\psi^{(re)},\psi^{(re)}\Big) = \frac{1}{4}\Big[T_{\mu\nu}\Big(\psi,\psi\Big) + T_{\mu\nu}\Big(\bar{\psi},\bar{\psi}\Big) + 2T_{\mu\nu}\Big(\psi,\bar{\psi}\Big)\Big], \tag{4.45}$$

with bar indicating complex conjugation. The ansatz (4.4) implies that the terms above will contain exponential prefactors, which reveal that the first and second one source outgoing waves with $\hat{m} = 2\,m$, $\hat{\omega} = 2\,\omega$ and $\hat{m} = -2\,m$, $\hat{\omega} = -2\,\omega$, respectively, whereas the third one corresponds to the energy of the cloud, given by the gravitational mode with $\hat{m} = \hat{\omega} = 0$.

The LHS of (4.41) can be separated into angular and radial parts as in the vacuum case [175], allowing us to solve for ψ_4 as an infinite sum of separable solutions using Green's method. This is what we explain in detail next.

4.4.1 Determining Outgoing Gravitational Radiation

We take the ansatz

$$\psi_4 = e^{-i\,\hat{\omega}\,t}e^{i\,\hat{m}\,\phi}\,\rho^4\,\mathcal{R}(r)\,\mathcal{S}(\theta), \tag{4.46}$$

with spin coefficient $\rho = -1/(r - i\,a\,\cos\theta)$, and multiply both sides of (4.41) by $2\,\Sigma(r,\theta)/\rho^4$. $\mathcal{S}(\theta)$ can be identified with a spin-weighted spheroidal harmonic, satisfying

$$\frac{1}{\sin\theta}\Big[\sin\theta\,{}_s\mathcal{S}_{\hat{\ell}\hat{m},\theta}\Big]_{,\theta} + \Big[(c\,\cos\theta)^2 - 2\,c\,s\,\cos\theta + s + {}_sA_{\hat{\ell}\hat{m}\hat{\omega}} - \frac{(\hat{m} + s\,\cos\theta)^2}{\sin^2\theta}\Big]{}_s\mathcal{S}_{\hat{\ell}\hat{m}} = 0, \tag{4.47}$$

with $c = a\,\hat{\omega}$, ${}_sA_{\hat{\ell}\hat{m}\hat{\omega}}$ the separation constant and $s = -2$. Multiplying by ${}_s\bar{\mathcal{S}}_{\hat{\ell}\hat{m}}$ and integrating over θ results in the following equation for the radial function

$$\Delta_k^2\Big[\Delta_k^{-1}\mathcal{R}_{\hat{\ell}\hat{m},r}\Big]_{,r} + \Big[\frac{K^2 + 4\,i\,(r-M)\,K}{\Delta_k} - 8\,i\,\hat{\omega}\,r - a^2\,\hat{\omega}^2 + 2\,a\,\hat{m}\,\hat{\omega} - {}_sA_{\hat{\ell}\hat{m}\hat{\omega}}\Big]\mathcal{R}_{\hat{\ell}\hat{m}} = \mathcal{T}_{\hat{\ell}\hat{m}\hat{\omega}}, \tag{4.48}$$

where $K = (r^2 + a^2)\,\hat{\omega} - a\,\hat{m}$ and the source term is the integrated over angles stress-energy tensor

$$\mathcal{T}_{\hat{\ell}\hat{m}\hat{\omega}} = \frac{4\pi}{\eta_{\hat{\ell}\hat{m}}}\int\frac{2\,\Sigma(r,\theta)}{\rho^4}\,{}_s\bar{\mathcal{S}}_{\hat{\ell}\hat{m}}\,T_4\,\sin\theta\,\mathrm{d}\theta, \tag{4.49}$$

with the normalisation condition

$$\int_0^\pi |{}_s\mathcal{S}_{\hat{\ell}\hat{m}}\,(\theta)|^2 \sin\theta \,\mathrm{d}\theta = \eta_{\hat{\ell}\hat{m}}. \tag{4.50}$$

Equation (4.48) should be evaluated for $\hat{\omega} = \pm 2\,\omega$, $\hat{m} = \pm 2\,m$, $s = -2$ on the LHS with $T_{\mu\nu}\big(\psi,\psi\big)$, for the $+$, and $T_{\mu\nu}\big(\bar{\psi},\bar{\psi}\big)$, for the $-$, inside T_4 on the RHS, and for $m = \hat{\omega} = 0$ on the LHS with $T_{\mu\nu}\big(\psi,\bar{\psi}\big)$ in T_4 on the RHS.

However, the Teukolsky equation is invariant under complex conjugation followed by $m \to -m$ and $\omega \to -\omega$, hence for $\hat{m} \neq 0 \neq \hat{\omega}$ we only need to determine the contribution of $T_{\mu\nu}\big(\psi,\psi\big)$ and double the result.

Moreover, by looking at the asymptotic behaviour of the homogeneous radial equation ((4.48) with $\mathcal{T}_{\hat{\ell}\hat{m}\hat{\omega}} = 0$) we can show that the $\hat{m} = \hat{\omega} = 0$ mode is subleading to all the rest at spatial infinity. To this end, transform the homogeneous (4.48) with the help of

$$\mathcal{R}_{\hat{\ell}\hat{m}}(r) = \frac{\Delta_K^{-\frac{s}{2}}}{\sqrt{r^2+a^2}} Y_{\hat{\ell}\hat{m}}(r), \quad \frac{dr_*}{dr} = \frac{r^2+a^2}{\Delta_K}, \tag{4.51}$$

and then take the limit of $r \to \infty$, leaving us with

$$Y''_{\hat{\ell}\hat{m}}(r_*) + \left[\hat{\omega}^2 + \frac{2\,i\,s\,\hat{\omega}}{r}\right] Y_{\hat{\ell}\hat{m}}(r_*) = 0, \tag{4.52}$$

for finite frequency $\hat{\omega}$ and azimuthal number $\hat{m}$ (due to the aforementioned symmetry of the Teukolsky equation, we can work, without loss of generality, with the case of $\hat{\omega} = 2\,\omega$, $\hat{m} = 2\,m$ only.). The outgoing part of $Y_{\hat{\ell}\hat{m}}$ behaves as $e^{i\,r_*\,\hat{\omega}} r^{-s}$, leading to an $e^{i\,r_*\,\hat{\omega}} r^{-2s-1}$ asymptotic behaviour for $\mathcal{R}_{\hat{\ell}\hat{m}}$, which together with the definition (4.46) allows us to deduce that the outgoing contribution of ψ_4 near spatial infinity, for finite $\hat{\omega}$ and $\hat{m}$, behaves as

$$\lim_{r\to\infty} \psi_4 \sim e^{i\,\hat{\omega}\,r_*}/r \quad \text{(outgoing mode)}. \tag{4.53}$$

However, were we to set $\hat{\omega} = \hat{m} = 0$ before we take the limit of $r \to \infty$, instead of (4.52), we are left with

$$Y''_{00}(r_*) - \frac{\ell(\ell+1)}{r^2} Y_{00}(r_*) = 0, \tag{4.54}$$

where we have used ${}_sA_{\hat{\ell}00} = \ell(\ell+1) - s(s+1)$. The solution with finite energy at infinity corresponds to asymptotic behaviour of the form $r^{-\ell-3}$ for ψ_4, which is clearly subleading to non-zero $\hat{\omega}$ and $\hat{m}$ modes.

Therefore, for the computation of the gravitational radiation from the scalar clouds, which is performed at spatial infinity, we only need to look at the $\hat{\omega} = 2\,\omega$, $\hat{m} = 2\,m$ case for (4.48), with $T_{\mu\nu}\Big(\psi,\psi\Big)$ inside T_4 on the RHS.

In this way, ψ_4 has been projected onto a basis of spin-weighted spheroidal harmonics

$$\psi_4 = e^{-i\,\hat{\omega}\,t} e^{i\,\hat{m}\,\phi}\,\rho^4 \sum_{\hat{\ell}} \mathcal{R}_{\hat{\ell}\hat{m}}(r)\,{}_s\mathcal{S}_{\hat{\ell}\hat{m}}(\theta), \tag{4.55}$$

where the definition of ${}_s\mathcal{S}_{\hat{\ell}\hat{m}}(\theta)$ requires $\hat{\ell} \geq \hat{m}$.

Thus, given a Kerr BH, for fixed $M\,\mu$ and J/M^2, and its $\ell = m$ scalar superradiant spectrum, we can use the latter as a source on the RHS of (4.48), which sets the values of the GW frequency $\hat{\omega}$ and mode-number $\hat{m}$, letting us solve (4.48) for any allowed value of $\hat{\ell}$.

From ψ_4, Teukolsky [176] showed us how to compute the rate of gravitational radiation at future null infinity

$$\frac{\mathrm{d}^2 E_s}{\mathrm{d}t\mathrm{d}\Omega} = \lim_{r\to\infty} \frac{r^2}{4\,\pi\,\hat{\omega}^2}\,|\psi_4|^2\,, \tag{4.56}$$

where $\hat{\omega} = 2\,\omega$ and $\mathrm{d}\Omega$ is the induced volume on a unit 2-sphere. We work with the scaled expression

$$P_E = \frac{\mathrm{d}E_s}{\mathrm{d}t}\left(\frac{M}{\mathcal{M}_s}\right)^2\,, \tag{4.57}$$

where

$$\mathcal{M}_s = \int_{r_+}^{+\infty}\int_0^{\pi}\int_0^{2\pi} \sqrt{-g}\,T^t_{\ t}\,\mathrm{d}\phi\,\mathrm{d}\theta\,\mathrm{d}r \tag{4.58}$$

is the total scalar field energy - the energy of the perturbed initial data. P_E is independent of the scalar field amplitude and measures the energy radiated per m mode in the initial data.

One can also use the NP scalar, ψ_4, as a measure of curvature, monitoring the maximum of the Weyl tensor component it represents, $\psi_4 = C_{n\,\bar{m}\,n\,\bar{m}}$. To this end, we look at the following time independent quantity as a function of m:

$$\chi \equiv \max_{r,\theta}\,\left(|\psi_4|^2/\mathcal{M}_s^2\right). \tag{4.59}$$

The radial and azimuthal location of the maximum of (4.59), $(r,\theta)=(r_\star,\theta_\star)$, track the maximum of $[\psi^{(1)}]^2$. The argument for ignoring the $\hat{m}=\hat{\omega}=0$ mode in the computation of the gravitational radiation at infinity does not hold for the maximum of ψ_4, as the latter is expected to be located at a finite distance from the black hole, near the peak of the scalar cloud, as we find in our numerics. Nevertheless, we have checked numerically that its contribution to the maximum is negligible compared to the rest.

Before proceeding with the numerical integration of Teukolsky equation, we will briefly detail an approximate analytic calculation of χ for large ℓ that will be compared with our numerical results later.

4.5 Analytic approximation for the curvature

In this section, we outline the steps for a WKB approximation of χ (4.59). We work with $\ell=m$ and $\ell\gg 1$.

First, we need a WKB expansion of the scalar field near its maximum - i.e. $R_{\omega\ell m}(r)$, $S_{\omega\ell m}(\theta)$, Λ and $\tilde{\omega}$, as well as the location of the minimum of the potential of the radial KG equation expanded for large $\ell=m$.

We start with the angular equation (4.6b), which rewriten in our numerical coordinates (4.38), together with the redefinition (4.39), looks like

$$(1-z)\,z\,\mathcal{S}''_{\omega\ell m}(z)+(m+1)(2z-1)\mathcal{S}'_{\omega\ell m}(z)-\left[\Lambda-m(m+1)-\tilde{a}^2\,\tilde{k}\,(2z-1)^2\right]\mathcal{S}_{\omega\ell m}(z)=0. \tag{4.60}$$

Expand the variables in series in m

$$\begin{aligned}\mathcal{S}_{\omega\ell m}(z)&=1+\frac{S_1(z)}{m}+\frac{S_2(z)}{m^2}+\mathcal{O}(m^{-3}),\\ \Lambda&=\lambda_1\,m^2+\lambda_2\,m+\lambda_3+\mathcal{O}(m^{-1}),\\ \tilde{\omega}&=\tilde{\mu}-\frac{(1+\tilde{a}^2)^2\,\tilde{\mu}^3}{8\,m^2}+\frac{\omega_3}{m^3}+\mathcal{O}(m^{-4}),\end{aligned} \tag{4.61}$$

plug them in and solve order by order, requiring regularity of the solution. The known behaviour of $\tilde{\omega}$, (4.36a) from before, is utilised. In this way one can obtain $S_i(z)$ and λ_i to any order as a function of the ω_i.

Afterwards, we transform the radial equation (4.6a) using the coordinate transformation

$$r = \frac{2\,r_+\,m(m+1)}{(1+\tilde{a}^2)\tilde{\mu}^2}u. \tag{4.62}$$

The resulting equation is cumbersome and will thus not be given here - the above transformation correponds to the first two terms in the expansion for large $\ell = m$ of the position of the minimum of the radial potential. This is straightforward to get, after deriving the leading order behaviour of the angular eigenvalue $\Lambda = m(m+1) + \mathcal{O}(1)$, for which no knowledge of ω_3 or higher is required. Afterwards, we take

$$R_{\omega\ell m}(u) = e^{m\,f(u)}\Big[1 + \frac{R_1(u)}{m} + \mathcal{O}(m^{-2})\Big], \tag{4.63}$$

and solve order by order for $f(u)$, $R_i(u)$ and ω_i, again demanding regularity of the solution. This can be done to any order, but we only give the first few here

$$\begin{aligned} S_1(z) &= c_2, \quad S_2(z) = c_3, \\ f(u) &= c_0 - u + \log\,u, \\ R_1(u) &= c_1 - \frac{\tilde{\mu}^2}{4}(1+\tilde{a}^2)^2\Big[u + \frac{1}{u} + 3\log\,u\Big], \\ \lambda_1 &= \lambda_2 = 1, \quad \lambda_3 = 0, \quad \omega_3 = \frac{(1+\tilde{a}^2)^2\,\tilde{\mu}^3}{4}, \end{aligned} \tag{4.64}$$

whereby c_i are constants that can for example be chosen so that the scalar field is unity at the maximum ($u = 1$), which is what we do to compare with the numerics (where we can just divide by the numerical maximum).

Next, we move onto the Teukolsky equation (4.48). The expressions are very lengthy and not illuminating at all, so we will give only the most important ones. Treating the angular equation (4.47) as the scalar one produces

$$\begin{aligned} {}_s\mathcal{S}_{\hat{\ell}\hat{m}} &= z^{|\frac{2m-s}{2}|}(1-z)^{|\frac{2m+s}{2}|}\Big[1 - \frac{2\,\tilde{a}\,\tilde{\mu}\,z(s+\tilde{a}\,\tilde{\mu}\,(1-z)) + d_1}{m} + \mathcal{O}(m^{-2})\Big], \\ {}_sA_{\hat{\ell}\hat{m}\hat{\omega}} &= 2\,m\,(2\,m+1) - s(s+1) + \mathcal{O}(m^{-1}), \end{aligned} \tag{4.65}$$

whereby we have accounted for $\hat{m} = 2\,m$ and d_1 is a constant that can be chosen to make the normalisation of the function easier. It should be noted that, depending on the method of obtaining the spheroidal harmonics numerically, ${}_s\bar{\mathcal{S}}_{\hat{\ell}\hat{m}}$ inside T_4 might also need to be normalised. Afterwards, we need to obtain a series expansion in $\ell = m$

for $\mathcal{T}_{\hat{\ell}\hat{m}\hat{\omega}}$ (4.49). The normalisation $\eta_{\hat{\ell}\hat{m}}$ has to be obtained by plugging (4.65) in (4.50) and integrating. The final result is

$$\mathcal{T}_{\hat{\ell}\hat{m}\hat{\omega}} = e^{2\,m(1-u+\log u)}\frac{16\sqrt{2}\,\pi\,r_+^2\,u^4}{(1+\tilde{a}^2)^4\,\tilde{\mu}^6}m^9\left[1-\frac{4}{m}-\frac{2\,i\,\tilde{\mu}(1+\tilde{a}^2)+3\,\tilde{\mu}^2(1+\tilde{a}^2)^2\log(u)}{2\,m}\right.$$
$$\left.-\frac{\tilde{\mu}^2\Big[3\,(1+\tilde{a}^4)(u-1)^2+\tilde{a}^2(u\,(6\,u-13)+6)\Big]}{6\,u\,m}+\mathcal{O}\Big[\frac{1}{m^2}\Big]\right]. \quad (4.66)$$

With all ingredients present, we change variables in (4.48) with (4.62) and WKB expand $\mathcal{R}_{\hat{\ell}\hat{m}}$ for large $\ell = m$. Matching order by order results in

$$\mathcal{R}_{\hat{\ell}\hat{m}} = -e^{2\,m(1-u+\log u)}\frac{\sqrt{2}\,\pi\,r_+^2\,u^2}{(1+\tilde{a}^2)^2\,\tilde{\mu}^4}m^5\left[1-\frac{2}{m}-\frac{2\,i\,\tilde{\mu}(1+\tilde{a}^2)+3\,\tilde{\mu}^2(1+\tilde{a}^2)^2\log(u)}{2\,m}\right.$$
$$\left.-\frac{\tilde{\mu}^2\Big[3\,(1+\tilde{a}^4)(u-1)^2+\tilde{a}^2(u\,(6\,u-13)+6)\Big]}{6\,u\,m}+\mathcal{O}\Big[\frac{1}{m^2}\Big]\right], \quad (4.67)$$

allowing us to to rebuild ψ_4 for $\ell = m$ via (4.55).

We also need an expression for the scalar cloud energy

$$\mathcal{M}_s = \int_{r_+}^{+\infty}\int_0^{\pi}\int_0^{2\pi}\sqrt{-g}\,T^t_{\ t}\,\mathrm{d}\phi\,\mathrm{d}\theta\,\mathrm{d}r. \quad (4.68)$$

Working with coordinates z and u, we substitute our expansions for the scalar field in the definition of $\mathcal{M}_s$, and after simplifications, the angular integrals can be done analytically - with *Mathematica* or with a book on integrals. The resulting expression is expanded in $\ell = m$ and integrated over u from $\frac{\tilde{\mu}^2(1+\tilde{a}^2)}{2\,m\,(m+1)}$ to infinity, producing

$$\mathcal{M}_s = \frac{e^{2\,m}\pi^{\frac{3}{2}}\,\Gamma\Big[3+2m,\frac{(1+\tilde{a}^2)\tilde{\mu}^2}{m+1}\Big]}{2^{4\,m-1}m^{2\,m-\frac{5}{2}}(1+\tilde{a}^2)^3\,\tilde{\mu}^4}\Big[1+\mathcal{O}(m^{-1})\Big], \quad (4.69)$$

where we also have higher order terms, but the expressions are several lines long and will not be presented here.

Having ψ_4 and $\mathcal{M}_s$ in the large $\ell = m$ limit allows one to derive an expression for χ_{WKB}, the maximum of the curvature component represented by ψ_4 in the spacetime, by dividing them and expanding in series in $\ell = m$:

$$\chi_{\mathrm{WKB}} = \frac{(1+\tilde{a}^2)^{10}\tilde{\mu}^{16}}{2^{16}m^{16}\pi^2}+\mathcal{O}\left(m^{-17}\right). \quad (4.70)$$

We can consistently correct this approximation to next-to-leading order, however, as with previous lengthy formulae, the result will not be given here.

4.5.1 Numerical integration of Teukolsky equation

We use the same numerical method for (4.47) and (4.48) as for (4.6a) and (4.6b).

The angular equation

(4.47) is an eigenvalue problem which we integrate using Newton's method. We write

$$ {}_s\mathcal{S}_{\ell m} = z^{\iota_-}(1-z)^{\iota_+}\,{}_s\mathbb{S}_{\ell m}, \tag{4.71} $$

where $\iota_\pm = |\frac{m\pm s}{2}|$ and solve for ${}_s\mathbb{S}_{\ell m}$. We drop the hats on m and ω, as we solve the equation generally. The eigenvalue ${}_sA_{\ell m\omega}$ is treated as an unknown and we normalise ${}_s\mathbb{S}_{\ell m}$ to 1 using (4.50). Appropriate boundary conditions are imposed at the edges of the domain. These can be obtained by expanding the equation for ${}_s\mathbb{S}_{\ell m}$ in power series around the poles. At $z=0$ we require

$$ \begin{aligned} &\left[4-(m-s)^2+8\,\iota_- +(2\,\iota_-)^2\right]\,\partial_z\,{}_s\mathbb{S}_{\ell m}(z)|_{z=0} = \\ &\left[m^2-4\,s+2\,m\,s-4\,{}_sA_{\ell m}-8\,\tilde{a}\,s\,\omega-4\,\tilde{a}^2\omega^2+(2\,\iota_-)^2+4\,\iota_+ +4\,\iota_-(1+2\,\iota_+)\right]\,{}_s\mathbb{S}_{\ell m}(z)|_{z=0}\,, \end{aligned} \tag{4.72} $$

and similarly at $z=1$

$$ \begin{aligned} &\left[-4+(m+s)^2-8\,\iota_+ -(2\,\iota_+)^2\right]\,\partial_z\,{}_s\mathbb{S}_{\ell m}(z)|_{z=1} = \\ &\left[m^2-4\,s-2\,m\,s-4\,{}_sA_{\ell m}+8\,\tilde{a}\,s\,\omega-4\,\tilde{a}^2\omega^2+(2\,\iota_+)^2+4\,\iota_+ +4\,\iota_-(1+2\,\iota_+)\right]\,{}_s\mathbb{S}_{\ell m}(z)|_{z=1}\,. \end{aligned} \tag{4.73} $$

A starting point to our iteration is the series solution, provided in [20], up to twelfth order.

The radial equation

(4.48) is a sourced ODE, which we can invert once the RHS is known. As explained above, we need the superradiant modes of the scalar field on a fixed Kerr background, which we have numerically, so we can integrate (4.48) for any $\hat{\ell}$. We take out the prefactors in (4.39) from the scalar field inside T_4, so that we can directly substitute our

numerical solutions $\mathcal{R}_{\omega\ell m}(x)$ and $\mathcal{S}_{\omega\ell m}(z)$. We then factor out the singular behaviour of $\mathcal{R}_{\hat{\ell}\hat{m}}$ at infinity and the horizon, derived via Frobenius analysis, and transfer them to the RHS. Specifically

$$\mathcal{R}_{\hat{\ell}\hat{m}}(x) = r_+^2 (1-x)^{\hat{\beta}}\, e^{\frac{\hat{\alpha}}{1-x}}\, x^{2+2\,\hat{\gamma}}\, \mathbb{R}_{\hat{\ell}\hat{m}}(x), \tag{4.74}$$

with $\mathbb{R}_{\hat{\ell}\hat{m}}(x)$ dimensionless and

$$\begin{aligned} \hat{\alpha} &= 2\,i\,\tilde{\omega}, \quad \hat{\beta} = -3 - 2\,i(1+\tilde{a}^2)\,\tilde{\omega}, \\ \hat{\gamma} &= -i\left(\tilde{\omega}\frac{1+\tilde{a}^2}{1-\tilde{a}^2} - \frac{\hat{m}\,\tilde{a}}{1-\tilde{a}^2}\right). \end{aligned} \tag{4.75}$$

Moreover, $x^{2\,\hat{\gamma}}$ gets cancelled by the x^{γ} from the radial scalar functions (4.39) inside T_4. We then solve for $\mathbb{R}_{\hat{\ell}\hat{m}}(x)$. We need to impose boundary conditions at spatial infinity, since [175] reveals that the ingoing behaviour of the radial function (the one we do not want) is subleading

$$\mathcal{R}_{\hat{\ell}\hat{m}}(x) \sim Z^{(in)}_{\hat{\ell}\hat{m}}\, e^{-\frac{2\,i\,\tilde{\omega}}{1-x}}(1-x) + Z^{(out)}_{\hat{\ell}\hat{m}}\frac{e^{\frac{2\,i\,\tilde{\omega}}{1-x}}}{(1-x)^3}, \tag{4.76}$$

The boundary condition that selects the outgoing waves only can be deduced by expanding the homogeneous Teukolsky equation for large radial variable , which shows that setting $Z^{(in)}_{\hat{\ell}\hat{m}} = 0$ is equivalent to demanding

$$\begin{aligned} &-\partial_{xx}\,\mathbb{R}_{\hat{\ell}\hat{m}}|_{x=1} = \\ &\frac{1}{4(1-\tilde{a}^2)^2\hat{\varpi}^2}\Big[(1-\tilde{a}^2)^2\,{}_sA_{\hat{\ell}\hat{m}\hat{\varpi}}{}^2 + 2(1-\tilde{a}^2)\,{}_sA_{\hat{\ell}\hat{m}\hat{\varpi}}\Big(2\,\tilde{a}\,\hat{m}\,\hat{\varpi} + \tilde{a}^4\hat{\varpi}^2 + 2\,\tilde{a}^6\hat{\varpi}^2 \\ &-(i+\hat{\varpi})^2 + \tilde{a}^2(-1+4\,i\,\hat{\varpi} - 3\,\hat{\varpi}^2)\Big) + 2\,\hat{\varpi}\Big(-3\,i - 12\,\hat{\varpi} + 20\,i\,\hat{\varpi}^2 + \tilde{a}^8(8\,i - \frac{11}{2}\hat{\varpi})\hat{\varpi}^2 \\ &+8\,\hat{\varpi}^3 + 2\,\tilde{a}^{12}\,\hat{\varpi}^3 + 2\,\tilde{a}^{10}\hat{\varpi}^2(i+\hat{\varpi} - 2\,\tilde{a}^7\,\hat{m}\,\hat{\varpi}(i-2\,\hat{\varpi}) + 4\,\tilde{a}^5\,\hat{m}(1+\frac{i}{2}\hat{\varpi} + \frac{1}{2}\hat{\varpi}^2) \\ &-8\,\tilde{a}^3\,\hat{m}(1-\frac{3\,i}{2}\hat{\varpi} + \frac{3}{4}\hat{\varpi}^2) + 4\,\tilde{a}\,\hat{m}(1-3\,i\,\hat{\varpi} - 2\,\hat{\varpi}^2) + \tilde{a}^4(3\,i - 2\,\hat{\varpi} - 20\,i\,\hat{\varpi}^2 + \frac{1}{2}\hat{\varpi}^3) \\ &+\tilde{a}^2(3\,i+19\,\hat{\varpi}+2\,\hat{m}^2\,\hat{\varpi} - 4\,i\,\hat{\varpi}^2 + 12\,\hat{\varpi}^3) - \tilde{a}^6(3\,i+5\,\hat{\varpi}+6\,i\,\hat{\varpi}^2+11\,\hat{\varpi}^3)\Big]\Big]\,\mathbb{R}_{\hat{\ell}\hat{m}}|_{x=1}\,, \end{aligned} \tag{4.77}$$

where $\hat{\varpi} = 2\,\tilde{\omega}$.

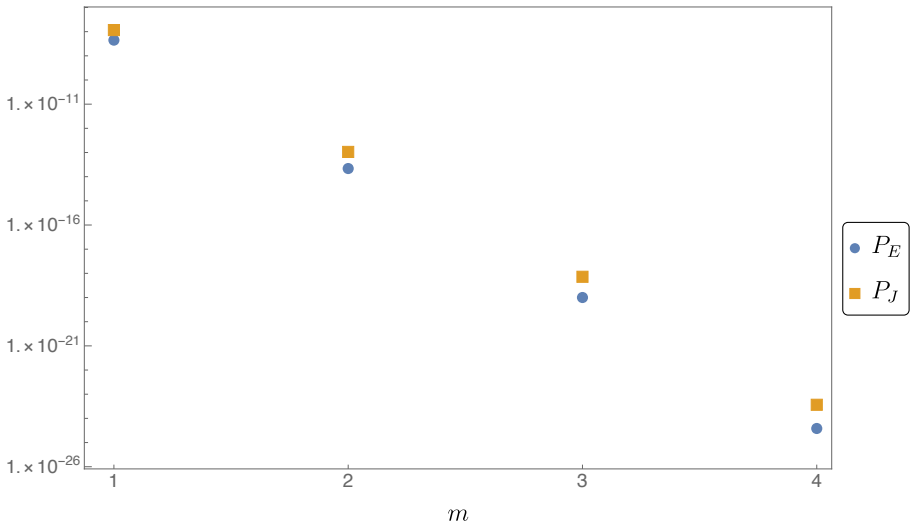

Figure 4.2 GW emission of energy and angular momentum, P_E, (4.57), and $P_J = \frac{m}{\mathrm{Re}(\omega M)} P_E$ respectively, for a single $\ell = m$ scalar cloud around Kerr as a function of m. Same parameters as in Fig. 4.1.

In terms of the functions for which we solve numerically, the formula for the gravitational radiation (4.56) takes the following form

$$\frac{dE_s}{dt} = \frac{1}{(2\,\tilde{\omega})^2} \sum_{\hat{\ell}} \eta_{\hat{\ell}\hat{m}} \left| \hat{\mathbb{R}}_{\hat{\ell}\hat{m}}(x) \right|^2_{x\to 1} , \tag{4.78}$$

where we have used (4.50), the orthogonality of the spin-weighted spheroidal harmonics, and have multiplied by 2 to account for the GWs with $\hat{m} = -2\,m$, $\hat{\omega} = -2\,\omega$.

4.5.2 GW emission results

Our results for the GW emission are shown in Fig. 4.2. The radiated angular momenta in this process is $P_J = \frac{m}{\mathrm{Re}(\omega M)} P_E$, in accordance with [176]. The fact that both P_E and P_J appear to decrease rapidly with increasing m, shows that the evolution occurs, to very good approximation, at fixed energy and angular momentum. This is akin to the time evolution of the superradiance instability with anti-de Sitter asymptotics [61, 143], simulated recently in [34], and showing hints of turbulent behaviour.

The data in Fig. (4.2) is for a fixed value of the dimensionless spin parameter a/M. However, during the aforementioned cascade, the BH will be gradually spinning down, hence, the gravitational radiation for each value of m should ideally be computed by accounting for the BH's loss of energy, due to the superradiant modes active prior to the one under consideration. Nevertheless, using the superradiant condition $\mathrm{Re}(\omega) > m\Omega_K$,

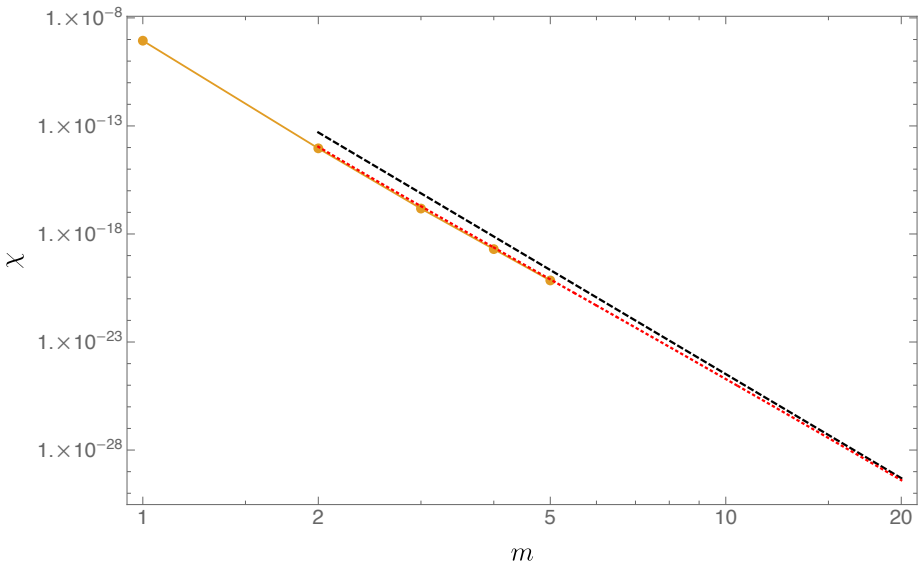

Figure 4.3 χ, a measure of the spacetime curvature, as a function of $\ell = m$. Same parameters as in Fig. 4.1. The black dashed curve shows our leading order approximation, whereas the dotted red line includes the next to leading order correction and the orange circles are numerical data.

one sees that $\Delta(a/M)$ for successive superradiant modes $\sim \ell^{-1}$ as $\ell \to \infty$, implying that in the regime of interest, the dimensionless spin will be approximately constant and Fig. (4.2) represents accurately the qualitative behaviour.

In Fig. 4.3 we show the dependence of χ on the initial data, here labelled by m. Our WKB-type analysis in the previous section revealed the leading order behaviour for χ as power law in $1/m$ (4.70).

Note that P_E is harder to compute numerically than χ, hence why we have extended results for χ up to $m = 5$.

Numerical convergence

As we cannot integrate (4.48) for infinitely many $\hat{\ell}$, we truncate the sum until (4.78) converges. We will look at the $m = 4$ case here ($\hat{m} = 8$ for the GWs), as this was the hardest one to tackle numerically. We include 9 GW modes, $\hat{\ell} = 8$ to $\hat{\ell} = 16$, to get good convergence for the radiated energy. Moreover, very high grid resolution was needed in the radial direction, in order to resolve the oscillating behaviour of the solution far away from the BH (exactly at spatial infinity the oscillating part is discarded by the boundary conditions). This is summarised in Figs. (4.4) and (4.5)

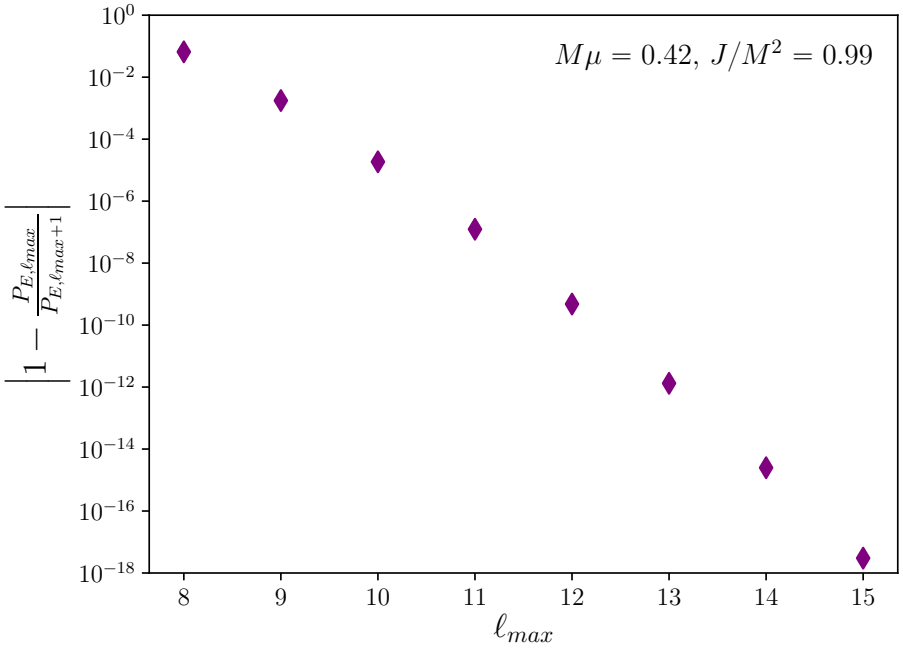

Figure 4.4 Convergence of the radiated GW energy at infinity, P_E, for the $m = 4$ scalar cloud as a function of the number of included $\hat{\ell}$ modes in the projection of ψ_4 onto the basis of spin-weighted spheroidal harmonics at the highest grid resolution.

4.6 *Gedanken* experiment

We are now ready to present our possible counterexample to WCCC with asymptotically flat boundary conditions. Consider generic initial data for the Einstein-Scalar system. These data are controlled by a large functional freedom coming from the fact that we can choose the initial metric, as well as the extrinsic curvature, on a constant time slice (so long as the Hamiltonian and momentum constraints are satisfied). In addition, we can also control the initial profile for the scalar field and its first time derivative on a constant time slice. We are going to choose our initial data to be close to that of the Kerr BH, so that deviations from the Kerr metric only occur at order $\mathcal{O}(\psi^2)$. This condition can be relaxed by considering initial data for the purely gravitational sector that is small in some norm. This essentially means that all the dynamics are being generated by the scalar field.

For generic scalar field initial data, we expect the scalar field profile to have some support on the unstable modes of the preceding sections, *i.e.* to excite unstable modes. Since all other modes decay with time[2], we expect the late time evolution to be dominated by the leading unstable modes and their backreaction. For each value of m

[2]This decay can be very complicated to determine and is not exponential with time.

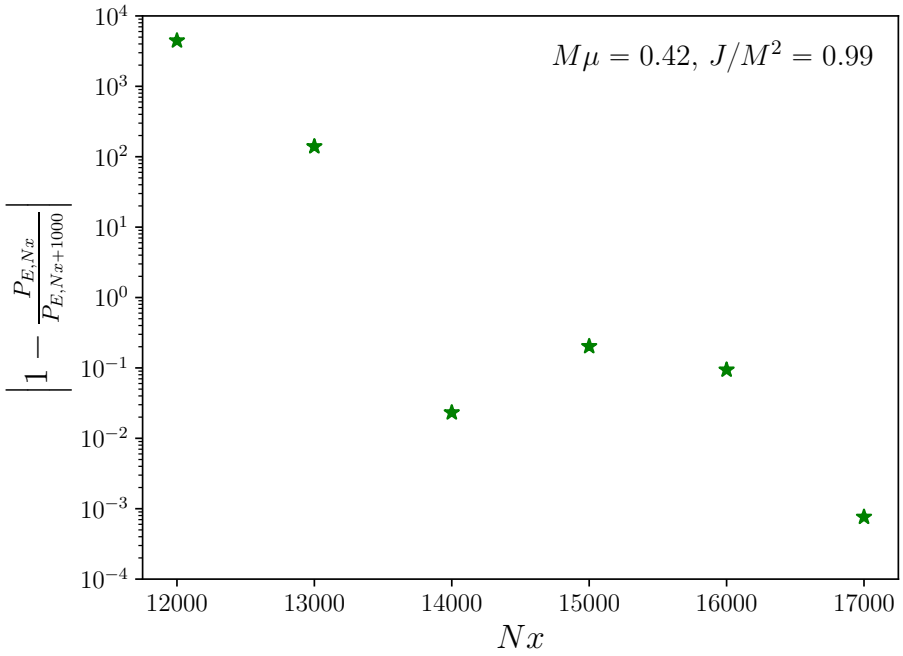

Figure 4.5 Convergence of the radiated GW energy at infinity, P_E, for the $m = 4$ scalar cloud as a function of the number of points in the radial direction Nx. Note that each point corresponds to a different number of included $\hat{\ell}$ modes, due to the low accuracy at lower resolutions, with the last two points having $\ell_{max} = 15$ - the highest we have used.

there is an infinite number of such modes labelled by $\ell \geq |m|$. However, all of these modes stop being unstable as soon as the condition $\mathrm{Re}(\omega) > m\Omega_K$ is no longer satisfied. The dynamics of this change in angular momentum and energy is entirely controlled by the $\ell = m$ modes, implying that, after some suitably long time, the dynamics of the Einstein-Scalar system can be well approximated by restricting our attention to scalar profiles of the form

$$\psi(t, r, \theta, \phi) = \mathrm{Re}\left[\sum_{\ell=0}^{+\infty} a_\ell e^{-i\omega_\ell + i\ell\phi}\, R_{\omega_\ell \ell\ell}(r)\, S_{\omega_\ell \ell\ell}(\theta)\right] , \tag{4.79}$$

and determining its leading order backreaction on the spacetime curvature. The coefficients a_ℓ are determined by our choice of initial data: for finite Sobolev norm initial data we expect a_ℓ to exhibit polynomial behaviour in $1/\ell$, whereas for C^∞ initial data we expect the coefficients a_ℓ to decay faster than any polynomial in $1/\ell$. Note that for real analytic initial data one can show that $a_\ell \approx e^{-\alpha\ell}$, for $\alpha > 0$.

Given that each ℓ mode evolves on an exponentially different timescale, as shown by Eq. (4.36b), they effectively decouple from each other, allowing us to study each term in Eq. (4.79) and its backreaction on the metric separately. Eventually, a given $\ell = \ell_\star$ mode becomes stable, but the system remains unstable to higher values of $\ell > \ell_\star$. This cascading happens slowly, since the timescales for this effect are exponentially large. One might worry that the energy contained in these high ℓ modes is radiated away as time passes by, but we have seen in Fig. (4.2) that this is not the case. In fact, the larger the value of ℓ, the smaller its radiative power is.

The intuitive picture is as follows: all the superradiant modes that the field has support on will be gradually condensating corotating scalar clouds around the BH. However, due to the exponentially separated timescales of their growth rates we can treat them independently. In particular, the fastest growing mode (the one with lowest mode number $\ell = m$) will be the first one to extract a significant amount of energy from the BH and form a scalar cloud, after which it will saturate (the superradiant mode will shut down) and stop extracting energy from the BH. The resulting cloud will partly disperse through GW emission and partly fall back into the BH, returning some of its energy. The evolution proceeds with the second fastest growing mode becoming dominant and condensating, further away, another cloud around the BH (while the first one is still dispersing), saturating, and then slowly decaying away. The process thus continues by gradually evolving the system to higher and higher mode numbers.

Finally, we have seen in Fig. (4.3) that χ decays as ℓ^{-16}. This in turn implies that a mode with weigh a_ℓ will depend on ℓ as $a_\ell^4\, \ell^{-16}$. The reason for this is simple: the

Teukolsky scalar ψ_4 is sourced by $[\psi^{(1)}]^2$, and χ is related to $|\psi_4|^2$, which translates into the overall scaling mentioned above. The curvatures are thus suppressed with time, and the evolution continues until all of the angular momentum is deposited into the scalar clouds, and the central black hole becomes Schwarzschild. However, one can show [64] that massive scalar field perturbations decay extremely slowly around Schwarschild black holes, with a dependence as weak as $1/\log(\log t)$, for large t. This suggests that the hypothetical endpoint is itself *non-linearly unstable* through a mechanism similar to the one reported in [79, 125, 126]. Namely, in some regions of spacetime matter will clump up enough that non-linear effects will become important, before its slow decay will have had the chance to disperse it. On the other hand, this slow decay warrants the question whether the gravitational radiation might not just disperse the clouds, before any non-linearities become problematic. We cannot answer this in our analysis, as our approximation for radiation emission breaks down at late times. Therefore, the outcome of our thought experiment depends on which of the competing processes - the GW emission or the nonlinear issues resulting from slower than logarithmic decay - wins over. If it is the latter, then the lack of a possible stationary endpoint leads us to conjecture that the spirit, if not the letter, of weak cosmic censorship is violated. Whether the curvature will be infinite in finite time is a question that we cannot settle with our current methods.

Note also that $r_\star(\ell)$ increases with ℓ, posing a problem from a numerical perspective: 1) the timescales involved are enormous; 2) the cascading towards high ℓ values makes this problem dependent on high frequency modes (as the simulation of turbulence in $3+1$ nonrelativitic fluids); and 3) the integration domain must extend to spatial infinity to observe this effect.

4.7 Conclusions

We have seen (Fig. 4.2) that the efficiency of superradiance cannot be counteracted by GW emission, implying that the system will continue advancing to higher values of m, with curvatures decreasing appropriately (as shown by Fig. 4.3), until a configuration with a central Schwarzschild black hole is reached. However, Schwarzschild is likely to be non-linearly unstable due to the very slow decay of perturbations induced by massive scalar fields. Reaching this troublesome regime, given that effects we cannot account for in our analysis do not prevent this, will involve timescales much longer than the age of our Universe, of course, as one will have to go to large values of $\ell = m$. Nevertheless

our scenario provides the first plausible example of a system with asymptotically flat boundary conditions, where WCCC is violated.

Chapter 5

Conclusions

5.1 Summary and Outlook

In this thesis we explored some aspects of the superradiant phenomenon in Einstein gravity minimally coupled to a massive scalar field in four, asymptotically flat dimensions.

In the case of a complex scalar, the equations of motion admit stationary, hairy scalar black hole solutions, which can coexist with the known Kerr black hole in certain regions of the parameter space, and branch off from the latter at the onset of scalar superradiance. Their existence is not in conflict with the known no-hair theorems, as these newly discovered hairy solutions avoid one of the assumptions of the theorems - namely, they possess only a single KVF that generates the horizon - whereas the theorems also require the existence of a Killing vector that is not normal to the event horizon.

We investigated the linear mode stability under scalar perturbations of these hairy black holes, and showed that, in the region of parameter space that we explored, they are also subject to a superradiant instability, however, only towards perturbations with mode number larger than that of the superradiant mode from whose onset the hairy solution branched off. This behaviour is analogous to what happens with superradiance in Kerr-AdS, and even if we did not explore the stability properties of hairy scalar black holes with $\tilde{m} > 1$, we do believe that the picture will not be qualitatively different for hairy solutions that emerge from higher m superradiant modes (recall that $\tilde{m}$ denotes the azimuthal quantum number of the background solution, and m the quantum number of the corresponding perturbations).

Even though we do not know of any complex scalars present in nature, one can still ask whether a hairy black hole exists, whose parameters allow for an instability

timescale that will be comparable with, or longer than, the age of the Universe. If that were the case, one could imagine, modulo the assumption of the existence of a complex scalar degree of freedom, that such solutions might have an astrophysical significance. Although, for the range of parameters that we have investigated that is not the case, we have seen that increasing the hair amplitude, while keeping $M\,\mu$ fixed, leads to smaller instability rates. Such arguments have been proposed in the literature, nevertheless, a more detailed study has not been performed. Therefore, it would be interesting to extend the analysis in chapter (3.1) to hairy solutions with progressively more hair for a fixed dimensionless mass $M\,\mu$, supposedly finding longer lived hairy black holes, in order to identify a possible domain of effective stability.

The findings in chapter (3.1) together with the parallels between the superradiant instability in flat space for a massive field, and in a spacetime with AdS asymptotics, prompted us to also look at the Einstein-Klein-Gordon system in flat four dimensions in the case of a real field, in an attempt to provide a plausible counterexample to the Weak Cosmic Censorship Conjecture. Although, in this setup, stationary solutions to the equations of motion with a non-trivial scalar profile do not exist, superradiance still leads to the formation of scalar clouds around the Kerr black hole. Our analysis indicated that this process cannot be prevented by the emission of gravitational waves, and hence, scalar clouds will continue forming with even higher mode numbers, until all the angular momentum of the black hole has been deposited in them. The resulting configuration of a Schwarzschild black hole surrounded by a sea of scalar clouds is believed to be non-linearly unstable, due to the very slow decay of massive scalar perturbations on a Schwarzschild background. Whether this can be countered by the emission of gravitational waves, given that superradiance is not present any more, is something that our linearised analysis cannot determine. Unfortunately, the timescales involved in the process are extremely long, rendering a numerical time-evolution in order to determine the endstate of the system impractical.

On the other hand, an interesting line of work that can follow from (4.1), albeit not connected to the WCCC in any way, is to investigate the gravitational waves spectrum from the scalar clouds around the Kerr black hole in more detail. In particular, it turns out that $m \geq 2$ scalar modes can have an overtone structure that includes crossings - that is, for particular values of the scalar mass, μ, and the black hole angular momentum, J, the fundamental mode $n = 0$ will not be the fastest growing one. This overtone mixing becomes more pronounced and easier to access[1] the higher

[1]For $m = 2$ one needs to be very close to black hole extremality in order to see the crossing. For larger m the behaviour occurs at lower values of the black hole spin.

the mode number is. This implies that in a time-dependent situation, there will be phases in the evolution of the system, when scalar modes with different overtone numbers will be active at the same time. This leads to a gravitational wave signature consisting of multiple frequencies, as one also needs to allow for cross-terms in the matter stress-tensor, arising from addition and subtraction of the different overtones' frequencies. Some of these might fall into various bands of astrophysical interest - for example, LIGO/LISA in the case of the difference between two overtones. Such a study has already been carried out for vector fields [168] and we are currently working on the just-described scalar case.

Finally, the numerical techniques utilised throughout the completion of this thesis can be used in numerous other systems with gravity and matter. The Einstein-DeTurck method has proven to be a viable tool in constructing various kinds of stationary black hole solutions - be it with different types of matter, or for spacetimes with AdS asymptotics. One can, for example, envisage deforming the spherical part of the AdS boundary or even putting a black hole there in order to investigate different phases of CFTs on curved backgrounds. Furthermore, such newly discovered stationary solutions can be subjected to a linearised analysis, which can always be complemented by a numerical study with the help of spectral methods. The latter are a powerful tool for solving systems of differential equations and physics does not fall short of providing us with such equations to deal with.

References

[1] B. P. Abbott et al., *GW151226: Observation of Gravitational Waves from a 22-Solar-Mass Binary Black Hole Coalescence*, Phys. Rev. Lett., 116 (2016), p. 241103.

[2] B. P. Abbott et al., *Observation of Gravitational Waves from a Binary Black Hole Merger*, Phys. Rev. Lett., 116 (2016), p. 061102.

[3] B. P. Abbott et al., *Tests of general relativity with GW150914*, Phys. Rev. Lett., 116 (2016), p. 221101.

[4] B. P. Abbott et al., *GW170104: Observation of a 50-Solar-Mass Binary Black Hole Coalescence at Redshift 0.2*, Phys. Rev. Lett., 118 (2017), p. 221101.

[5] B. P. Abbott et al., *GW170814: A Three-Detector Observation of Gravitational Waves from a Binary Black Hole Coalescence*, Phys. Rev. Lett., 119 (2017), p. 141101.

[6] B. P. Abbott et al., *GW170817: Observation of Gravitational Waves from a Binary Neutron Star Inspiral*, Phys. Rev. Lett., 119 (2017), p. 161101.

[7] B. P. Abbott et al., *GWTC-1: A Gravitational-Wave Transient Catalog of Compact Binary Mergers Observed by LIGO and Virgo during the First and Second Observing Runs*, Phys. Rev., X9 (2019), p. 031040.

[8] B. P. Abbott et al., *GW190425: Observation of a Compact Binary Coalescence with Total Mass* $\sim 3.4 M_{\odot}$, Astrophys. J. Lett., 892 (2020), p. L3.

[9] A. Adam, S. Kitchen, and T. Wiseman, *A numerical approach to finding general stationary vacuum black holes*, Class. Quant. Grav., 29 (2012), p. 165002.

[10] M. T. Anderson, P. T. Chrusciel, and E. Delay, *Nontrivial, static, geodesically complete, vacuum space-times with a negative cosmological constant*, JHEP, 10 (2002), p. 063.

[11] L. Andersson, S. Ma, C. Paganini, and B. F. Whiting, *Mode stability on the real axis*, J. Math. Phys., 58 (2017), p. 072501.

[12] R. L. Arnowitt, S. Deser, and C. W. Misner, *The Dynamics of general relativity*, Gen. Rel. Grav., 40 (2008), pp. 1997–2027.

[13] A. Ashtekar, *Asymptotic Structure of the Gravitational Field at Spatial Infinity.*, PhD thesis, University of Chicago, 1978.

[14] A. Ashtekar and R. O. Hansen, *A unified treatment of null and spatial infinity in general relativity. I - Universal structure, asymptotic symmetries, and conserved quantities at spatial infinity*, J. Math. Phys., 19 (1978), pp. 1542–1566.

[15] A. Ashtekar and J. D. Romano, *Spatial infinity as a boundary of space-time*, Class. Quant. Grav., 9 (1992), pp. 1069–1100.

[16] J. M. Bardeen, B. Carter, and S. Hawking, *The Four laws of black hole mechanics*, Commun. Math. Phys., 31 (1973), pp. 161–170.

[17] J. M. Bardeen, W. H. Press, and S. A. Teukolsky, *Rotating black holes: Locally nonrotating frames, energy extraction, and scalar synchrotron radiation*, Astrophys. J., 178 (1972), p. 347.

[18] J. M. Bardeen, W. H. Press, and S. A. Teukolsky, *Rotating black holes: Locally nonrotating frames, energy extraction, and scalar synchrotron radiation*, Astrophys. J., 178 (1972), p. 347.

[19] J. D. Bekenstein, *Extraction of energy and charge from a black hole*, Phys. Rev., D7 (1973), pp. 949–953.

[20] E. Berti, V. Cardoso, and M. Casals, *Eigenvalues and eigenfunctions of spin-weighted spheroidal harmonics in four and higher dimensions*, Phys. Rev., D73 (2006), p. 024013. [Erratum: Phys. Rev.D73,109902(2006)].

[21] S. Bhattacharya and A. Lahiri, *Black-hole no-hair theorems for a positive cosmological constant*, Phys. Rev. Lett., 99 (2007), p. 201101.

[22] S. Bhattacharyya, V. E. Hubeny, S. Minwalla, and M. Rangamani, *Nonlinear Fluid Dynamics from Gravity*, JHEP, 02 (2008), p. 045.

[23] Y. Brihaye, C. Herdeiro, and E. Radu, *Myers–Perry black holes with scalar hair and a mass gap*, Phys. Lett., B739 (2014), pp. 1–7.

[24] R. Brito, V. Cardoso, and P. Pani, *Black holes as particle detectors: evolution of superradiant instabilities*, Class. Quant. Grav., 32 (2015), p. 134001.

[25] R. Brito, V. Cardoso, and P. Pani, *Superradiance*, Lect. Notes Phys., 906 (2015), pp. pp.1–237.

[26] R. Brito, S. Ghosh, E. Barausse, E. Berti, V. Cardoso, I. Dvorkin, A. Klein, and P. Pani, *Gravitational wave searches for ultralight bosons with LIGO and LISA*, Phys. Rev., D96 (2017), p. 064050.

[27] M. M. Caldarelli, O. J. Dias, R. Monteiro, and J. E. Santos, *Black funnels and droplets in thermal equilibrium*, JHEP, 05 (2011), p. 116.

[28] V. Cardoso and O. J. Dias, *Rayleigh-Plateau and Gregory-Laflamme instabilities of black strings*, Phys. Rev. Lett., 96 (2006), p. 181601.

[29] V. Cardoso, O. J. Dias, G. S. Hartnett, L. Lehner, and J. E. Santos, *Holographic thermalization, quasinormal modes and superradiance in Kerr-AdS*, JHEP, 04 (2014), p. 183.

[30] B. Carter, *Axisymmetric Black Hole Has Only Two Degrees of Freedom*, Phys. Rev. Lett., 26 (1971), pp. 331–333.

[31] B. Carter, *Republication of: Black hole equilibrium states*, General Relativity and Gravitation, 41 (2009), p. 2873.

[32] S. Chandrasekhar, *The Solution of Dirac's Equation in Kerr Geometry*, Proc. Roy. Soc. Lond. A, A349 (1976), pp. 571–575.

[33] S. Chandrasekhar, *The mathematical theory of black holes*, Clarendon Press, 1985.

[34] P. M. Chesler and D. A. Lowe, *Nonlinear evolution of the AdS_4 superradiant instability*, Phys. Rev. Lett., 122 (2019), p. 181101.

[35] O. Chodosh and Y. Shlapentokh-Rothman, *Time-Periodic Einstein-Klein-Gordon Bifurcations of Kerr*, Commun. Math. Phys., 356 (2017), pp. 1155–1250.

[36] M. W. Choptuik, *Universality and scaling in gravitational collapse of a massless scalar field*, Phys. Rev. Lett., 70 (1993), pp. 9–12.

[37] Y. Choquet-Bruhat and R. P. Geroch, *Global aspects of the Cauchy problem in general relativity*, Commun. Math. Phys., 14 (1969), pp. 329–335.

[38] D. Christodoulou, *Reversible and irreversible transforations in black hole physics*, Phys. Rev. Lett., 25 (1970), pp. 1596–1597.

[39] D. Christodoulou, *Violation of cosmic censorship in the gravitational collapse of a dust cloud*, Commun. Math. Phys., 93 (1984), pp. 171–195.

[40] D. Christodoulou, *A Mathematical Theory of Gravitational Collapse*, Commun. Math. Phys., 109 (1987), pp. 613–647.

[41] D. Christodoulou, *Examples of naked singularity formation in the gravitational collapse of a scalar field*, Annals Math., 140 (1994), pp. 607–653.

[42] D. Christodoulou, *On the global initial value problem and the issue of singularities*, Classical and Quantum Gravity, 16 (1999), pp. A23–A35.

[43] P. T. Chrusciel, *On uniqueness in the large of solutions of einstein's equations*, in Mathematical Aspects of Classical Field Theory: Proceedings of the AMS-IMS-SIAM Joint Summer Research Conference Held July 20-26, 1991, with Support from the National Science Foundation, vol. 132, American Mathematical Soc., 1992, p. 235.

[44] P. T. Chrusciel, *On rigidity of analytic black holes*, Commun. Math. Phys., 189 (1997), pp. 1–7.

[45] P. T. Chrusciel, J. Lopes Costa, and M. Heusler, *Stationary Black Holes: Uniqueness and Beyond*, Living Rev. Rel., 15 (2012), p. 7.

[46] P. T. Chrusciel and R. M. Wald, *On the topology of stationary black holes*, Class. Quant. Grav., 11 (1994), pp. L147–L152.

[47] T. Crisford, G. T. Horowitz, and J. E. Santos, *Testing the Weak Gravity - Cosmic Censorship Connection*, Phys. Rev., D97 (2018), p. 066005.

[48] T. Crisford and J. E. Santos, *Violating the Weak Cosmic Censorship Conjecture in Four-Dimensional Anti–de Sitter Space*, Phys. Rev. Lett., 118 (2017), p. 181101.

[49] M. Dafermos, *Stability and Instability of the Cauchy Horizon for the Spherically Symmetric Einstein-Maxwell-Scalar Field Equations*, Ann. Math, 158 (2003), pp. 875–928.

[50] M. Dafermos, *The Interior of charged black holes and the problem of uniqueness in general relativity*, Commun. Pure Appl. Math., 58 (2005), pp. 0445–0504.

[51] M. Dafermos, G. Holzegel, and I. Rodnianski, *The linear stability of the Schwarzschild solution to gravitational perturbations*, Acta Math., 222 (2019), pp. 1–214.

[52] M. Dafermos and I. Rodnianski, *A Proof of Price's law for the collapse of a selfgravitating scalar field*, Invent. Math., 162 (2005), pp. 381–457.

[53] M. Dafermos and I. Rodnianski, *Lectures on black holes and linear waves*, Clay Math. Proc., 17 (2013), pp. 97–205.

[54] T. Damour, N. Deruelle, and R. Ruffini, *On Quantum Resonances in Stationary Geometries*, Lett. Nuovo Cim., 15 (1976), pp. 257–262.

[55] T. Damour, N. Deruelle, and R. Ruffini, *On Quantum Resonances in Stationary Geometries*, Lett. Nuovo Cim., 15 (1976), pp. 257–262.

[56] S. de Haro, S. N. Solodukhin, and K. Skenderis, *Holographic reconstruction of space-time and renormalization in the AdS / CFT correspondence*, Commun. Math. Phys., 217 (2001), pp. 595–622.

[57] J. C. Degollado, C. A. R. Herdeiro, and E. Radu, *Effective stability against superradiance of Kerr black holes with synchronised hair*, arXiv, (2018).

[58] N. Deppe, L. E. Kidder, M. A. Scheel, and S. A. Teukolsky, *Critical behavior in 3D gravitational collapse of massless scalar fields*, Phys. Rev., D99 (2019), p. 024018.

[59] D. M. DeTurck, *Deforming metrics in the direction of their ricci tensors*, J. Differential Geom., 18 (1983), pp. 157–162.

[60] S. L. Detweiler, *Klein-Gordon equation and rotating black holes*, Phys. Rev., D22 (1980), pp. 2323–2326.

[61] O. J. Dias, G. T. Horowitz, and J. E. Santos, *Black holes with only one Killing field*, JHEP, 07 (2011), p. 115.

[62] O. J. Dias, J. E. Santos, and B. Way, *Black holes with a single Killing vector field: black resonators*, JHEP, 12 (2015), p. 171.

[63] O. J. C. Dias and J. E. Santos, *Boundary Conditions for Kerr-AdS Perturbations*, JHEP, 10 (2013), p. 156.

[64] O. J. C. Dias, J. E. Santos, H. S. Reall, and B. Ganchev, *In preparation*, , ( ).

[65] O. J. C. Dias, J. E. Santos, and B. Way, *Black holes with a single Killing vector field: black resonators*, JHEP, 12 (2015), p. 171.

[66] O. J. C. Dias, J. E. Santos, and B. Way, *Numerical Methods for Finding Stationary Gravitational Solutions*, Class. Quant. Grav., 33 (2016), p. 133001.

[67] R. Dicke, *Coherence in Spontaneous Radiation Processes*, Phys. Rev., 93 (1954), pp. 99–110.

[68] S. R. Dolan, *Instability of the massive Klein-Gordon field on the Kerr spacetime*, Phys. Rev., D76 (2007), p. 084001.

[69] S. R. Dolan, *The Quasinormal Mode Spectrum of a Kerr Black Hole in the Eikonal Limit*, Phys. Rev., D82 (2010), p. 104003.

[70] W. E. East, *Superradiant instability of massive vector fields around spinning black holes in the relativistic regime*, Phys. Rev., D96 (2017), p. 024004.

[71] W. E. East and F. Pretorius, *Superradiant Instability and Backreaction of Massive Vector Fields around Kerr Black Holes*, Phys. Rev. Lett., 119 (2017), p. 041101.

[72] J. Eggers, *Nonlinear dynamics and breakup of free-surface flows*, Rev. Mod. Phys., 69 (1997), pp. 865–930.

[73] H. Elvang, R. Emparan, and P. Figueras, *Phases of five-dimensional black holes*, JHEP, 05 (2007), p. 056.

[74] H. Elvang and P. Figueras, *Black Saturn*, JHEP, 05 (2007), p. 050.

[75] R. Emparan, T. Harmark, V. Niarchos, and N. A. Obers, *Essentials of Blackfold Dynamics*, JHEP, 03 (2010), p. 063.

[76] R. Emparan and H. S. Reall, *A Rotating black ring solution in five-dimensions*, Phys. Rev. Lett., 88 (2002), p. 101101.

[77] R. Emparan and H. S. Reall, *Black Holes in Higher Dimensions*, Living Rev. Rel., 11 (2008), p. 6.

[78] F. C. Eperon, B. Ganchev, and J. E. Santos, *Plausible scenario for a generic violation of the weak cosmic censorship conjecture in asymptotically flat four dimensions*, Phys. Rev. D, 101 (2020), p. 041502.

[79] F. C. Eperon, H. S. Reall, and J. E. Santos, *Instability of supersymmetric microstate geometries*, JHEP, 10 (2016), p. 031.

[80] P. Figueras, M. Kunesch, L. Lehner, and S. Tunyasuvunakool, *End Point of the Ultraspinning Instability and Violation of Cosmic Censorship*, Phys. Rev. Lett., 118 (2017), p. 151103.

[81] P. Figueras, M. Kunesch, and S. Tunyasuvunakool, *End Point of Black Ring Instabilities and the Weak Cosmic Censorship Conjecture*, Phys. Rev. Lett., 116 (2016), p. 071102.

[82] P. Figueras, J. Lucietti, and T. Wiseman, *Ricci solitons, Ricci flow, and strongly coupled CFT in the Schwarzschild Unruh or Boulware vacua*, Class. Quant. Grav., 28 (2011), p. 215018.

[83] P. Figueras, J. Lucietti, and T. Wiseman, *Ricci solitons, Ricci flow, and strongly coupled CFT in the Schwarzschild Unruh or Boulware vacua*, Class. Quant. Grav., 28 (2011), p. 215018.

[84] P. Figueras and T. Wiseman, *Stationary holographic plasma quenches and numerical methods for non-Killing horizons*, Phys. Rev. Lett., 110 (2013), p. 171602.

[85] P. Figueras and T. Wiseman, *On the existence of stationary Ricci solitons*, Class. Quant. Grav., 34 (2017), p. 145007.

[86] A. E. Fischer and J. E. Marsden, *The einstein evolution equations as a first-order quasi-linear symmetric hyperbolic system. I*, Comm. Math. Phys., 28 (1972), pp. 1–38.

[87] S. Fischetti and D. Marolf, *Flowing Funnels: Heat sources for field theories and the AdS_3 dual of CFT_2 Hawking radiation*, Class. Quant. Grav., 29 (2012), p. 105004.

[88] S. Fischetti, D. Marolf, and J. E. Santos, *AdS flowing black funnels: Stationary AdS black holes with non-Killing horizons and heat transport in the dual CFT*, Class. Quant. Grav., 30 (2013), p. 075001.

[89] Y. Foures-Bruhat, *Theoreme d'existence pour certains systemes derivees partielles non lineaires*, Acta Mat., 88 (1952), pp. 141–225.

[90] V. P. Frolov and I. D. Novikov, *Black hole physics: Basic concepts and new developments*, Kluwer Academic Publishers, 1998.

[91] H. Furuhashi and Y. Nambu, *Instability of massive scalar fields in Kerr-Newman space-time*, Prog. Theor. Phys., 112 (2004), pp. 983–995.

[92] G. J. Galloway, *On the topology of the domain of outer communication*, Classical and Quantum Gravity, 12 (1995), pp. L99–L101.

[93] G. J. Galloway, S. Surya, and E. Woolgar, *A Uniqueness theorem for the AdS soliton*, Phys. Rev. Lett., 88 (2002), p. 101102.

[94] G. J. Galloway, S. Surya, and E. Woolgar, *On the geometry and mass of static, asymptotically AdS space-times, and the uniqueness of the AdS soliton*, Commun. Math. Phys., 241 (2003), pp. 1–25.

[95] B. Ganchev and J. E. Santos, *Scalar Hairy Black Holes in Four Dimensions are Unstable*, Phys. Rev. Lett., 120 (2018), p. 171101.

[96] G. Gibbons, *Collapsing shells and the isoperimetric inequality for black holes*, Class. Quant. Grav., 14 (1997), pp. 2905–2915.

[97] G. W. Gibbons, S. W. Hawking, G. T. Horowitz, and M. J. Perry, *Positive Mass Theorems for Black Holes*, Commun. Math. Phys., 88 (1983), p. 295.

[98] R. Gregory and R. Laflamme, *Black strings and p-branes are unstable*, Phys. Rev. Lett., 70 (1993), pp. 2837–2840.

[99] S. S. Gubser, *Phase transitions near black hole horizons*, Class. Quant. Grav., 22 (2005), pp. 5121–5144.

[100] S. S. Gubser, *Breaking an Abelian gauge symmetry near a black hole horizon*, Phys. Rev., D78 (2008), p. 065034.

[101] R. S. Hamilton, *Three-manifolds with positive ricci curvature*, J. Differential Geom., 17 (1982), pp. 255–306.

[102] S. A. Hartnoll, C. P. Herzog, and G. T. Horowitz, *Building a Holographic Superconductor*, Phys. Rev. Lett., 101 (2008), p. 031601.

[103] S. Hawking and G. Ellis, *The Large Scale Structure of Space-Time*, Cambridge Monographs on Mathematical Physics, Cambridge University Press, 2011.

[104] S. W. Hawking, *Black holes in general relativity*, Communications in Mathematical Physics, 25 (1972), pp. 152–166.

[105] M. Headrick, S. Kitchen, and T. Wiseman, *A New approach to static numerical relativity, and its application to Kaluza-Klein black holes*, Class. Quant. Grav., 27 (2010), p. 035002.

[106] M. Headrick, S. Kitchen, and T. Wiseman, *A New approach to static numerical relativity, and its application to Kaluza-Klein black holes*, Class. Quant. Grav., 27 (2010), p. 035002.

[107] C. Herdeiro and E. Radu, *Ergosurfaces for Kerr black holes with scalar hair*, Phys. Rev., D89 (2014), p. 124018.

[108] C. Herdeiro, E. Radu, and H. Runarsson, *Kerr black holes with Proca hair*, Class. Quant. Grav., 33 (2016), p. 154001.

[109] C. A. R. Herdeiro and E. Radu, *Kerr black holes with scalar hair*, Phys. Rev. Lett., 112 (2014), p. 221101.

[110] T. Hertog, *Towards a Novel no-hair Theorem for Black Holes*, Phys. Rev., D74 (2006), p. 084008.

[111] S. Hollands and A. Ishibashi, *Black hole uniqueness theorems in higher dimensional spacetimes*, Class. Quant. Grav., 29 (2012), p. 163001.

[112] S. Hollands, A. Ishibashi, and R. M. Wald, *A Higher dimensional stationary rotating black hole must be axisymmetric*, Commun. Math. Phys., 271 (2007), pp. 699–722.

[113] G. Holzegel and J. Smulevici, *Quasimodes and a Lower Bound on the Uniform Energy Decay Rate for Kerr-AdS Spacetimes*, Anal. PDE, 7 (2013), pp. 1057–1090.

[114] G. T. Horowitz, N. Iqbal, J. E. Santos, and B. Way, *Hovering Black Holes from Charged Defects*, Class. Quant. Grav., 32 (2015), p. 105001.

[115] G. T. Horowitz and M. J. Perry, *Gravitational energy cannot become negative*, Phys. Rev. Lett., 48 (1982), p. 371.

[116] G. T. Horowitz, J. E. Santos, and B. Way, *Evidence for an Electrifying Violation of Cosmic Censorship*, Class. Quant. Grav., 33 (2016), p. 195007.

[117] G. T. Horowitz and A. Strominger, *Black strings and P-branes*, Nucl. Phys. B, 360 (1991), pp. 197–209.

[118] V. E. Hubeny, D. Marolf, and M. Rangamani, *Black funnels and droplets from the AdS C-metrics*, Class. Quant. Grav., 27 (2010), p. 025001.

[119] V. E. Hubeny, D. Marolf, and M. Rangamani, *Hawking radiation from AdS black holes*, Class. Quant. Grav., 27 (2010), p. 095018.

[120] V. E. Hubeny, D. Marolf, and M. Rangamani, *Hawking radiation in large N strongly-coupled field theories*, Class. Quant. Grav., 27 (2010), p. 095015.

[121] R. A. Hulse and J. H. Taylor, *Discovery of a pulsar in a binary system*, Astrophys. J., 195 (1975), pp. L51–L53.

[122] W. Israel, *Event horizons in static vacuum space-times*, Phys. Rev., 164 (1967), pp. 1776–1779.

[123] W. Israel, *Event horizons in static electrovac space-times*, Commun. Math. Phys., 8 (1968), pp. 245–260.

[124] B. R. Iyer and A. Kumar, *Note on the Absence of Massive Fermion Superradiance from a Kerr Black Hole*, Phys. Rev. D, 18 (1978), pp. 4799–4801.

[125] J. Keir, *Slowly decaying waves on spherically symmetric spacetimes and ultracompact neutron stars*, Class. Quant. Grav., 33 (2016), p. 135009.

[126] J. Keir, *Wave propagation on microstate geometries*, Annales Henri Poincare, 21 (2019), pp. 705–760.

[127] R. P. Kerr, *Gravitational field of a spinning mass as an example of algebraically special metrics*, Phys. Rev. Lett., 11 (1963), pp. 237–238.

[128] W. Kinnersley, *Type D Vacuum Metrics*, J. Math. Phys., 10 (1969), pp. 1195–1203.

[129] B. Kleihaus and J. Kunz, *Static axially symmetric Einstein Yang-Mills dilaton solutions: 1. Regular solutions*, Phys. Rev. D, 57 (1998), pp. 834–856.

[130] B. Kleihaus and J. Kunz, *Static axially symmetric Einstein Yang-Mills dilaton solutions. 2. Black hole solutions*, Phys. Rev. D, 57 (1998), pp. 6138–6157.

[131] B. Kleihaus and J. Kunz, *Rotating hairy black holes*, Phys. Rev. Lett., 86 (2001), pp. 3704–3707.

[132] B. Kleihaus, J. Kunz, M. List, and I. Schaffer, *Rotating Boson Stars and Q-Balls. II. Negative Parity and Ergoregions*, Phys. Rev., D77 (2008), p. 064025.

[133] B. Kleihaus, J. Kunz, and E. Radu, *New nonuniform black string solutions*, JHEP, 06 (2006), p. 016.

[134] B. Kol and T. Wiseman, *Evidence that highly nonuniform black strings have a conical waist*, Class. Quant. Grav., 20 (2003), pp. 3493–3504.

[135] H. Kudoh and T. Wiseman, *Properties of Kaluza-Klein black holes*, Prog. Theor. Phys., 111 (2004), pp. 475–507.

[136] H. Kudoh and T. Wiseman, *Connecting black holes and black strings*, Phys. Rev. Lett., 94 (2005), p. 161102.

[137] L. Lehner and F. Pretorius, *Black Strings, Low Viscosity Fluids, and Violation of Cosmic Censorship*, Phys. Rev. Lett., 105 (2010), p. 101102.

[138] D. Marolf and J. E. Santos, *Phases of Holographic Hawking Radiation on spatially compact spacetimes*, JHEP, 10 (2019), p. 250.

[139] M. Mars, *Present status of the Penrose inequality*, Class. Quant. Grav., 26 (2009), p. 193001.

[140] C. Martinez, R. Troncoso, and J. Zanelli, *De Sitter black hole with a conformally coupled scalar field in four-dimensions*, Phys. Rev., D67 (2003), p. 024008.

[141] P. Mazur, *Proof of Uniqueness of the Kerr-Nweman Black Hole Solution*, J. Phys. A, 15 (1982), pp. 3173–3180.

[142] B. E. Niehoff, J. E. Santos, and B. Way, *Towards a violation of cosmic censorship*, Class. Quant. Grav., 33 (2016), p. 185012.

[143] B. E. Niehoff, J. E. Santos, and B. Way, *Towards a violation of cosmic censorship*, Class. Quant. Grav., 33 (2016), p. 185012.

[144] V. Paschalidis and N. Stergioulas, *Rotating Stars in Relativity*, Living Rev. Rel., 20 (2017), p. 7.

[145] R. Penrose, *Gravitational collapse and space-time singularities*, Phys. Rev. Lett., 14 (1965), pp. 57–59.

[146] R. Penrose, *Gravitational collapse: The role of general relativity*, Riv. Nuovo Cim., 1 (1969), pp. 252–276.

[147] R. Penrose, *Naked singularities*, Annals of the New York Academy of Sciences, 224 (1973), pp. 125–134.

[148] R. Penrose and R. M. Floyd, *Extraction of rotational energy from a black hole*, Nature, 229 (1971), pp. 177–179.

[149] E. Poisson and W. Israel, *Internal structure of black holes*, Phys. Rev. D, 41 (1990), pp. 1796–1809.

[150] W. H. Press and S. A. Teukolsky, *Perturbations of a Rotating Black Hole. II. Dynamical Stability of the Kerr Metric*, Astrophys. J., 185 (1973), pp. 649–674.

[151] R. H. Price, *Nonspherical perturbations of relativistic gravitational collapse. 1. Scalar and gravitational perturbations*, Phys. Rev. D, 5 (1972), pp. 2419–2438.

[152] R. H. Price, *Nonspherical Perturbations of Relativistic Gravitational Collapse. II. Integer-Spin, Zero-Rest-Mass Fields*, Phys. Rev. D, 5 (1972), pp. 2439–2454.

[153] A. Raychaudhuri, *Relativistic cosmology. I*, Phys. Rev., 98 (1955), pp. 1123–1126.

[154] H. Ringström, *Origins and development of the Cauchy problem in general relativity*, Class. Quant. Grav., 32 (2015), p. 124003.

[155] D. C. Robinson, *Uniqueness of the Kerr black hole*, Phys. Rev. Lett., 34 (1975), pp. 905–906.

[156] D. C. Robinson, *Four decades of black holes uniqueness theorems*, in Kerr Fest: Black Holes in Astrophysics, General Relativity and Quantum Gravity Christchurch, New Zealand, August 26-28, 2004, 2004.

[157] M. Rozali, J. B. Stang, and M. van Raamsdonk, *Holographic Baryons from Oblate Instantons*, JHEP, 02 (2014), p. 044.

[158] J. E. Santos, *To go or not to go with the flow: Hawking radiation at strong coupling*, (2020).

[159] M. Sasaki and H. Tagoshi, *Analytic black hole perturbation approach to gravitational radiation*, Living Rev. Rel., 6 (2003), p. 6.

[160] R. Schoen and S.-T. Yau, *The existence of a black hole due to condensation of matter*, Communications in Mathematical Physics, 90 (1983), pp. 575–579.

[161] R. Schon and S.-T. Yau, *On the Proof of the positive mass conjecture in general relativity*, Commun. Math. Phys., 65 (1979), pp. 45–76.

[162] R. Schon and S.-T. Yau, *Proof of the positive mass theorem. 2.*, Commun. Math. Phys., 79 (1981), pp. 231–260.

[163] B. F. Schutz and N. Comins, *On the existence of ergoregions in rotating stars*, Monthly Notices of the Royal Astronomical Society, 182 (1978), pp. 69–76.

[164] K. Schwarzschild, *Über das Gravitationsfeld eines Massenpunktes nach der Einsteinschen Theorie*, Sitzungsberichte der Königlich Preußischen Akademie der Wissenschaften, Berlin, (1916), pp. 189–196.

[165] J. M. M. Senovilla, *Singularity Theorems and Their Consequences*, Gen. Rel. Grav., 30 (1998), p. 701.

[166] Y. Shlapentokh-Rothman, *Exponentially growing finite energy solutions for the Klein-Gordon equation on sub-extremal Kerr spacetimes*, Commun. Math. Phys., 329 (2014), pp. 859–891.

[167] Y. Shlapentokh-Rothman, *Quantitative Mode Stability for the Wave Equation on the Kerr Spacetime*, Annales Henri Poincare, 16 (2015), pp. 289–345.

[168] N. Siemonsen and W. E. East, *Gravitational wave signatures of ultralight vector bosons from black hole superradiance*, Phys. Rev. D, 101 (2020), p. 024019.

[169] J. Sorce and R. M. Wald, *Gedanken experiments to destroy a black hole. II. Kerr-Newman black holes cannot be overcharged or overspun*, Phys. Rev. D, 96 (2017), p. 104014.

[170] A. A. Starobinsky, *Amplification of waves reflected from a rotating "black hole"*, Sov. Phys. JETP, 37 (1973), pp. 28–32. [Zh. Eksp. Teor. Fiz.64,48(1973)].

[171] D. Sudarsky and R. M. Wald, *Extrema of mass, stationarity, and staticity, and solutions to the Einstein Yang-Mills equations*, Phys. Rev. D, 46 (1992), pp. 1453–1474.

[172] D. Sudarsky and R. M. Wald, *Mass formulas for stationary Einstein Yang-Mills black holes and a simple proof of two staticity theorems*, Phys. Rev. D, 47 (1993), pp. 5209–5213.

[173] J. H. Taylor and J. M. Weisberg, *Further experimental tests of relativistic gravity using the binary pulsar PSR 1913+16*, Astrophys. J., 345 (1989), pp. 434–450.

[174] R. Teixeira da Costa, *Mode stability for the Teukolsky equation on extremal and subextremal Kerr spacetimes*, arXiv preprint arXiv:1910.02854, (2019).

[175] S. A. Teukolsky, *Perturbations of a rotating black hole. 1. Fundamental equations for gravitational electromagnetic and neutrino field perturbations*, Astrophys. J., 185 (1973), pp. 635–647.

[176] S. A. Teukolsky and W. H. Press, *Perturbations of a rotating black hole. III - Interaction of the hole with gravitational and electromagnet ic radiation*, Astrophys. J., 193 (1974), pp. 443–461.

[177] W. Unruh, *Separability of the Neutrino Equations in a Kerr Background*, Phys. Rev. Lett., 31 (1973), pp. 1265–1267.

[178] C. Vishveshwara, *Stability of the schwarzschild metric*, Phys. Rev. D, 1 (1970), pp. 2870–2879.

[179] R. M. Wald, *General Relativity*, Chicago Univ. Pr., Chicago, USA, 1984.

[180] R. M. Wald, *Gravitational collapse and cosmic censorship*, in Black Holes, Gravitational Radiation and the Universe: Essays in Honor of C.V. Vishveshwara, 10 1997, pp. 69–85.

[181] J. M. Weisberg, D. J. Nice, and J. H. Taylor, *Timing Measurements of the Relativistic Binary Pulsar PSR B1913+16*, Astrophys. J., 722 (2010), pp. 1030–1034.

[182] B. F. Whiting, *Mode Stability of the Kerr Black Hole*, J. Math. Phys., 30 (1989), p. 1301.

[183] E. Winstanley, *Existence of stable hairy black holes in SU(2) Einstein Yang-Mills theory with a negative cosmological constant*, Class. Quant. Grav., 16 (1999), pp. 1963–1978.

[184] T. Wiseman, *Static axisymmetric vacuum solutions and nonuniform black strings*, Class. Quant. Grav., 20 (2003), pp. 1137–1176.

[185] T. Wiseman, *Numerical construction of static and stationary black holes*, (2011), pp. 233–270.

[186] E. Witten, *Instability of the Kaluza-Klein Vacuum*, Nucl. Phys. B, 195 (1982), pp. 481–492.

[187] H. Yang, D. A. Nichols, F. Zhang, A. Zimmerman, Z. Zhang, and Y. Chen, *Quasinormal-mode spectrum of Kerr black holes and its geometric interpretation*, Phys. Rev., D86 (2012), p. 104006.

[188] H. Yoshino and H. Kodama, *Gravitational radiation from an axion cloud around a black hole: Superradiant phase*, PTEP, 2014 (2014), p. 043E02.

[189] Y. Zeldovich, *Amplification of cylindrical electromagnetic waves reflected from a rotating body*, Soviet Physics-JETP, 35 (1972), pp. 1085–1087.

[190] T. J. M. Zouros and D. M. Eardley, *Instabilities of massive scalar perturbations of a rotating black hole*, Annals Phys., 118 (1979), pp. 139–155.